ISOELECTRIC TRAPPING AND MASS SPECTROMETRY: TOOLS FOR PROTEOMICS

A Dissertation

by

STEPHANIE MARIE COLOGNA

Submitted to the Office of Graduate Studies of
Texas A&M University
in partial fulfillment of the requirements for the degree of

DOCTOR OF PHILOSOPHY

December 2010

Major Subject: Chemistry

ISOELECTRIC TRAPPING AND MASS SPECTROMETRY: TOOLS FOR PROTEOMICS

A Dissertation

by

STEPHANIE MARIE COLOGNA

Submitted to the Office of Graduate Studies of
Texas A&M University
in partial fulfillment of the requirements for the degree of

DOCTOR OF PHILOSOPHY

Approved by:

Chair of Committee,	David H. Russell
Committee Members,	Paul S. Cremer
	Arul Jayaraman
	Gyula Vigh
Head of Department,	David H. Russell

December 2010

Major Subject: Chemistry

ABSTRACT

Isoelectric Trapping and Mass Spectrometry: Tools for Proteomics. (December 2010)

Stephanie Marie Cologna, B.S., University of Arizona

Chair of Advisory Committee: Dr. David H. Russell

Mass spectrometry (MS) has played a major role in the proteomic analysis of an array of biological samples. Even so, inherent limitations exist such as sample complexity and the dynamic range. In an attempt to overcome these limitations, pre-fractionation is typically performed followed by reversed phase liquid chromatography coupled with MS. Pre-fractionation can be performed in several formats including chromatographic or electrophoretic based methods. Solution-based isoelectric point (pI) fractionation, specifically isoelectric trapping (IET), provides an attractive alternative for pre-fractionation in bottom-up proteomic studies.

A recently developed device, membrane separated wells for isoelectric focusing and trapping (MSWIFT), provides rapid separation on the basis of pI and resulting solutions are MS compatible without the need for extensive sample cleanup. Initial experiments demonstrate fractionation using MSWIFT, of peptide mixtures ranging from standards to a yeast lysate where resulting fractions are analyzed using matrix-assisted laser desorption/ionization (MALDI) – MS or further separated using reversed phase liquid chromatography followed by tandem MS (MS/MS) analysis. Identified yeast proteins range in size, pI and copy number illustrating an ability to increase the

depth of proteome coverage when using MSWIFT. Extensive studies were also performed using MSWIFT in a multi-stage fractionation platform to improve peptide and protein identifications for the first large-scale proteomic study of the model fungus, *Neurospora crassa.*

A second focus of this work is the development of a new sample preparation method for proteolytic digestion and high-throughput separations using MSWIFT. Histidine is used as a neutral pH, isoelectric, sample buffer for tryptic digestion of proteins and also assists in rapid separations using MSWIFT owing to the low conductivity. Tryptic digests of individual standard proteins and a mixture of standard proteins are used to illustrate these advantages. Finally, the histidine buffer sample preparation method is incorporated into a two-dimensional separation strategy. Tryptic peptides are fractionated using MSWIFT and resulting solutions are further separated using capillary electrophoresis (CE) coupled with MALDI-MS/MS. Performing the two-dimensional strategy allows for increased confidence in peptide and protein assignment owing to experimentally determined in-solution charge states and estimated pI values.

ACKNOWLEDGEMENTS

I would first like to acknowledge and thank my advisor, Dr. David H. Russell for his continual support and guidance and for providing me the opportunity to perform research in his laboratory. He encouraged my individual research, welcomed ideas and spent many hours helping me develop as a scientist. For these things and many others, I am greatly indebted.

I am also very appreciative of the guidance that was provided by Dr. Gyula Vigh and his willingness to open his laboratory to me. He is a great teacher and mentor and his excitement for chemistry is contagious. I have learned from him it is important to take a step back and think about the big picture and I am grateful for the many scientific and life lessons he has provided.

Sincere thanks to the members of the Russell Research Group both past and present, for their help and guidance. I would especially like to thank Dr. William K. Russell for being an outstanding mentor and for providing me with endless opportunities to expand my knowledge. I would also like to thank Dr. Stacy D. Sherrod for her friendship, constant support, encouragement and willingness to help develop ideas and critically evaluate my work. A special thank you to Dr. Jody C. May for being a great friend and providing a hand when I needed to construct a piece or fix an electrode and for his willingness to give me a lesson on an array of topics. I would like to acknowledge my friend and coworker, Dr. Brad J. Williams for his support, everlasting patience and for teaching me many valuable things along the way.

Finally, I would like to thank my undergraduate research advisor, Dr. Katrina M. Miranda for encouraging me to pursue my interests in chemistry, and to savor the joys of scientific research.

NOMENCLATURE

MS	Mass Spectrometry
MS/MS	Tandem Mass Spectrometry
MSWIFT	Membrane Separated Wells for Isoelectric Focusing and Trapping
IET	Isoelectric Trapping
IEF	Isoelectric Focusing
pI	Isoelectric Point
LC	Liquid Chromatography
MALDI	Matrix Assisted Laser Desorption/Ionization
ESI	Electrospray Ionization
CE	Capillary Electrophoresis
SCX	Strong Cation Exchange
HILIC	Hydrophilic Interaction Liquid Chromatography
GELLFrEE	Gel-eluted Liquid Fraction Entrapment Electrophoresis
GeLC	Gel Electrophoresis – Liquid Chromatography
MW	Molecular Weight
SDS	Sodium Dodecylsulfate
PAGE	Polyacrylamide Gel Electrophoresis
CIEF	Capillary Isoelectric Focusing
2D-GE	Two-Dimensional Gel Electrophoresis
MCE	Multicompartment Electrolyzer

IPG	Immobilized pH Gradient
CID	Collision Induced Dissociation

TABLE OF CONTENTS

CHAPTER Page

LIST OF FIGURES

Page

Page

Page

Page

Page

Page

LIST OF TABLES

Page

LIST OF SCHEMES

Page

CHAPTER I

INTRODUCTION

MASS SPECTROMETRY-BASED PROTEOMICS

The study of the protein compliment of a cell or organism is defined as proteomics. Proteomic studies often include but are not limited to protein identification, localization, determination of post-translational modifications, interactions and quantitation. The task of characterizing the entire proteome can be daunting considering the vast number of proteins present in any given organism and the dynamic range of protein concentrations encountered. For example, it has been estimated that the protein concentration in human plasma spans more than ten orders of magnitude.[1] Mass spectrometry (MS) has been at the forefront of advances in proteomics, specifically with the development of matrix assisted laser desorption/ionization (MALDI)[2] and electrospray ionization (ESI).[3] MS has been a valuable tool because of the excellent sensitivity, dynamic range and resolution that can be achieved.

The majority of mass spectrometry-based proteomic studies are typically performed in one of two experimental formats; bottom-up or top-down.[4, 5] Bottom-up proteomics consists of the treatment of proteins with an enzyme resulting in peptides which are then analyzed using MS. Most bottom-up proteomics experiments use

---

This dissertation follows the style of *Analytical Chemistry*.

trypsin as the proteolytic enzyme for reasons such as: (i) specific C-terminal cleavage after arginine and lysine residues which provides a basic amino acid residue to be the potential charge carrying site, (ii) tryptic peptides typically have a mass in the range of 700-3000Da which takes advantage of the sensitivity and resolution capabilities of modern mass spectrometers, (iii) *a priori* knowledge of the C-terminal amino acid assists in tandem MS interpretation and database searching and (iv) trypsin activity is optimal at neutral pH values where proteins are typically the most stable.

Peptides are typically analyzed to determine their mass-to-charge (m/z) value and those values are then submitted to a database search to obtain protein identification and amino acid sequence coverage. Using accurate mass measurement to obtain protein identification is commonly referred to as 'peptide mass mapping' where the m/z information is used to map the peptides to a specific protein. To increase the confidence of protein assignments obtained from peptide mass mapping, researchers have utilized tandem mass spectrometry (MS/MS) to obtain peptide sequence information.[6] The most common types of tandem MS experiments are performed such that peptide ions collide with a neutral gas to fragment the peptide into smaller components. The fragment ions are then used to determine the amino acid sequence composition of the peptide. These tandem MS spectra can then be subjected to database searching to identify the fragmented peptide sequence and assign a corresponding protein based on user-defined parameters. When peptides are analyzed from a protein with an unsequenced genome, protein sequence homology can be used to identify proteins based on other organisms or

de novo sequencing is used to empirically determine the peptide sequence which is typically performed by manual interpretation of the spectrum.

Opposite to bottom-up, top-down proteomic experiments analyze intact proteins to determine protein molecular weight based on the mass-to-charge ratio followed by fragmentation of the intact protein to get amino acid sequence information for regions of the protein.[7] Advantages of top-down experiments include; (i) direct analysis of a protein of interest, (ii) large fragments can result allowing for greater amino acid sequence coverage, and (iii) post-translational modifications can be determined without the need for enrichment.[8] However, several challenges are present in these experiments such as the need for pure, isolated proteins, high concentrations are required, and there is a lack of available databases to search resulting data. These limitations have led the majority of researchers to rely primarily on the bottom-up approach. Regardless of the method of choice, both methods have proven to be useful for proteomic studies and have also been shown to be complimentary for characterization of proteins, confirmation of amino acid sequences and determination of post-translational modifications, among other analyses.[9-12]

PRE-FRACTIONATION FOR PROTEOMIC STUDIES

The excellent sensitivity, mass resolution and dynamic range capabilities of most commercial mass spectrometers provide an easier means to studying the proteome. However, the extreme complexity and dynamic range of such samples still gives rise to several challenges. For reference, the protein concentration in human plasma has been

estimated to span more than ten orders of magnitude far exceeding the capabilities of modern mass spectrometers.[1] To mediate this, sample handling measures must be taken prior to MS analysis to reduce the complexity of proteomic samples. Several techniques have been successfully utilized to decrease sample complexity including chromatographic and electrophoretic methods. [13] Chromatographic separations rely on interactions of analytes with a stationary phase. The most commonly used chromatographic techniques for MS-based proteomic studies are reversed phase liquid chromatography (RPLC or LC), and ion-exchange chromatography such as strong cation exchange (SCX). Some of the advantages of using chromatographic separation methods include: (i) high column loading capacity and (ii) high peak capacity. However, features such as the high load capacity, high salt concentration used and the limited peak capacity can also become limitations when trying to analyze extremely complex mixtures leading to the coupling of different chromatographic and/or electrophoretic techniques.[14]

MULTI-DIMENSIONAL PROTEIN IDENTIFICATION TEHCHNOLOGY

One of the most utilized techniques for bottom-up proteomic studies was introduced by Yates and coworkers[15] termed 'multi-dimensional protein identification' (MudPIT) Technology. MudPIT takes advantage of a two-dimensional chromatographic separation prior to MS analysis. Proteolytically derived peptides are initially subjected to a charge-based separation using SCX, followed by a reversed phase liquid chromatographic separation. Eluent from the second separation is then directly subjected to ESI-MS and MS/MS analysis. In the initial work performed in the Yates

lab, 1484 yeast proteins were identified using this method. Since then, several groups have also reported significant numbers of protein identifications using this method[16] including the analysis of protein and peptide phosphorylation.[17] Additionally, several variant methods have been described such as high and low pH reversed phase LC,[18, 19] hydrophilic interaction LC (HILIC) - reversed phase LC[20] and gel electrophoresis – LC (referred to as GeLC) followed by MS analysis.[21, 22] This general experimental approach (separate peptides followed by MS) is typically referred to as 'shotgun proteomics' as a means to identify as many peptides and proteins from a sample without a specific target.[23]

ELECTROPHORETIC SEPARATIONS

In addition to chromatographic methods, several electrophoretic separation techniques have also been used to fractionation both peptides and proteins. The most commonly used techniques are sodium dodecylsulfate – polyacrylamide gel electrophoresis (SDS-PAGE) for size based separations and two-dimensional gel electrophoresis (2D-GE) which incorporates isoelectric point (pI)-based separation using isoelectric focusing (IEF) in the first dimension followed by size-based (SDS-PAGE) separation in the second dimension.[24] Many researchers prefer an experimental platform that utilizes 1D or 2D-GE followed by excision of each protein band (or entire gel lanes) and tryptic digestion.[25] The resulting peptides are then subjected to MS analysis or are separated using LC (GeLC) prior to MS analysis. Although this experimental platform has resulted in several successful experiments, limitations to the method are

prevalent such as; (i) the need for extensive sample handling, (ii) limited sample load capabilities and (iii) the need for automation for high-throughput analyses. Additionally, researchers are limited to studying proteins at the peptide level since proteolytic digestion is required to release the protein from the gel matrix. Recently, molecular weight-based separations were carried out in tubular gels and were coupled with solution-based recovery for proteomic studies. This method is called gel-eluted liquid fraction entrapment electrophoresis (GELFrEE).[26] The GELFrEE approach allows for protein-based separations but does not require proteolytic digestion for downstream processing. In fact, the GELFrEE method has been shown to be advantageous for first dimensional protein separation followed by pI-based separations and also for top-down proteomic applications.[27-29]

ISOELECTRIC FOCUSING (IEF)

Isoelectric focusing (IEF) is the separation of ampholytic molecules based on their isoelectric point (pI) in the presence of small ampholytic molecules called carrier ampholytes. The pI values of carrier ampholytes span a large pH range, provide high buffering capacity at their pI values and their solutions have low conductivity.[30] In a typical IEF experiment, the protein or peptide sample is mixed with carrier ampholytes (composed of poly(amino)-poly(carboxylic acid) molecules) and upon application of an electric field, the carrier ampholytes and proteins and/or peptides migrate until becoming focused at a point where the pH of the solution equals their respective pI value. It has been estimated that over 1000 different species of carrier ampholytes are present in each

pH unit interval. [31, 32] Therefore, a continuous, linear, pH-gradient is formed between the two electrodes and any migration away from the 'focusing point' will result in recharging of the molecule which in turn results in electrophoretic migration back to the focusing position again.

IEF can be carried out in a variety of formats such as in a capillary, on a gel slab, on beads, in strips or in a segmented device termed a multicompartment electrolyzer (MCE).[33-37] Until recently, the majority of IEF was carried on in a capillary (termed capillary isoelectric focusing (cIEF)), or on strips where acrylamido weak acids and bases (Immobilines) were co-polymerized with acrylamide and bisacrylamide to create an immobilized pH gradient across the strip.[35, 36] These immobilized pH gradients (IPG's) provided the breakthrough technology for two-dimensional gel electrophoresis (2D-GE) and the majority of early mass spectrometry-based proteomics relied on this advancement for the study of complex protein mixtures.[38, 39] Although the use of cIEF and IPGs both provide a means for pI-based separations, several limitations are also present. In cIEF, once ampholytes are focused, an external force (i.e., pressure) is required to pass the ampholytes across the detector and secondly, the carrier ampholytes must be removed prior to further investigation using mass spectrometry. IPGs clearly started a new paradigm for proteomics; however, their low sample capacity, protein precipitation at or near the pI and slow separation times all hinder the use of this approach.

Of particular interest to this work are pI-based separation techniques performed in MCEs. In a typical MCE setup, each well is separated by a semi-permeable buffering

membrane (Figure 1). Hydrogel buffering membranes with covalently attached weak acids and bases are used and have been formed from agarose,[40] acrylamide[36] and poly(vinyl alcohol)[41-44] with the latter being more stable because of resistance to hydrolysis at high and low pH values. By changing the ratio of concentration (and pKa value) of the weak acid and base, buffering membranes can be synthesized to cover a broad pH range.

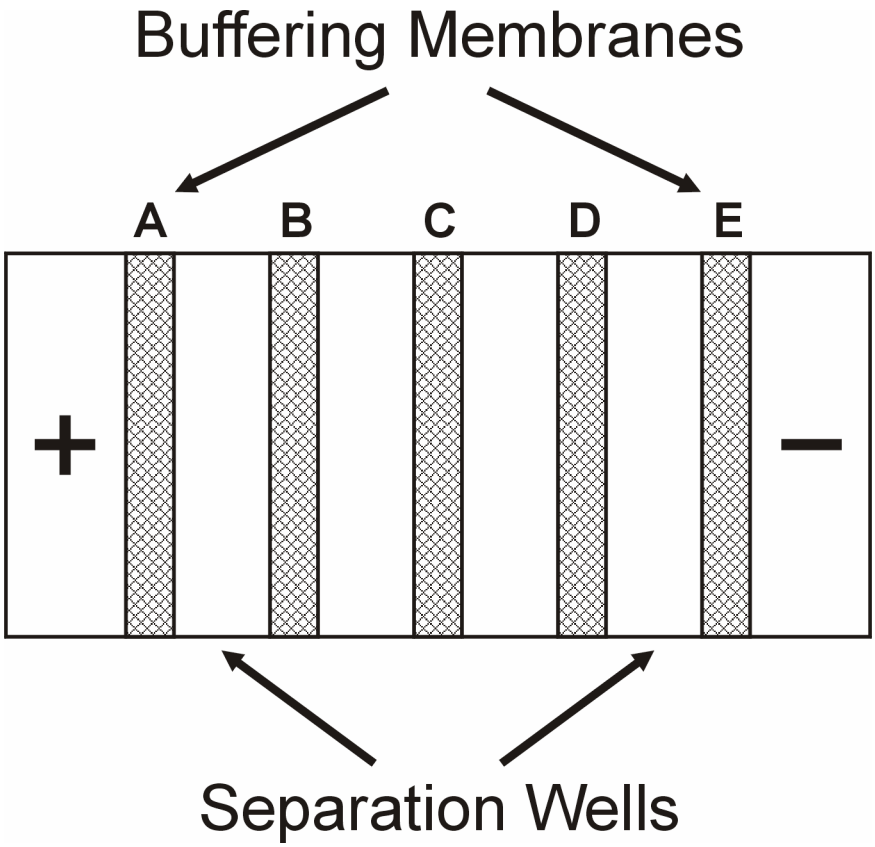

Figure 1. General schematic of a typical multicompartment electrolyzer. Components include anode (+) and cathode (-) compartments, separation wells (white) and buffering membranes (checkered, labeled A-E) whose pH increases from left to right.

Several small scale IEF devices have been described and are commercially available. The most common include the Zoom IEF Fractionator (Invitrogen), the microRotofor (Bio-Rad), the digital ProteomeChip Fractionator (Cell Biosciences) and the OFFGEL^{TM} Fractionator (Agilent). In addition, several in-house devices have also been described. [45-47] Of the commercially available devices, the Agilent OFFGEL^{TM} system has been the most promising for mass spectrometry-based proteomic studies. The OFFGEL^{TM} uses an IPG gel strip onto which small cups are placed to form the compartments. In the commercial format, either 12 or 24 cups can be used to make separation compartments that hold ~300 μL of solution. The OFFGEL^{TM} was first introduced by Ros and coworkers[48] and a cartoon schematic of the concept is depicted in Figure 2**.**

The OFFGEL^{TM} Fractionator was initially used for protein purification and separation of an *Escherichia coli* lysate.[48, 49] Since, several researchers have reported separation of protein mixtures,[50] peptide mixtures[51] and have shown that very small protein amounts (ca. 10 μg) can be digested and fractionated followed by MS analysis resulting in a large number of identified proteins.[52] Although the OFFGEL system has proven to be an advantageous fractionation tool, several limitations are associated with the technology. Namely, (i) separation times are typically very long (typically 12-24 hours), (ii) carrier ampholytes are added to the sample solutions so cleanup is needed prior to MS analysis and (iii) IPG strips are synthesized with defined pH ranges limiting the ability to customize the experiment.

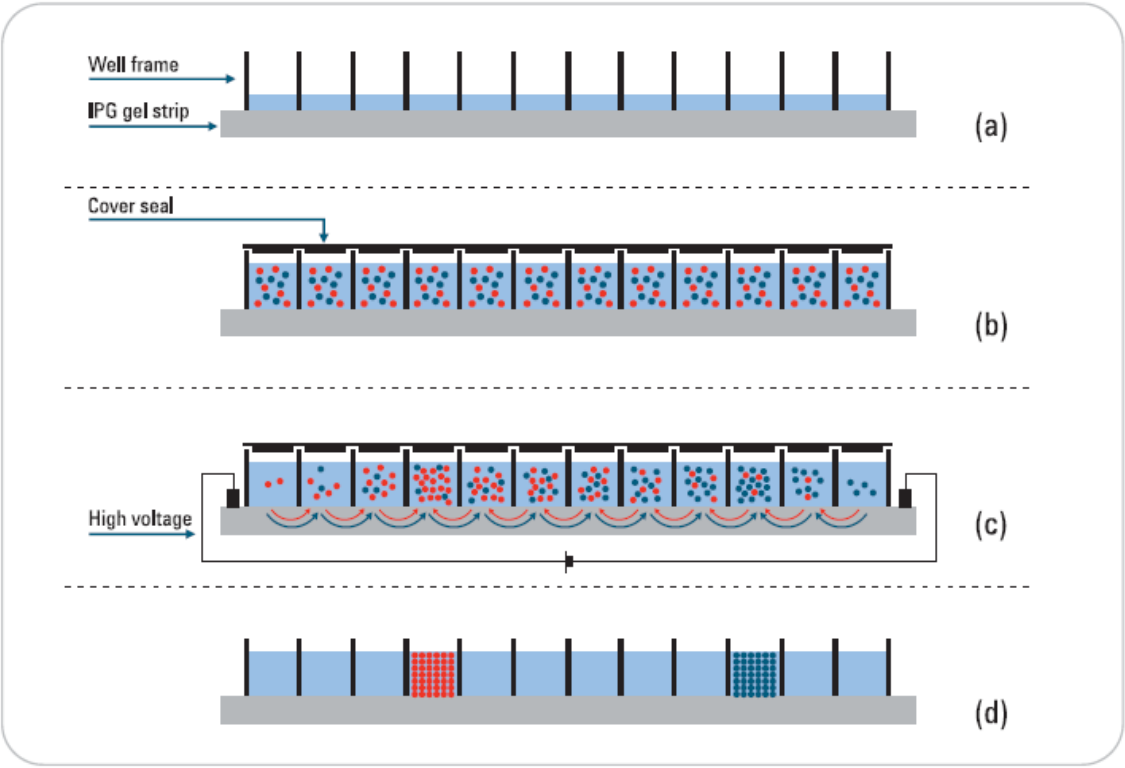

Figure 2. Schematic of the OFFGEL™ separation principle. Small cups are placed over an IPG strip with a given pH range (a) the peptide or protein solution is loaded into the cups and voltage is applied for pI-based separation (b). Peptides or proteins migrate through the IPG strip (c) and are retained in solution following separation (d). (Adapted from www.agilent.com)

ISOELECTRIC TRAPPING (IET)

The separation of analytes based on pI performed in MCEs without carrier ampholytes is termed isoelectric trapping (IET). In IET, ampholytic components are separated and trapped using buffering membranes that create a step-wise pH gradient.

Specifically, consider a mixture of two ampholytes of pI 10 and pI 4 in a solution whose pH is buffered to 7. At pH 7, the solution pH is less than the pI of the pI 10 component therefore, the ampholyte is cationic. Conversely, since the pH of the solution is greater than the pI of the pI 4 component, it is anionic. Therefore, in an electric field, the pI 10 ampholyte will migrate towards the cathode and the pI 4 ampholyte will migrate towards the anode compartment. A schematic of this is provided in Figure 3A. During the migration of the ampholytic components, they will approach a buffering membrane. It is at this interface that the ampholyte will be titrated. When the anionic components (pI 4 ampholyte) experiences a membrane environment that buffers at a lower pH, the ampholyte becomes titrated and therefore becomes positively charged and starts to migrate towards the cathode. Upon experiencing a buffering membrane environment with a pH higher than its pI value, the ampholyte is titrated to become negatively charged again. A similar situation would be observed with the pI 10 component. Therefore, trapping occurs by constant titration occurring at the buffering membranes as represented in Figure 3B.

In order to assists in buffering and maintaining proteins and peptides in solution, a concept termed pH-biased IET has been described.[53] Typical pH-biased experiments utilize small ampholytic molecules (such as amino acids) that buffer at their isoelectric points serving two purposes. First, charge and pH are maintained within a compartment

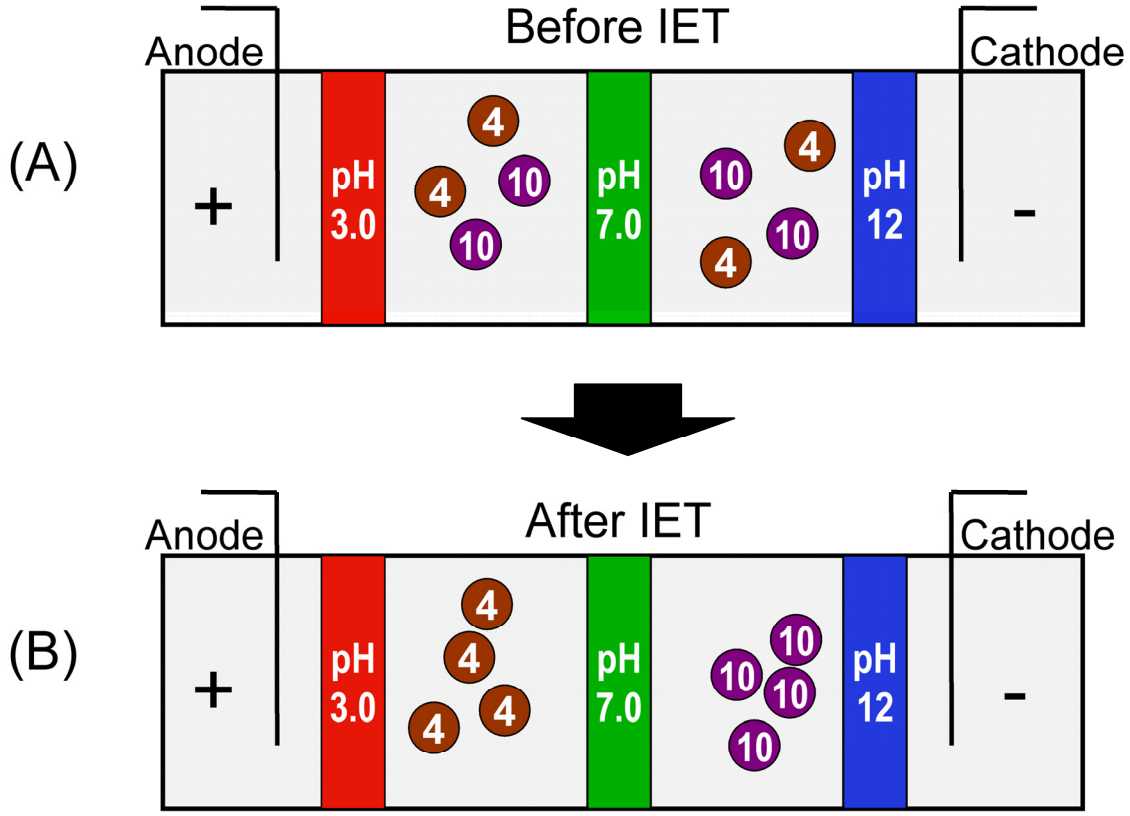

Figure 3. Demonstration of the concept of isoelectric trapping (IET). A mixture of ampholytic components is placed in the separation wells of a multicompartment electrolyzer. Upon applying a voltage, the ampholytes will migrate until they reach a well in which their pI falls between the pH values of the two buffering membranes.

of the MCE reducing protein precipitation that is known to occur near the protein pI [54] and secondly, since the buffers are 'isoelectric' the conductivity of the solution in the well is relatively low allowing for high field strengths to be applied across the well and/or device. Using isoelectric buffers during IET also eliminates the need for sample cleanup prior to MS analysis which is often required when using carrier ampholytes for traditional IEF separations.

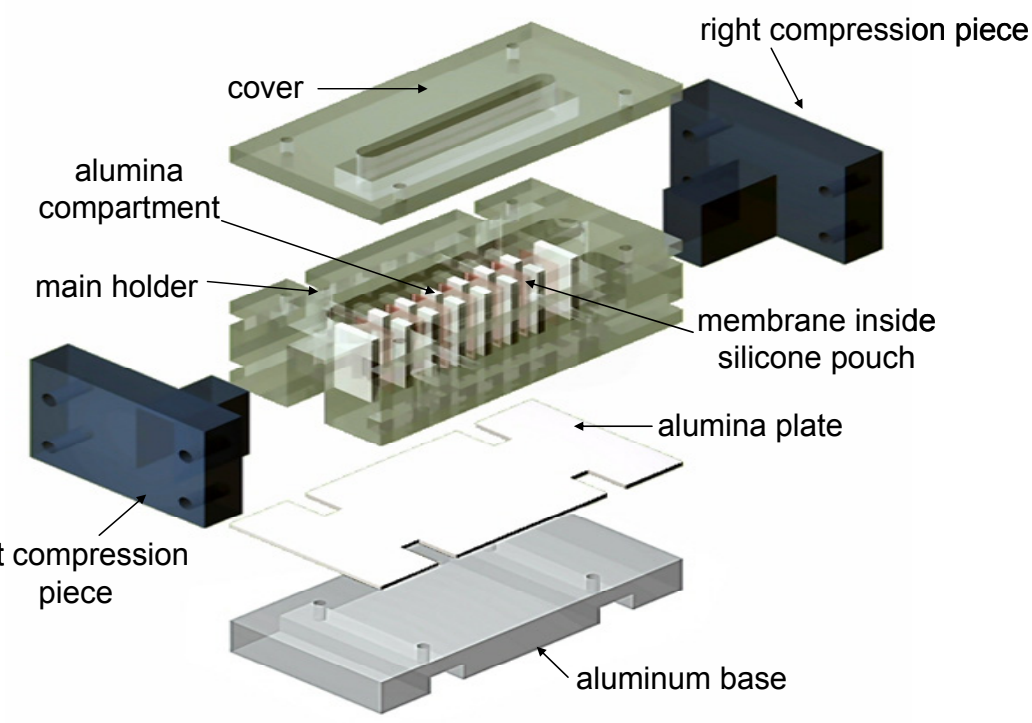

Figure 4. Expanded view of the MSWIFT device. Major features of the device include the aluminum base, alumina plate and separation wells, the main holder, the compression pieces and the silicone pouches which hold the buffering membranes. Once assembled, the MSWIFT device can contain up to 20 separation wells to quickly separate ampholytic species.

MEMBRANE SEPARATED WELLS FOR ISOELECTRIC FOCUSING AND TRAPPING (MSWIFT)

Recently, a new IET device termed membrane separated wells for isoelectric focusing and trapping (MSWIFT) was introduced by Lim and coworkers.[55, 56] The MSWIFT device can be assembled to contain between 2-20 separation compartments and was designed to overcome some of the limitations associated commercial devices. An expanded view drawing of the MSWIFT device is provided in Figure 4. The major components of the device include the main housing, compression pieces and cover fabricated from polycarbonate, the alumina separation compartments and plates, silicone pouches which hold the pH-buffering membranes, and the aluminum base which serves as a heat sink.

The MSWIFT was designed and manufactured to overcome some of the limitations associated with the currently available commercial devices such as; (i) help with the removal of Joule heat owing to the material and design of the compartment and the aluminum heat sink, (ii) short anode to cathode distances as well as inter-membrane distances which allow for application of high field strengths, and (iii) a high sample load capacity. Initial proof-of-concept experiments were performed to illustrate the desalting capabilities, isolation of major and minor components from a reaction mixture, and fractionation of a protein mixture using the MSWIFT device. [56]

The goal of this work is to further expand upon the initial applications performed using MSWIFT, and to separate and analyze more complex mixtures while incorporating MS analysis to develop an experimental platform for proteomic studies.

The included studies fall into four categories: (i) proof-of-concept experiments illustrating MSWIFT fractionation followed by MS and LC-MS/MS analysis for increasingly complex mixtures, (ii) introduction of a multi-stage fractionation scheme coupled with LC-MS/MS for the proteomic analysis of the model fungus *Neurospora crassa*, (iii) development of a new sample preparation method using histidine as a sample buffer, proteolytic digestion buffer and compatible buffer for rapid electrophoretic separations and (iv) implementation of the histidine buffering system for MSWIFT fractionation followed by CE-MS analysis to maximize informational content in proteomic studies. The experiments described within were all performed using the bottom-up proteomics approach which allowed quick separation of peptides (Scheme 1).

Scheme 1. Experimental workflow for bottom-up proteomic studies using MSWIFT fractionation. Isolated proteins or protein mixtures are subjected to proteolytic cleavage (typically using trypsin) resulting in small peptides. The peptides are subjected to pI-based fractionation using the MSWIFT device and the solutions from each separation well are then separated and analyzed using LC-MS/MS followed by database searching to identify peptides and proteins.

Some advantages of using the bottom-up proteomics method include ease of sample handling (overcoming protein solubility and quantitation limitations was not required), high resolution separations in which theoretical pI values can be accurately calculated and used for validation (compared to estimated values calculated for proteins) and fractions obtained following MSWIFT fractionation could be directly coupled with MS and LC-MS/MS analysis. We utilize MALDI mass spectrometry for the work described within because it leads to predominantly singly charged ions facilitating easy interpretation of the collected mass spectra. While these experiments incorporate peptide-based separations and MALDI mass spectrometry, these are not a limitation to the device or the technique. Solutions obtained from MSWIFT fractionation could easily be coupled with ESI mass spectrometry or LC-ESI-MS/MS. Additionally, proteins could be separated using the MSWIFT device followed by proteolytic digestion and LC-MS/MS analysis or peptide-based MSWIFT fractionation and LC-MS/MS analysis. While we demonstrate compatibility with reversed phase LC and capillary electrophoresis, it is viable to consider coupling MSWIFT fractionation with a variety of other separation methods such as SCX, affinity chromatography, or gel electrophoresis to maximize the information content of proteomic experiments and to increase the number of identified proteins.

CHAPTER II

COMBINING ISOELECTRIC POINT-BASED FRACTIONATION, LIQUID CHROMATOGRAPHY AND MASS SPECTROMETRY TO IMPROVE PEPTIDE DETECTION AND PROTEIN IDENTIFICATION*

INTRODUCTION

Sample pre-fractionation techniques are widely used to decrease the complexity of proteomic samples prior to liquid chromatographic and tandem mass spectrometric (LC-MS/MS) analysis.[13] Isoelectric focusing (IEF) separations of ampholytic compounds such as peptides or proteins based on differences in isoelectric point (pI) [57, 58] is becoming increasingly useful for many different types of mass spectrometry (MS)-based proteomics.[39, 59, 60] Early MS-based proteomics utilized two-dimensional gel electrophoresis (2D-GE); [33, 61] however, IEF also can be achieved in gel matrices, capillaries, and multi-compartment electrolyzers (MCE's). Although considerable improvements have been made in 2D-GE, [38, 62, 63] there are significant problems associated with the technology,[64] specifically 2D-GE performs poorly for very large and small proteins, hydrophobic proteins, and proteins with extremely acidic or basic pI values. Furthermore, proteomic studies based on the coupling of gel electrophoresis and

---

*Reprinted from Journal of the American Society for Mass Spectrometry, Cologna, S.M., *et. al.,* Combining Isoelectric Point-Based Fractionation, Liquid Chromatography and Mass Spectrometry to Improve Peptide Detection and Protein Identification, Copyright (2010), with permission from Elsevier.

mass spectrometry are labor intensive. To circumvent these limitations, alternative IEF methods such as analytical scale MCE's have been developed and combined successfully with MS for proteomic applications.[48, 50, 65-70] Pre-fractionation devices based on solution IEF enhance several key aspects of the analysis, *e.g.,* (i) they increase the dynamic range owing to a partitioning of high and low abundance species across multiple fractions and (ii) increase the sample loading capability because analyte incorporation into a gel matrix is not required. In addition, separations can be performed in a few hours and analytes are captured and retained in the solution phase.[71] On the other hand, a significant limitation of solution IEF is the increased sample handling required to remove carrier ampholytes prior to MS analysis.

An alternative carrier ampholyte-free pI-based separation method called isoelectric trapping (IET) has been described.[65, 72, 73] IET uses buffering membranes to create a step-wise pH gradient, thereby establishing a series of separation wells bracketed by membranes with well-defined pH values. In IET, proteins or peptides migrate under the influence of an electric field until the individual components reach a compartment in which the pH values of the buffering membranes bracket the pI value of the analyte. In order to reduce protein precipitation, which can occur near or at the isoelectric point,[54] the individual compartments can be buffered using small ampholytic molecules, *e.g.,* amino acids.[53] These buffering molecules do not interfere with MS analysis such as matrix assisted laser desorption/ionization (MALDI) owing to their low molecular weights which fall below the m/z range of interest.

Lim and coworkers developed an IET device termed membrane separated wells for isoelectric focusing and trapping (MSWIFT).[56] The primary advantages of the MSWIFT device for MS-based proteomics include (i) small volume wells (~200 μl), (ii) tunable membranes that cover a wide pH range (pH 2-12), (iii) option for the taking of a large number of fractions, (iv) absence of sample cleanup after IET and (v) membrane compatibility with both aqueous and organic solvent systems. They demonstrated the utility of MSWIFT for separation and concentration of ampholytes while minimizing the detrimental effects associated with fast electrophoretic techniques, *i.e.,* Joule heating and sample overloading. Preliminary experiments from their work include demonstration of desalting capabilities, enrichment of a minor component from a synthetic mixture and fractionation of egg white proteins, which has implications for proteomics experiments. For comparison, one of the most highly utilized pI-based separation devices for proteomic studies is the OFFGEL^{TM} Fractionator (Agilent Technologies). Much of the work on the OFFGEL^{TM} device has been centered on peptide separations followed by MS analysis. Samples including cerebral spinal fluid,[74] brain tissue [75] and yeast [52, 76] have been analyzed and quantitative studies incorporating Itraq labeling have been reported.[77, 78] The OFFGEL^{TM} is an attractive device for peptide fractionation considering its multiplexing abilities – running several strips simultaneously, small sample volume and low sample quantity requirements. However, several inherent limitations are associated with the technology such as long separation times, sample cleanup requirements, the need for an insulated cooling system and a lack in the ability to customize the number of wells or pH ranges. These restrictions however, are not

associated with using the MSWIFT device. Several proof-of-concept experiments, specifically focused on bottom-up proteomics are included here to illustrate the compatibility and advantages of using MSWIFT as a pre-fractionation device for mass spectrometry-based studies.

EXPERIMENTAL SECTION

Chemicals were obtained from Sigma (St. Louis, MO), unless noted otherwise. HPLC grade acetonitrile was purchased from EMD Chemicals, Inc. (Gibbstown, NJ). Peptide standards from American Peptide Company (Sunnyvale, CA) were used without further purification. All experiments were performed using purified 18 MΩ water (Barnstead International, Dubuque, IA).

Membrane Separated Wells for Isoelectric Focusing and Trapping (MSWIFT)

The design and assembly of MSWIFT have been previously described.[55, 56] Briefly, the main housing of MSWIFT was built using polycarbonate and equipped with an aluminum heat sink. Poly(vinyl-alcohol) based buffering membranes with tunable pH values were synthesized in-house.[41-44] A cartoon representation of the MSWIFT assembly is displayed in Figure 5**.** Features include the anode and cathode compartments, variable number of separation wells and buffering membranes

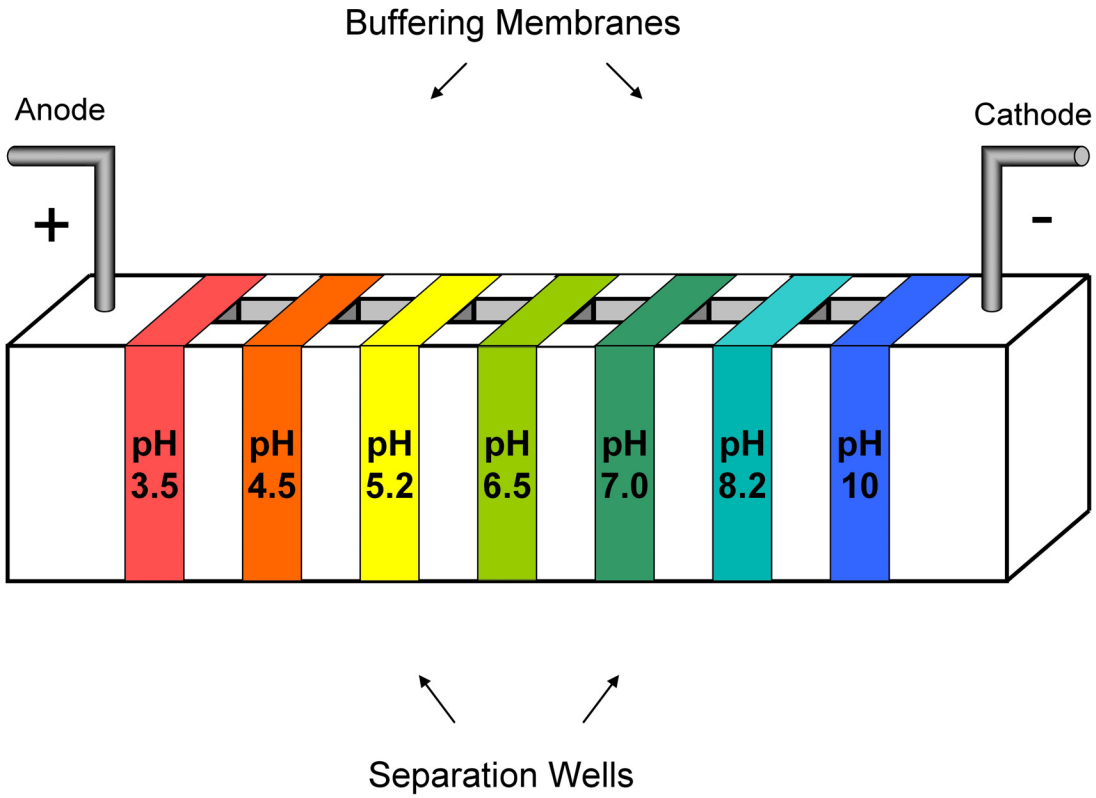

Figure 5. Cartoon schematic of MSWIFT assembly including anode and cathode compartments, separation wells and buffering membranes. The number of separation wells and pH values of buffering membranes can be tailored for each experiment.

IET

Alumina separation wells were assembled serially and buffering membranes were inserted into silicone pouches in between each well. The wells were filled with 200µL of either the peptide sample solution and/or an isoelectric buffer. The anode solution was 3 mM methanesulfonic acid, and the cathode solution was 3 mM sodium hydroxide. Compartment solutions were pH biased by ampholytic buffers as previously

described.[53] Typical separation times ranged from 45-60 minutes at 5W constant power. Theoretical pI values were calculated using the compute pI/MW tool from ExPASy.[79]

IET of a Five Peptide Mixture

The five peptides, leptin (93-105) (NVIQISNDLENLR, pI 4.4), angiotensin II (DRVYIHPF, pI 6.7), angiotensin I (DRVYIHPFHL, pI 6.9), angiotensin III (RVYIHPF, pI 8.8) and bradykinin fragment 1-7 (RPPGFSP, pI 9.8) were mixed to final concentrations of 0.05 mg mL^{-1} for leptin and bradykinin and 0.025 mg mL^{-1} for the angiotensin peptides. The pH values of the five buffering membranes were 2.9, 5.4, 7.6, 9.0 and 11.0. The peptide mixture was loaded in the fourth separation well bracketed by pH 9.0 and 12.0 membranes then separated. After fractionation, an aliquot from each separation well was analyzed using MALDI-MS.

Proteolytic Digestion and IET of a Five Protein Mixture

A protein mixture containing bovine α-casein, bovine serum albumin, bovine apo-transferrin, bovine ribonuclease A and horse cytochrome c (10 μg each) was prepared in 50 mM ammonium bicarbonate buffer, pH 8. The protein mixture was reduced by adding dithiothreitol to a final concentration of 5 mM followed by incubation at 60 °C for 1 hour. Alkylation was performed by adding methane methylthiosulfonate (MMTS) (20 mM final concentration) and the solution was incubated at room temperature for 10 minutes. Trypsin (Promega Corp., Madison, WI) was added at an enzyme to protein ratio of 1:50 (w/w) and digestion was carried out at 37 °C overnight.

The resulting peptides were loaded into the second separation well of MSWIFT (bracketed by pH 4.5-5.4 membranes) and subjected to IET separation. The pH values of all the membranes were as follows: 2.0, 4.5, 5.4, 6.5, 7.6, 8.2 and 12.0. Following separation, MALDI-MS analysis was performed using an aliquot obtained from each fraction.

Isolation, Proteolytic Digestion and Separation of Escherichia coli *Peptides*

70S ribosomes were isolated from *E. coli* as previously described.[80] Ribosomal RNA was removed by acid precipitation (1% TFA) followed by centrifugation at 14,000 rpm x 10 minutes. The supernatant containing 100 µg soluble proteins was diluted in 100 mM triethyl ammonium bicarbonate buffer pH 8. The proteins were denatured thermally at 90 °C for ten minutes then quenched by freezing. Trypsin was added at a 1:50 enzyme:protein ratio and digestion was carried out by incubation at 37 °C overnight. The pH values of the buffering membranes used for this separation were: 2.0, 4.5, 5.4, 6.5, 7.6, 8.2, and 12.0. For comparison, an aliquot from the digestion stock, aliquots from each fraction were analyzed using MALDI-MS/MS. Additionally, an aliquot from each fraction was subjected to reversed phase liquid chromatography (LC) MALDI-MS/MS analysis via a robotic spotting device as previously described.[81]

Proteolytic Digestion, IET and LC-MS/MS Analysis of Yeast Lysate

Soluble yeast proteins (*Saccharomyces cerevisiae*) were prepared in 100 mM 3-morpholinopropane sulfonic acid (MOPS), 100 mM sodium chloride, 5 mM

ethylenediaminetetraacetic acid (EDTA) with protease inhibitors. Protein concentrations were determined using the Bradford Assay.[82] A total of 180 μg of protein was reduced using tris-(2-carboxyethyl) phosphine at a final concentration of 5 mM and incubated at 60 °C for 1 hour. Alkylation using MMTS and trypsin digestion were carried out as outlined for the five-protein mixture. The pH values of the membranes were as follows: 2.0, 4.7, 5.4, 6.5, 7.0, 8.2 and 12.0. The sample was loaded in the fourth separation well (bracketed by pH 6.5-7.0 membranes) and IET was carried out. Following separation, an aliquot from each compartment solution was subjected to LC-MS/MS analysis. In the two-stage MSWIFT separation of yeast peptides, an additional 200 μg of yeast was digested as above and fractionated. The pH values of the buffering membranes were: 2.9, 4.0, 5.4, 6.8, 7.5, 9.8 and 11.0 (1^{st} stage) and 4.0, 4.5, 5.0 and 5.4 (2^{nd} stage). An aliquot of the contents of the pH 4.0-5.4 well in the first dimension separation were analyzed using LC-MS/MS then the remaining solution was subjected to further IET fractionation followed by LC-MS/MS analysis.

MALDI – MS and Database Searching

Samples (excluding yeast) were mixed 1:1 (v/v) with the MALDI matrix (5 mg mL^{-1} α-cyano-4-hydroxycinnamic acid, 50% (v/v) acetonitrile, 10 mM ammonium dihydrogen phosphate, 0.1% trifluoroacetic acid) and 1 μL of the resulting mixture was spotted onto a MALDI target. MALDI mass spectra were acquired using either a Voyager DE-STR, Model 4700 or 4800 Proteomics Analyzer (Applied Biosystems, Framingham, MA). Collision-induced dissociation (CID) spectra were acquired using

air as the collision gas (medium pressure setting) and at 1 kV of collision energy. Tandem MS data collected for the five-protein mixture, ribosomal protein digest and yeast lysate experiments were analyzed using the GPS Explorer Software (Applied Biosystems, Framingham, MA) and an in-house license of the search engine MASCOT (v. 2.1).[83] The five-protein mixture data and ribosomal protein digest data were searched against the Swiss-Prot database with the following search parameters: taxonomy, metazoa/*E.coli*; enzyme, trypsin; missed cleavages, 1; variable modifications, oxidation (M) and MMTS I (five protein mix only).

Data collected from the yeast separation experiment were searched against the *Saccharomyces* Genome Database (www.yeastgenome.org, downloaded March 4, 2010, 6717 sequences) with the following parameters: precursor tolerance, 100 ppm; fragment ion tolerance, 0.8Da; enzyme: trypsin; missed cleavages, 1; and variable modifications, oxidation (M) and MMTS I. Protein assignments were made using a minimum of two peptides and a score of 21 ($p<0.05$) determined by MASCOT. For reference, a table is provided of the top 989 protein assignments (99.990% confidence interval, 2 peptide minimum) which includes the 593 identifications obtained from the MASCOT search (APPENDIX A). The same criteria were used for protein identifications in the two-stage separation experiment. Data reporting peptide assignments (two-stage experiment) included all matched peptides without implementing an ion score cut-off.

RESULTS AND DISCUSSION

Lim and coworkers previously reported proof-of-concept analyte fractionation experiments for a variety of different analytes, ranging from small molecules to egg white proteins. Here, we focus on developing applications of MSWIFT-MALDI-MS for protein identification using 'bottom-up' techniques. For example, MSWIFT provides an ideal option for bottom-up proteomics for peptide-based fractionation followed by MS, MS/MS and/or reversed phase LC-MS/MS analysis owing to the flexibility in arrangement and operation of the device. Oftentimes, the analysis of minor components or even major components that do not ionize well by MALDI or ESI in complex mixtures is severely limited, and a rapid, reproducible fractionation technique can be used to circumvent such problems. Several proof-of-concept experiments, specifically focused on bottom-up proteomics are included to illustrate the compatibility and advantages of using MSWIFT as a pre-fractionation device.

Fractionating a mixture of peptides having very different pI values illustrates the basic operation of the device. A mixture composed of five standard peptides, leptin (pI 4.4), angiotensin II (pI 6.7), angiotensin I (pI 6.9), angiotensin III (pI 8.8) and bradykinin 1-7 (pI 9.8) was analyzed using MALDI-MS before and after fractionation. Note, that a signal for the $[M + H]^+$ ion of leptin (m/z 1527.81) is not observed in the MALDI spectrum of the mixture (Figure 6), possibly owing to analyte suppression effects. [84] This same peptide mixture was then fractionated using MSWIFT under conditions where individual peptides should be trapped in wells in which buffering membranes bracket the

pI value of each peptide. The pI values for angiotensin II and angiotensin I peptides are similar (6.7 and 6.9, respectively).

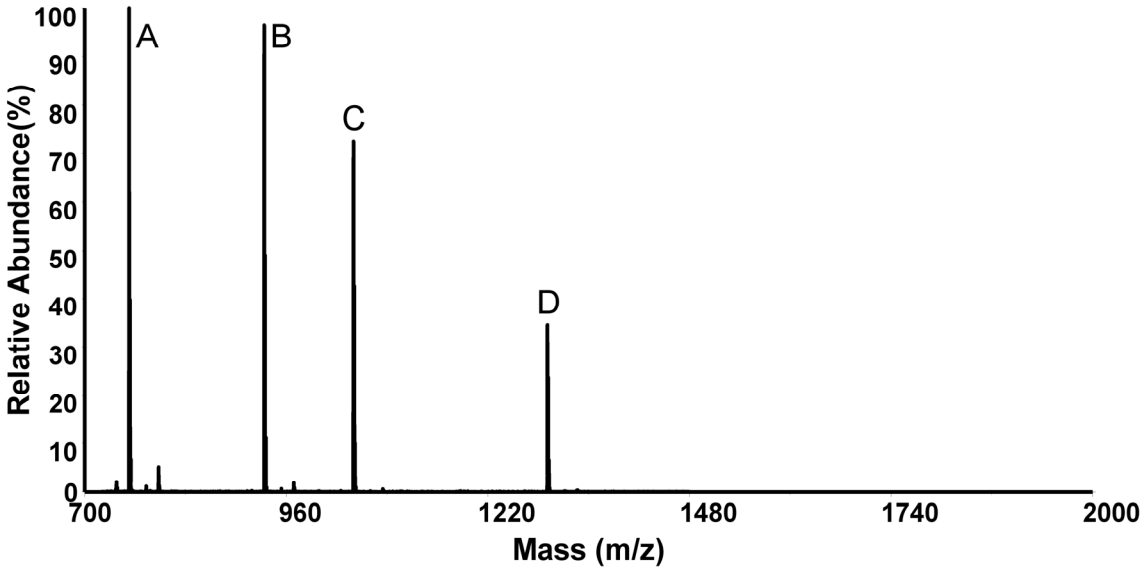

Figure 6. MALDI mass spectrum of a mixture of five peptides before separation. The mixture contains (A) Bradykinin 1-7 (pI 9.8, $[M+H]^{+}_{obs}$ = 757.39 Da), (B) Angiotensin III (pI 8.8, $[M+H]^{+}_{obs}$ = 931.54 Da), (C) Angiotensin II (pI 6.7, $[M+H]^{+}_{obs}$ = 1046.58 Da), (D) Angiotensin I (pI 6.9, $[M+H]^{+}_{obs}$ = 1296.75 Da). Each ion signal is labeled with the appropriate peptide with the exception of Leptin (pI 4.4, $[M+H]^{+}_{calc}$ = 1527.81 Da) which is not observed.

Thus these two peptides should be trapped in the same compartment. Following fractionation, an aliquot from each fraction was analyzed by MALDI-MS. Figure 7(A-D) contains the MALDI mass spectra for each of the wells which are defined by pH buffering membranes: pH 2.9-5.4 (2B), pH 5.4-7.6 (2C), pH 7.6-9.0 (2D) and pH 9.0-12.0 (2E). Each of the standard peptides is observed in the predicted well based on the

calculated pI values of the peptides and the pH values of the buffering membranes used. In Figure 7E (pH 9.0-12.0), a low abundance signal (< 5% relative abundance to the bradykinin signal) at m/z 931.68 is also observed and corresponds to the $[M + H]^+$ ion of angiotensin III (pI 8.8), which may indicate a slightly insufficient electrophoresis time.

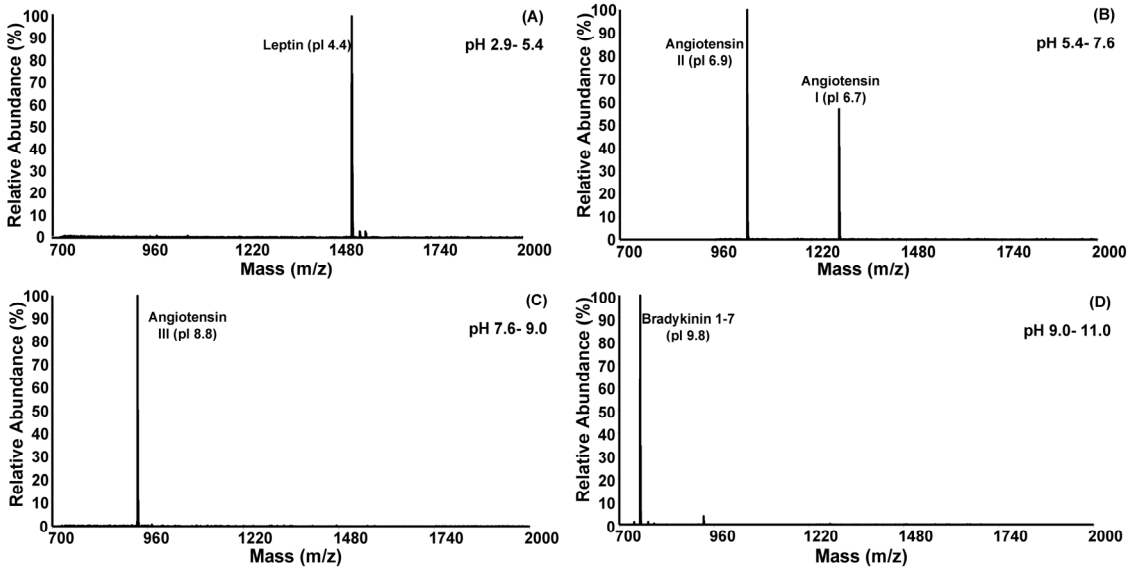

Figure 7. (A-D)MALDI mass spectra taken from an aliquot of each separation well following IET using MSWIFT. The pH values of the buffering membranes used are indicated in each spectrum. Peptide ion signals are labeled as follows: Leptin (pI 4.4, $[M+H]^+_{obs}$ = 1527.99 Da) (A), Angiotensin II (pI 6.7, $[M+H]^+_{obs}$ = 1046.68 Da), Angiotensin I (pI 6.9, $[M+H]^+_{obs}$ = 1296.88 Da) (B), Angiotensin III (pI 8.8, $[M+H]^+_{obs}$ = 931.66 Da) (C), Bradykinin 1-7 (pI 9.8, $[M+H]^+_{obs}$ = 757.50 Da) (D).

On the basis of these experiments we conclude that the MSWIFT device is capable of separating ampholytic components (*i.e.,* peptides) where the resulting fractions can be analyzed using MALDI-MS. Peptides are trapped according to their pI

values and experimental results are in agreement with theoretical pI calculations. Additional signals, (*i.e.,* leptin) are observed following fractionation highlighting an advantage to using this device and technique.

Separation of a Five Protein Tryptic Digest

To demonstrate an IET separation of a more complex sample in MSWIFT, a solution obtained by the proteolytic digestion of a mixture of five proteins: α-casein, albumin, apo-transferrin, ribonuclease A, and cytochrome c was analyzed. *In silico* digestion of this five-protein mixture yields a mixture of 345 possible peptides with molecular weights ranging from 500-4500 Da, assuming a single missed-cleavage. The MALDI mass spectra obtained from an aliquot of each fraction following the IET separation is shown in Figure 8(A-F). Inspection of the six resulting mass spectra display varying ion signal patterns which indicates that the peptides present in each separation well differ from each other. Note that numerous ion signals that are observed following IET are not observed in the non-fractionated samples, and are denoted with filled circles (●). The peptides observed from the five-protein mixture digest generally have theoretical pI values that fall within the pH values of the buffering membranes used in their respective separation wells, which verifies that MSWIFT is trapping the ampholytic components as it should. For example, the signal at m/z 1871.95 in the well bracketed by pH 4.5 and 5.4 buffering membranes (Figure 8B) corresponds to the theoretical m/z of the α_{s1}-casein peptide at residues 119-134 (YKVPQLEIVPNSAEER). A MASCOT database search performed on the six post-fractionation spectra results in the identification of four out of five proteins at the >99.990% confidence interval.

Ribonuclease A, which is not identified from database searching, has very few tryptic cleavage sites (13 R or K residues), thus a limited number of tryptic peptides are observed. Low abundance ion signals corresponding to ribonuclease A peptides are observed but were not selected for fragmentation by the automated software. By manual inspection of the mass spectrum obtained from the well bracketed by pH 6.5 and 7.6 membranes, the signals observed at m/z 2353.87 and 2495.12 can be assigned to tryptic ribonuclease A fragments 37-57 (QHMDSSTSAASSSNYCNQMMK, $[M+H]^+_{calc}$ – 2353.91 Da) and 66-87 (CKPVNTFVHESLADVQAVCSQK, $[M+H]^+_{calc}$ – 2495.18 Da), respectively. The theoretical pI value calculated for both of these peptides is 6.7, which falls between the pH values of the buffering membranes. Therefore, the protein can be assigned with increased confidence based on accurate mass and peptide pI.[85] The amino acid sequence coverage values obtained for the four proteins identified by database searching using only tandem MS data acquired after MSWIFT fractionation are as follows: albumin – 20%, apo-transferrin – 24%, cytochrome c – 58% and α_{s1}-casein – 28%. The amino acid sequence coverage of these proteins may be low owing to the

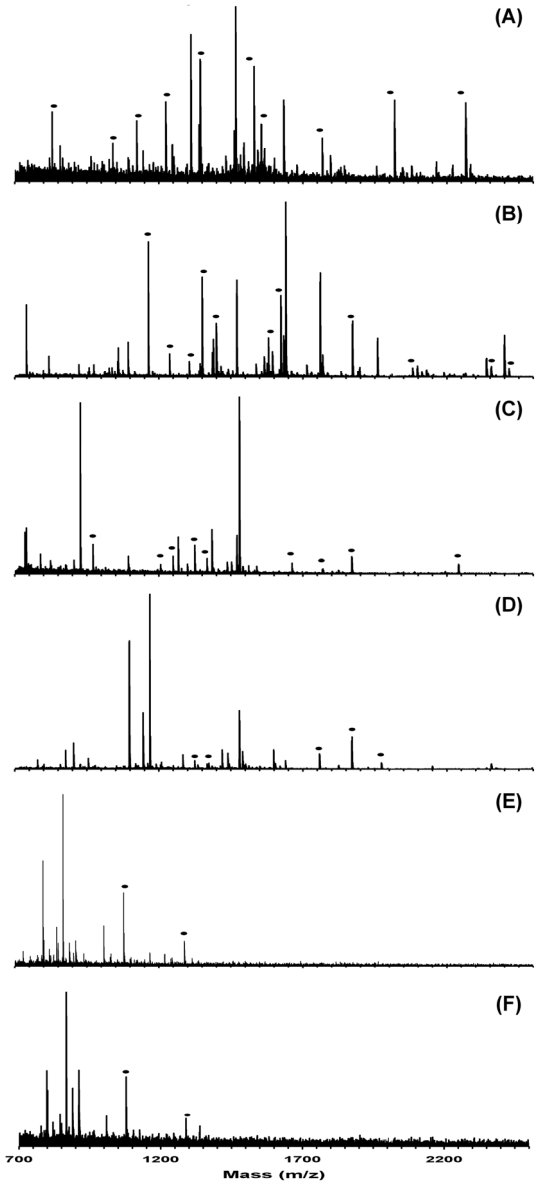

Figure 8. (A-F) MALDI mass spectrum of the contents of each MSWIFT separation well from the IET separation of the five protein digestion mixture. The pH values of the buffering membranes used were as follows: (1) pH 2.0-4.5, (2) pH 4.5-5.4, (3) pH 5.4-6.5, (4) pH 6.5-7.6, (5) pH 7.6-8.2 and (6) pH 8.2-12.0. Peptide ion signals denoted with a filled circle (●) are those which are not observed in the mass spectrum acquired prior to separation.

limited number of tandem MS spectra acquired for each MALDI spot based on software settings and prior to sample consumption on the specific spot. For comparison, MS/MS analysis of a tryptic digest of the five-protein mixture without fractionation results in the following sequence coverage values: albumin – 18%, apo-transferrin – 13%, cytochrome c – 26% and α_{s1}-casein – 26%. Most notable are the increases for cytochrome c (32%) and apo-transferrin (11%) observed with fractionation. A more significant increase in amino acid sequence coverage would be observed given additional IET experiments or analyzing each fraction using LC-MS/MS. However, the goal of this work does not encompass maximizing the coverage for a standard mixture. Note that the majority of peptide ion signals are observed from fractions taken from the first three separation wells (pI values 2.0-7.6) and very few signals are observed in the most basic wells. This trend observed from the five-protein mixture digest is also observed by plotting the calculated peptide molecular weight versus theoretical pI value pairs for the *in silico* digestion of bovine serum albumin where 74% of the tryptic peptides have pI values less than 7.6 (Figure 9). Separation of the five-protein digestion mixture illustrates the ability of MSWIFT to provide initial fractionation after which the resulting fractions can be analyzed using MALDI-MS. However, more sophisticated techniques such as LC or additional IET separations are needed for the analysis of more complex mixtures.

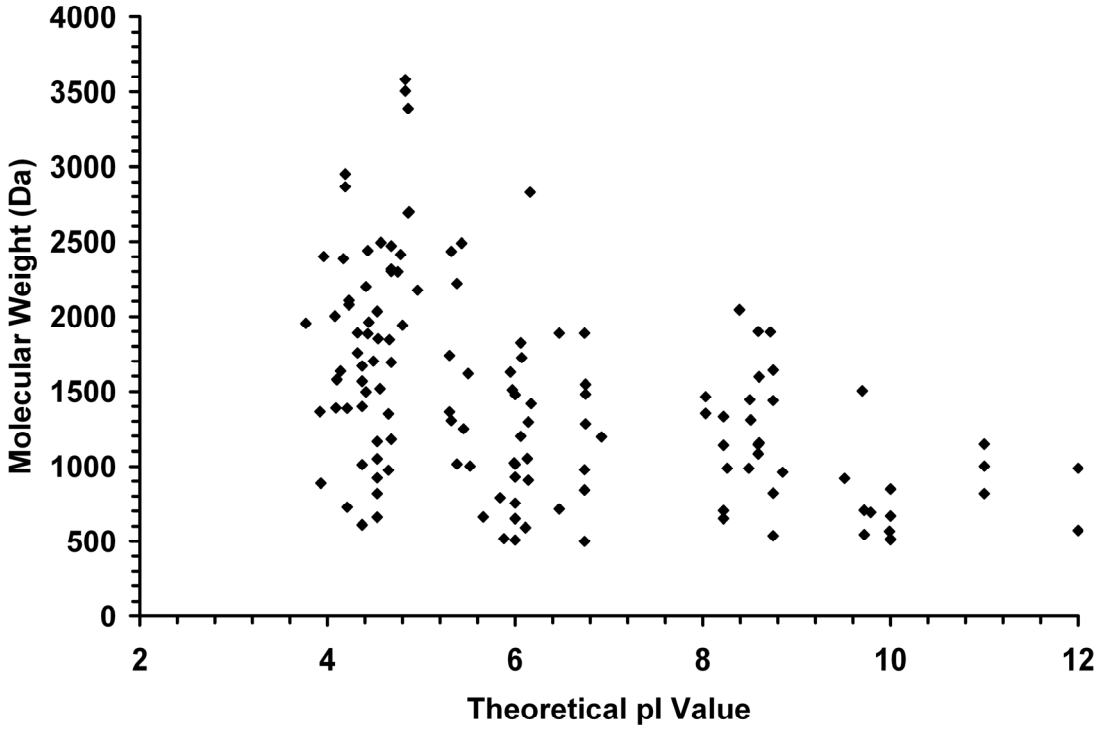

Figure 9. Plot of peptide molecular weight (MW) versus theoretical pI for an *in silico* tryptic digestion of bovine serum albumin allowing for one missed cleavage and peptide mass ranging from 500-3500 Da.

Analysis of a Ribosomal Protein Tryptic Digest

Ribosomal proteins isolated from *Escherichia coli* ribosomes provide an increasingly complex mixture to further demonstrate the separation capabilities of MSWIFT in bottom-up proteomic studies. These proteins range in molecular weight from *ca*. 3-30 kDa, isoelectric point from 4-11 and are rich in basic residues making tryptic digestion and MS analysis ideal. There are 56 ribosomal proteins contained in the *E. coli* ribosome proving an increase in sample complexity compared to the previous experiment. In this study, we analyzed peptides resulting from the tryptic digestion of

ribosomal proteins by subjecting this mixture to pI-based separation using the MSWIFT device. Following separation, an aliquot from each separation well was directly analyzed using MALDI-MS. The positive ion MALDI mass spectra collected for each compartment are displayed in Figure 10 (labeled A-F corresponding to Fractions 1-6 from low to high pH).

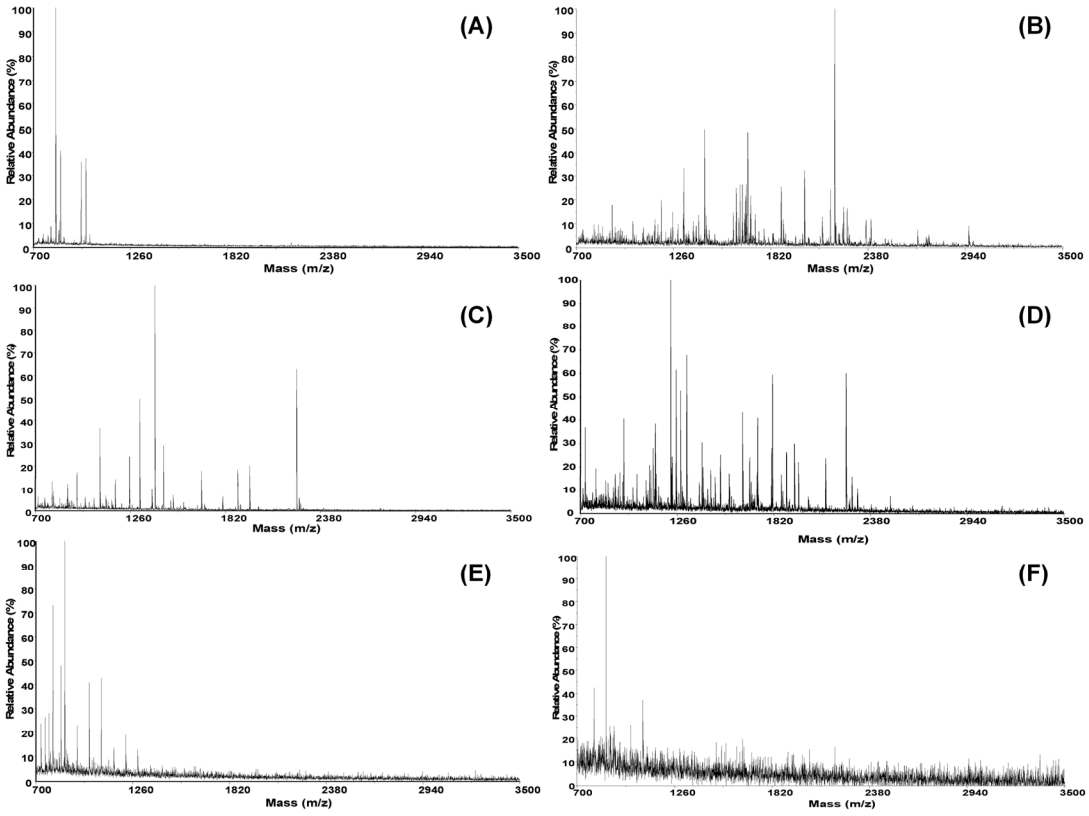

Figure 10. MALDI mass spectrum taken for an aliquot of each MSWIFT fraction following the pI-based separation of tryptic peptides derived from ribosomal proteins. The pH ranges for each compartment are fraction 1: pH 2.0- 4.5 (A), fraction 2: pH 4.5-5.4 (B), fraction 3: pH 5.4-6.5 (C), fraction 4: pH 6.5-7.6 (D), fraction 5: pH 7.6-8.2 (E), and fraction 6: pH 8.2-12.0 (F).

Similar to the results observed in the separation of the five-protein mixture digest, the majority of ion signals are observed in fractions 2-4 corresponding to peptide pI values between 4.5 and 7.6. In order to validate that the separation was occurring as predicted the MALDI mass spectrum collected from the third fraction was further analyzed. Several tryptic peptides corresponding to ribosomal proteins were observed and confirmed by tandem mass spectrometry (Figure 11). Additionally, the theoretical pI value for each tandem MS confirmed peptide is denoted in parenthesis and all fall within the pH values of the respective buffering membranes. Upon further analysis, the ion signal observed at m/z 1315.79 (outlined in red) could correspond to two tryptic peptide sequences derived from ribosomal proteins within the set mass error tolerance. The two peptide sequences, LQAFEGVVIAIR and VMCIKVLGGSHR have theoretical pI values of 6.0 and 9.6, respectively. Considering the theoretical pI value and the accurate mass measurement, the pI 6.0 peptide sequence would be assigned with higher confidence. Confirmation of this assignment was made using tandem mass spectrometry illustrating an added dimension of information that can be validated for peptide assignment when tandem MS is insufficient or absent. As a side note, approximately 19,000 mass resolving power would be needed to separate signals at these two calculated masses if both were present corresponding to the two potential peptides. A summary of the peptides assigned from the pH 4.5-5.4 fraction is provided in Table 1. Peptides denoted in bold correspond to those not observed in the MALDI-MS/MS analysis of the

digest alone. Following MSWIFT fractionation and MALDI-MS/MS analysis, database searching resulted in the confident identification of 20 ribosomal proteins, doubling the number of identifications made without any fractionation. For comparison, performing reversed phase LC, coupled off-line with MALDI-MS/MS results in 25 ribosomal protein identifications thus suggesting that coupling the two separation methods would result in an even larger increase in the number of identified proteins.

Indeed, performing MSWIFT-LC-MALDI-MS/MS analysis on the tryptic peptides resulted in 43 ribosomal protein identifications. The analysis of tryptic peptides from ribosomal proteins demonstrates the separation capabilities of MSWIFT, its compatibility with reversed phase LC, and the advantages of using a pI-based separation technique. Additionally, the separation is performed in a quick, high-throughput manner and additional depth of proteome coverage is observed by coupling these two separation methods followed by MS analysis.

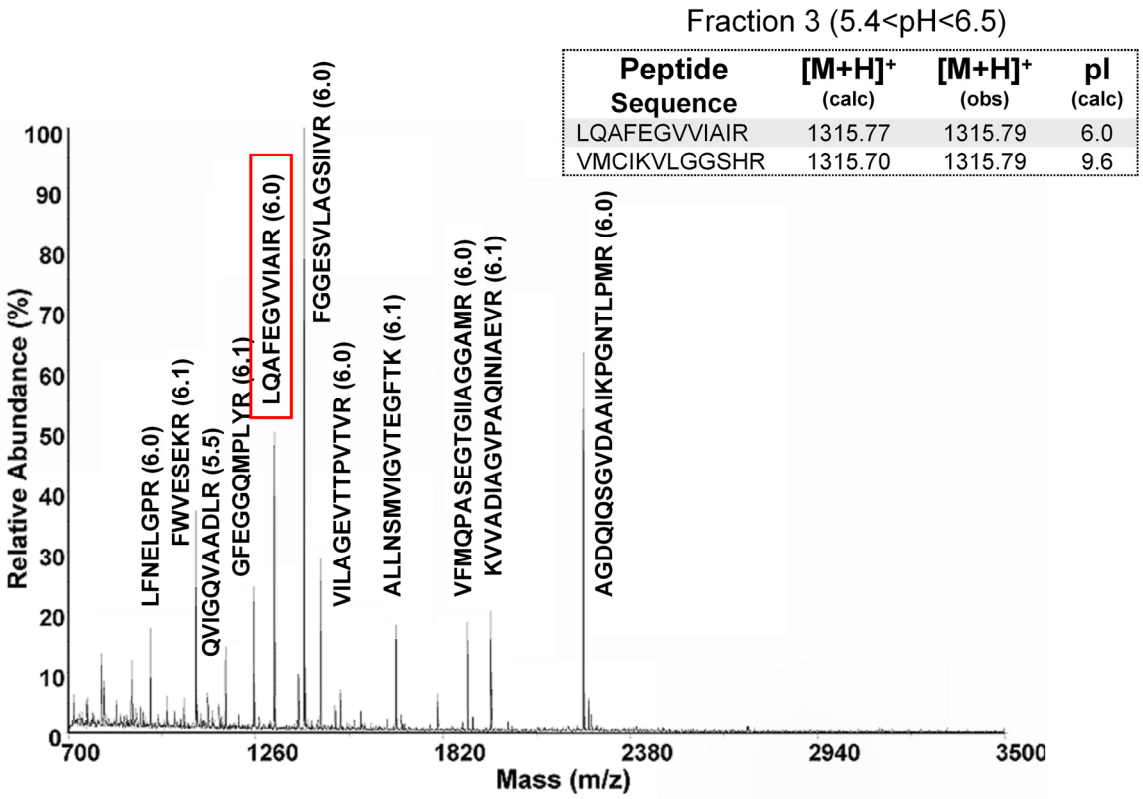

Figure 11. Expanded view of the MALDI mass spectrum acquired for the third fraction from the MSWIFT device which was bracketed by pH 5.4 and 6.5 buffering membranes. Peptides confirmed by tandem MS experiments are provided with the theoretical pI values denoted in parenthesis. The peptide LQAFEGVVIAIR is outlined with a red box to illustrate the advantage of pI-based separations when two there are two possible amino acid sequences corresponding to the same m/z.

Table 1. Fraction three (pH 5.4-6.5) peptide identifications from the MSWIFT separation of ribosomal protein tryptic peptides. Bolded sequences denote peptides not observed in the MALDI-MS spectrum prior to fractionation.

Summary of MSWIFT Fraction 3 (pH 5.4-6.5) Ribosomal Peptides

Ribosomal Protein	Peptide Sequence	$[M+H]^+_{obs}$	Theoretical pI[a]
L2	AGDQIQSGVDAAIKPGNTI	2239.06	6.0
L6	**APVVVPAGVDVK**	1004.54	5.9
L6	QVIGQVAADLR	1169.63	5.8
L6	ALLNSMVIGVTEGFTK	1679.83	6.1
L7/L12 (L8)	FGVSAAAAVAVAAGPVEA	2014.97	4.3
L11	**AQLQEIAQTK**	1129.58	6.1
L11	**GLPIPVVITVYADR**	1512.82	5.8
L15	GFEGGQMPLYR	1254.55	6.0
L15	AANIIGIQIEFAK	1387.73	6.1
L15	VILAGEVTTPVTVR	1454.81	6.0
L16	**GNVEYWVALIQPGK**	1573.76	6.0
L19	**LQAFEGVVIAIR**	1315.73	6.0
L24	**EAAIQVSNVAIFNAATGK**	1803.88	6.1
L25	MFTINAEVR	1080.51	5.8
L27	FGGESVLAGSIIVR	1404.74	6.0
S3	KVVADIAGVPAQINIAEVR	1963.06	6.1
S5	**VFMQPASEGTGIIAGGAM**	1892.86	6.0
S13	**LMDLGCYR**	1016.40	5.8

a - Theoretical pI values were calculated using Expasy pI/MW Tool (http://ca.expasy.org/tools/pi_tool.html)

Analysis of a Yeast Protein Digest

Successful analysis of complex mixtures typically relies on two separation techniques. When the separation principles of the two techniques are different, they are considered orthogonal, and the resulting separation or peak capacity is maximized. Therefore, fractions obtained from MSWIFT which have been separated based on pI, can be further separated using other techniques such as capillary electrophoresis or LC.

To illustrate this, we chose to separate and analyze the tryptic peptides from soluble *S. cerevisiae* proteins. Tryptic peptides were first subjected to IET separation using MSWIFT, followed by reversed phase LC-MS/MS analysis of the contents of each MSWIFT separation well. From database searching, 593 proteins were identified from a single analysis with high confidence. Similarly, Yates and coworkers successfully identified yeast proteins by separating peptides using strong cation exchange and reversed phase LC-MS/MS known as the MudPIT approach.[15] Haynes *et al.* analyzed yeast proteins using a variety of separation techniques including strong cation exchange and reversed phase chromatography as well as electrophoretic methods (*i.e.,* SDS-PAGE, IEF).[86] Analysis of our data indicates that fractionation was successful as observed in Figure 12 where the number of unique protein assignments from each fraction is plotted along with the total number of unique protein identifications (last column). The breakdown of the number of protein identifications by fraction is: 0 (pH 2.0-4.7), 256 (pH 4.7-5.4), 116 (pH 5.4-6.5), 305 (pH 6.5-7.0), 257 (pH 7.0-8.2), 153 (pH 8.2-12.0) and 593 combined. The analysis of proteins with high and low values of pI or MW is not compromised using the MSWIFT device and LC-MS/MS in a bottom-up approach. For example, Stress Protein DDR48 and 60S Ribosomal Protein L19A were both identified and have calculated pI values of 4.22 and 11.35 respectively. Furthermore, protein size is not problematic since peptides are being fractionated. For example, the 245Kd protein URA2 and 12Kd Heat Shock Protein were both identified. An additional benefit is the amount of material that was loaded. Compared to gel-based methods, there is no practical limit (within reason) to the amount of sample that can be

fractionated. Although our experiment utilizes 180 μg, much larger amounts (*i.e.,* mg scale) could easily be fractionated as was demonstrated in early experiments.[56] Furthermore, using this experimental scheme allows incorporation of pI for low scoring peptides to improve confidence in their assignment. Take for example the peptide ^{85}IDSVIHFAGLK^{95} from UDP-glucose-4-epimerase (GAL10). Based on tandem MS data, and a MASCOT score of 15, peptide assignment may not be regarded as highly confident. However, considering that the peptide has a theoretical pI value of 6.7 and is observed in the pH 6.5-7.0 well, increases the confidence in the peptide assignment.[87] Utilizing pI to improve peptide assignment may not always be feasible because the theoretical pI value is for an aqueous environment assuming that all residues are exposed and does not account for peptide or protein structure. Nevertheless, in cases such as the above example, pI clearly assists in the peptide assignment.

Another feature of the MSWIFT device is the ability to fractionate a sample multiple times. To demonstrate the utility of multi-stage separation experiments, we fractionated tryptic peptides from yeast into six fractions. Based on manual inspection of the MALDI mass spectrum taken of each fraction, the second well (pH 4.0-5.4)

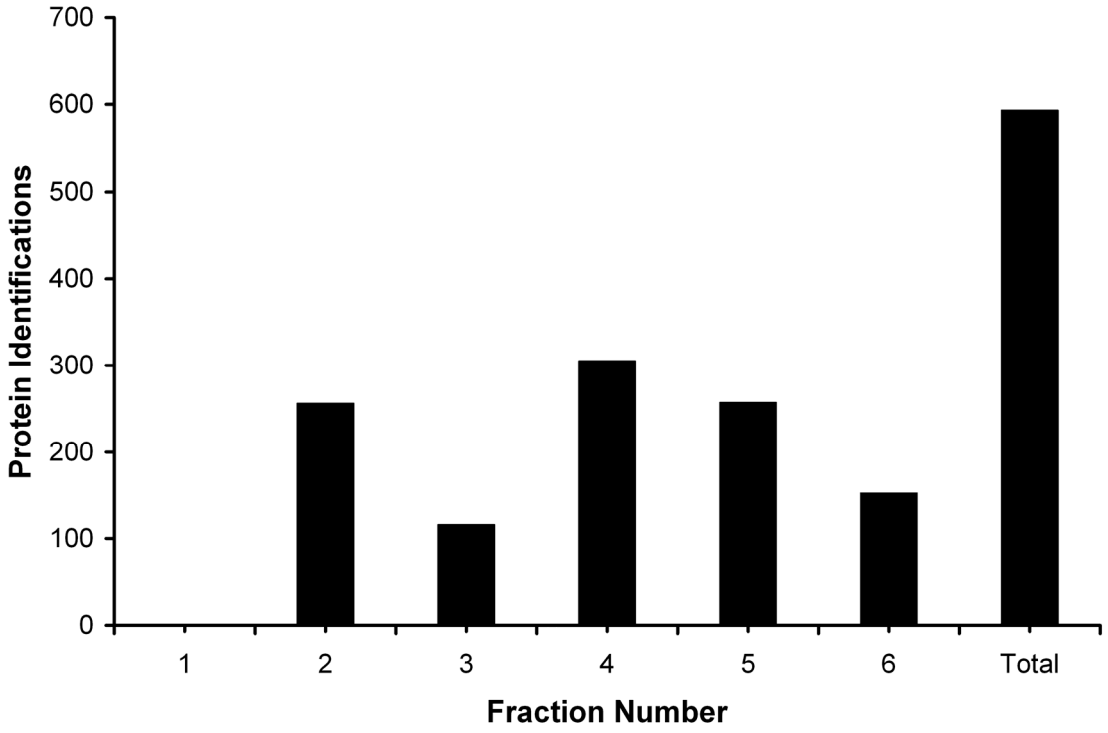

Figure 12. Plot of the number of unique proteins identified in each fraction from the MSWIFT. The final column represents the total number of proteins identified (from all six fractions) by database searching.

looked the most complex; this assumption is supported by earlier studies for *Escherichia coli* tryptic peptides.[88] Following initial fractionation, an aliquot of the contents of the pH 4.0-5.4 well was analyzed using LC-MS/MS and the remaining solution was then fractionated a second time using MSWIFT into three additional wells (pH 4.0-4.5, pH 4.5-5.0 and pH 5.0-5.4). Figure 13 is a cartoon schematic of the experimental scheme. The contents of the three wells from the second stage were also analyzed using LC-MS/MS. Preliminary data from this experiment results in 696 identified peptides

corresponding to 155 protein identifications from the first dimension of separation. Following a second stage of fractionation, the combined LC-MS/MS data resulted in an approximate two-fold increase in the number of identified peptides to 1436 corresponding to 231 protein identifications. The LC-MS/MS data obtained from each of the three wells in the second stage of fractionation was also subjected to database searching and the number of peptides and protein assignments are provided in Table 2. The greatest number of peptide and protein identifications (813 peptides and 203 proteins) from the second stage separation was observed in the pH 4.5-5.0 fraction.

Manual inspection of the preliminary data suggests that the majority of peptides are observed in their proper well and very few peptides are being assigned in multiple wells serving as additional indicators that MSWIFT works as an efficient pI-based separation device. Utilizing a multi-stage separation scheme increases the ability to identify low abundance proteins in the presence of highly abundant proteins.

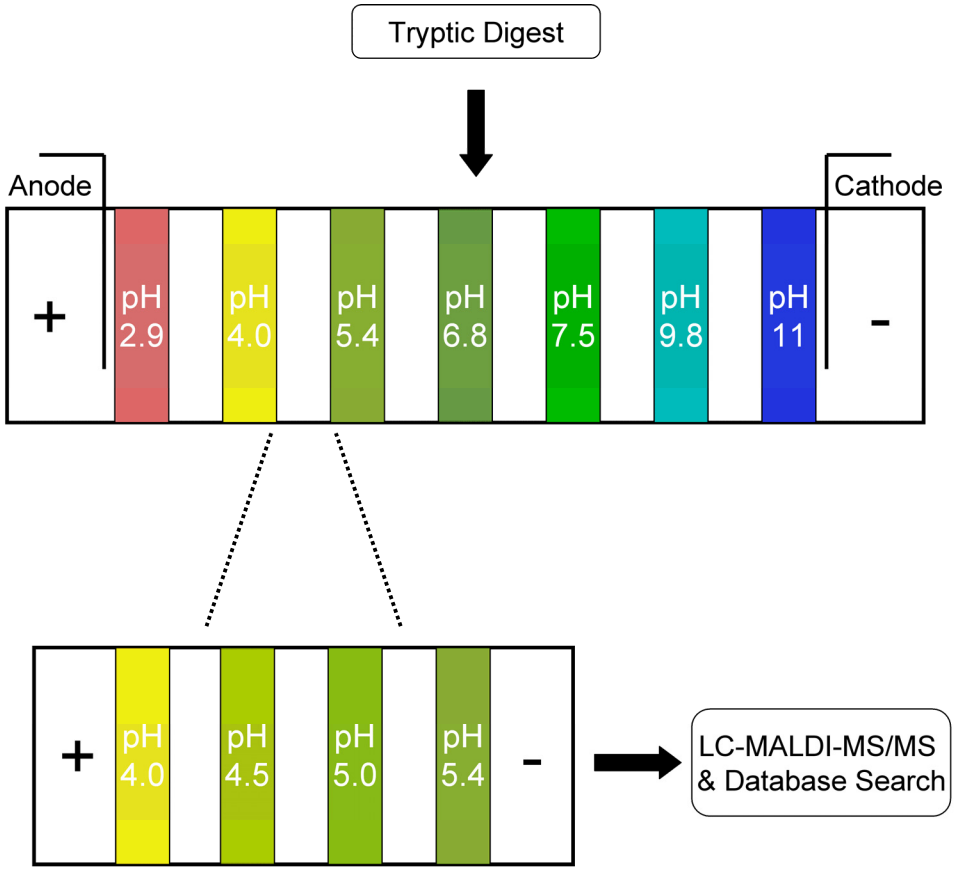

Figure 13. Experimental scheme for a two-stage separation of yeast tryptic peptides to increase peptide and protein identifications. A yeast tryptic digest was subjected to separation using MSWIFT over a broad range of pH values. The contents of the pH 4.0-5.4 fraction were then subjected to a second stage of fractionation into three compartments. The solutions from the three compartments in the second stage fractionation were then subjected to LC-MS/MS analysis and database searching to obtain peptide and protein identifications.

An example from these data is the identified proteins proteinase B which is known to be present at 1600 copies per cell and pyruvate kinase which is present at 291,000 copies per cell (www.yeastgenome.org). These results suggest that in order to identify low abundance proteins and peptides, fractionation is essential and the ability to perform several dimensions of fractionation followed by LC-MS/MS analysis greatly increases the number of peptides that can be identified. In turn, the number of protein identifications will increase as well as the confidence in protein assignment.

Table 2. Summary of the number of peptide and protein assignments made from a single stage and dual stage separation of yeast tryptic peptides.

	1st Stage Fraction 1 pH 4.0-5.4	2nd Stage Fraction 1 pH 4.0-4.5	2nd Stage Fraction 2 pH 4.5-5.0	2nd Stage Fraction 3 pH 5.0-5.4	2nd Stage Fractions 1-3 Combined
Peptides	696	769	813	84	1436
Proteins	155	151	203	31	231

CONCLUSIONS

The utility of MSWIFT for fractionation of peptides on the basis of pI followed by MALDI-MS and LC-MS/MS analysis is demonstrated for both model peptide mixtures, sub-proteome analysis (ribosomal protein digest) and for the analysis of a complex proteome (yeast lysate). Amino acid sequence coverage values obtained for peptide mass mapping and tandem MS are typically higher following fractionation compared to direct analysis of the mixture. For example, numerous peptide ion signals

which are not observed in crude mixtures are observed following MSWIFT fractionation. We have successfully used MSWIFT for a large scale proteomic analysis by separating tryptic peptides from yeast followed by LC-MS/MS and demonstrated that several hundred proteins can be assigned from a single analysis and that the number of peptide identifications is distributed throughout the MSWIFT fractions. Peptides with low MASCOT scores can be assigned with increased confidence when theoretical pI values fall between the pH values of the buffering membranes. Finally, we have performed initial experiments showing the ability to carry out multiple separations on a single sample by taking a first stage fraction and further fractionating the contents. By implementing a two-stage MSWIFT separation strategy, the number of peptide and protein identifications increased. Further experiments are currently underway investigating multi-stage separations using the MSWIFT device to increase the depth of proteome coverage. These proof-of-concept experiments illustrate the utility of MSWIFT as a high-throughput device that provides flexibility, increased sample load capacity and eliminates the need for sample clean-up for mass spectrometry-based proteomic studies.

CHAPTER III

MULTI-STAGE, ISOELECTRIC POINT-BASED SEPARATIONS FOR THE PROTEOMIC ANALYSIS OF THE MODEL FUNGUS: *NEUROSPORA CRASSA*

INTRODUCTION

Mass spectrometry (MS) plays an important role in the identification of peptides and proteins from complex mixtures such as human plasma, parasites, bacteria and fungi.[4] However, one of the remaining challenges in most proteomic studies is obtaining sufficient MS data resulting in accurate peptide and protein assignments of all expressed proteins owing to the low copy numbers at which some proteins are expressed.[39, 89, 90] In an attempt to overcome limitations associated with dynamic range, researchers rely on various separation techniques which, when used in tandem, allows for multi-dimensional separations. Guidelines for producing optimal multi-dimensional separations have been recently re-visited.[91] The most extensively studied model system is the fungus *Saccharomyces cerevisiae*: its' complexity has lead to the development of several separation strategies and ultimately generated the beginning of a field dedicated to fungal proteomics. To date, several large-scale studies have been performed on *S. cerevisiae* with the most extensive recently reporting more than 4000 identified proteins.[76] Additionally, several studies have attempted to identify other fungal proteins, and determine their post-translational modifications.[92,93] The recent completion of several fungal genomes [94, 95] now sets the stage for extensively studying their respective proteomes using mass spectrometry to reveal qualitative and quantitative information

regarding the protein complement of several different fungi proteomes.

Another model system, *Neurospora crassa,* is a filamentous fungus whose genome is more complex than that of the extensively studied *S. cerevisiae,* with more than 9000 protein encoding genes;[96] however, proteomic studies utilizing *N. crassa* have been limited. Recently, MS-based studies have been performed to identify *N. crassa* mitochondrial ribosomal proteins,[97] to explore the mitochondrial outer membrane proteome[98] and investigate the role of phosphorylation associated with the circadian clock.[99] Furthermore, sample preparation techniques applicable to fungal proteomics have been presented.[100] The recent completion of the determination of the *N. crassa* genome[96] generates the opportunity for more extensive proteomic studies, however, a large-scale proteomic analysis of *N. crassa* has not been performed to date.

Successful analyses of complex protein samples such as *N. crassa* often relies on pre-fractionation followed by liquid chromatography (LC)- tandem mass spectrometry (MS/MS) analysis. We have recently shown that an isoelectric point (pI) – based fractionation device termed membrane separated wells for isoelectric focusing and trapping (MSWIFT) provides fast separations of peptides for MS-based proteomic studies and is directly compatible with matrix-assisted laser desorption/ionization (MALDI) – MS and LC-MS/MS.[101] The MSWIFT device is advantageous owing to (i) the flexibility of its design where a variable number of compartments can be assembled, (ii) the use of buffering membranes whose pH can be tuned and (iii) a wide range of sample loading capacity. In this work, we present a multi-stage fractionation scheme for the analysis of the *Neurospora crassa* proteome. This multi-stage experimental platform

is unique to the MSWIFT device and allows for customizable separations to increase the number of identified peptides and proteins by providing fractioned samples that can be directly analyzed using LC-MS/MS.

EXPERIMENTAL SECTION

Chemicals were obtained from Sigma (St. Louis, MO) unless noted otherwise. HPLC grade acetonitrile was purchased from EMD Chemicals, Inc. (Gibbstown, NJ). Peptide standards from American Peptide Company (Sunnyvale, CA) were used without further purification. All experiments were performed using purified 18 MΩ water (Barnstead International, Dubuque, IA).

Membrane Separated Wells for Isoelectric Focusing and Trapping (MSWIFT)

The design and assembly of MSWIFT have been previously described.[55,56] Briefly, the main housing of MSWIFT was built using polycarbonate and equipped with an aluminum heat sink. Poly(vinyl-alcohol) based buffering membranes with tunable pH values were synthesized in-house.[41-44]

IET

Alumina separation wells were assembled serially and filled with 200 μL of either the peptide sample solution or an isoelectric buffer. The anolyte was a 3 mM methanesulfonic acid solution, the catholyte a 3 mM sodium hydroxide solution. Compartment solutions were pH biased using ampholytic buffers as previously

described.[53] Typical separation times ranged from 45-60 minutes at 5W constant power. Theoretical pI values were calculated using the compute pI/MW tool from ExPASy.[79]

Proteolytic Digestion of Neurospora crassa *Proteins*

Proteins isolated from *N. crassa* (vegetative state) were provided as a generous gift from Professor Rodolfo Aramayo's Laboratory, Department of Biology, Texas A&M University. Protein concentrations were determined using the Bradford Assay.[82] Pelleted proteins were re-suspended in 25 mM ammonium bicarbonate buffer. A total of 500 μg of protein was reduced using tris-(2-carboxyethyl) phosphine at a final concentration of 5 mM and incubated at 60 °C for 1 hour. Alkylation was performed using 15 mM methylmethane thiosulfonate and allowed to react at room temperature for ten minutes. Tryptic digestion was carried out by trypsin addition at a 1:100 enzyme to protein ratio and the solution was incubated at 37°C for 4 hours. The trypsin addition was repeated two additional times.

Two-stage fractionation of a Neurospora crassa *proteolytic digest*

Tryptic peptides from *N. crassa* were fractionated using MSWIFT in a two-stage experimental design. The second stage of fractionation was performed such that two of the initial fractions were further separated simultaneously. A schematic representation of the experimental design is provided in Figure 14. The pH values of the membranes in the first stage fractionation were as follows: 2.9, 4.7, 5.4, 6.6, 7.5, 9.5 and 11. The sample was loaded in the fourth and fifth separation wells and IET was carried out. Following separation, an aliquot of the solution from each compartment was subjected to LC-MS/MS analysis. Results of the LC-MS/MS analysis indicated that the fractions in the second, third, fourth and fifth compartments were most complex and therefore subjected to a second stage of fractionation. The pH values of the buffering membranes used for the pH 4.7-5.4 and pH 5.4-6.6 fractions were: 2.9, 4.6, 4.9, 5.2, 5.5, 5.8, 6.0 and 11.0. The pH values of the buffering membranes used for the second stage fractionation of the pH 6.6-7.5 and 7.5-9.5 wells were 2.9, 6.0, 6.8, 7.1, 7.6, 8.6, 9.0 and 11.0. This experimental scheme resulted in six fractions in the first stage and fourteen additional fractions in the second stage. The peptide solution contents of each fraction were then subjected to reversed phase LC coupled offline to MALDI-MS/MS analysis.

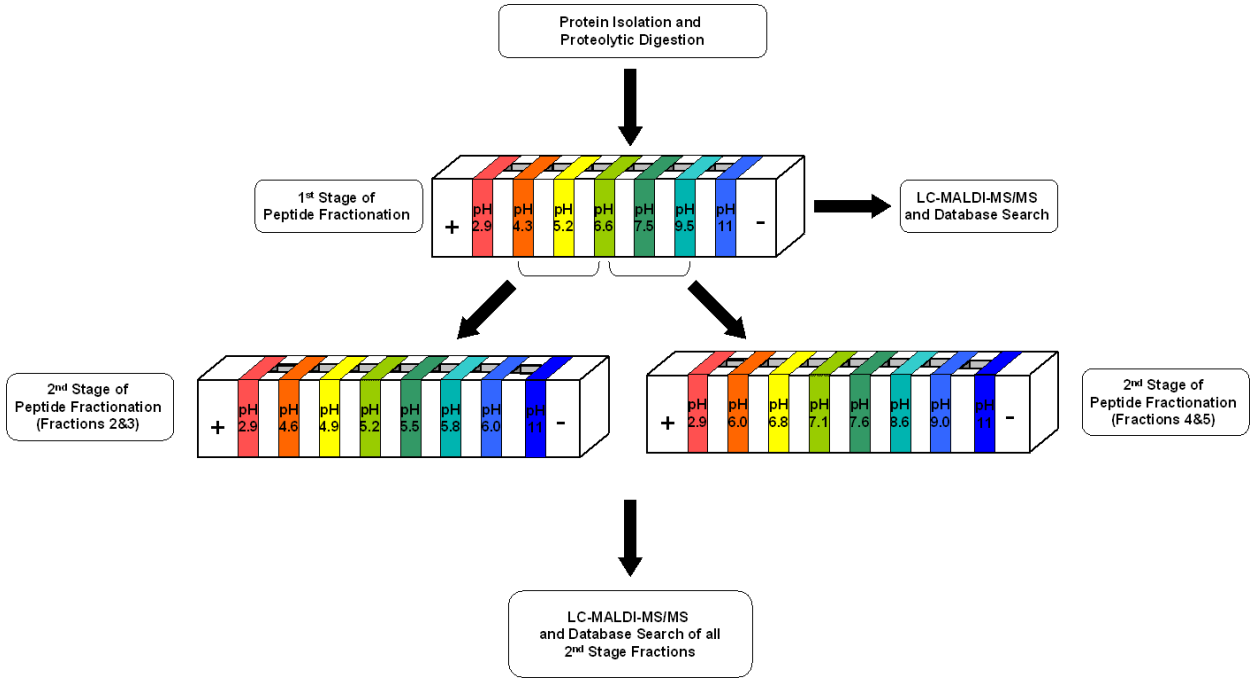

Figure 14. Schematic representation of the experimental workflow used. *Neurospora crassa* proteins were subjected to proteolytic digestion using trypsin followed by a first stage fractionation using MSWIFT and LC-MS/MS analysis. The contents of the pH 4.3-5.2, 5.2-6.6, 6.6-7.5 and 7.5-9.5 wells were then further fractionated in a second stage. Following the second stage of fractionation, the contents of each well was analyzed by LC-MS/MS and the resulting data was analyzed to obtain peptide and protein assignments.

LC-MALDI – MS/MS Analysis

Assuming equal distribution of the sample mass across all wells, approximately 3 μg of each was subjected to reversed phase liquid chromatography for additional separation coupled off-line with MALDI-MS/MS as previously described.[81] The column eluent was mixed with the MALDI matrix (7 mg mL^{-1} α-cyano-4-hydroxycinnamic acid, 60% (v/v) acetonitrile, 10 mM ammonium dihydrogen phosphate, 10% isopropanol) and the resulting mixture was spotted onto a MALDI target via a robotic spotting device. MALDI mass spectra were acquired using a 4800 Proteomics Analyzer (Applied Biosystems, Framingham, MA). External calibration was performed using the standard peptides bradykinin fragment 2-9 and adrenocorticotropic hormone fragment 18-39. Collision-induced dissociation (CID) spectra were acquired using air as the collision gas (medium pressure setting) at 1 kV of collision energy. Tandem mass spectrometry data were searched against the *Neurospora crassa* database (downloaded 02/12/2010, www.broadinstitute.org) using the Protein Pilot Software v. 3.0 and the Paragron™ Algorithm (Applied Biosystems, Framingham, MA). Peptide and protein assignments were made at the 95% (N>1.3) confidence level. For protein identification, at least one 95% level peptide was required. A table of protein identifications is provided in Appendix B.

RESULTS AND DISCUSSION

The recent sequencing of the *Neurospora crassa* genome now allows for MS – based large scale proteomic profiling of this model fungus. To perform such a daunting task, we utilize the MSWIFT device for pI-based fractionation of peptides prior to LC-MS/MS analysis. Furthermore, we have developed a dual stage separation scheme using the MSWIFT to increase the number of peptides and proteins identified in bottom-up proteomic studies.

MSWIFT-LC-MS/MS of N. crassa

Initial experiments were aimed at performing the first large-scale proteomic profiling study of the *Neurospora crassa* proteome. Tryptic peptides were first subjected to fractionation based on pI using the MSWIFT in a six-compartment setup. The contents of each well was further separated by reverse phase LC followed by MALDI-MS/MS. Database searching of the tandem MS data resulted in 2558 and 672 high confidence identifications for peptides and proteins, respectively. Since the bottom-up proteomic approach was utilized in these experiments, complications associated with the analysis of proteins with high and low MW or pI are not observed. Take for example the two proteins, Elongation Factor 3 which is 117 kDa and 60S Ribosomal Protein L13 which is 24 kDa. The theoretical pI values for these two proteins are 5.83 and 10.92 respectively. Table 3 contains a summary of the protein properties and database search results obtained from these two protein assignments. In order to determine the success of the MSWIFT fractionation, the MS/MS data from each

fraction was also subjected to database searching. The number of peptide assignments obtained from searching each fraction is provided in Figure 15. The number of tandem MS spectra acquired as well as the number of peptide identifications obtained from each fraction formed the basis for the design of the additional experiments. Based on our initial experimental results, we can conclude that using MSWIFT for peptide pre-fractionation followed by LC-MS/MS analysis provides an effective method for large scale proteomic profiling.

Table 3. Example of two proteins identified from the analysis of *N. crassa*

Protein Name	Accession #	MW (kDa)	Amino Acids	pI	Peptide IDs	AA Seq.Cov.
Elongation Factor 3	NCU07922T0	117	1057	5.83	14	27%
60S Ribosomal Protein L13	NCU05554T0	24	215	10.92	10	47%

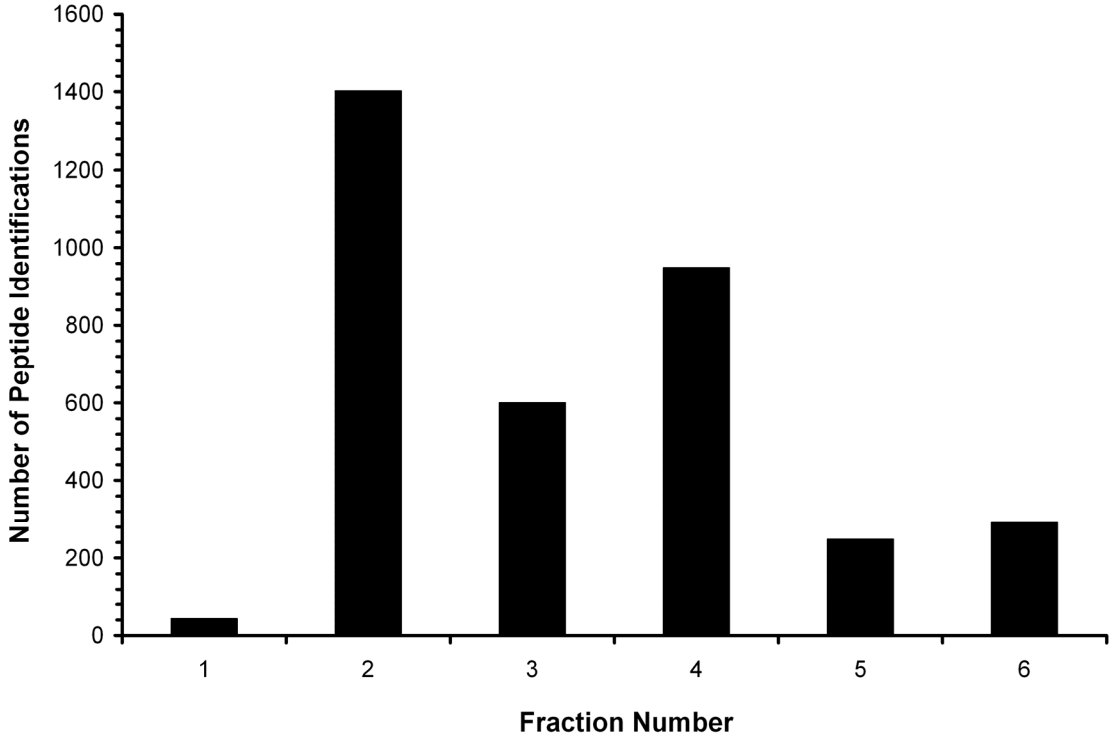

Figure 15. Plot of the number of peptides identified in fractions by the MSWIFT-LC-MS/MS analysis of *Neurospora crassa*. The MS/MS data obtained from each fraction was subjected to database searching individually to determine the number of peptides identified for that specific fraction. These results led to the development of the dual stage separation method used in further work to increase the number of peptides and proteins identified.

Although the initial fractionation was successful and yielded several hundred protein identifications, complete (or maximal) proteome identification is the overall goal of this work. Since the *Neurospora crassa* genome encodes for more than 9000 gene products, less than ten percent of the predicted proteins were identified. Therefore,

another method is needed to enhance the depth of proteome coverage. To accomplish this, we developed a multi-stage separation platform using the MSWIFT device to perform pI-based fractionation followed by LC-MS/MS analysis. The two stage fractionation experiment is performed such that tryptic peptides are first subjected to fractionation in broad pI ranges. Following initial fractionation, the contents of the most complex wells are then further separated into narrow pI ranges. From the first stage MSWIFT fractionation of *N. crassa* tryptic peptides, the second, third, fourth and fifth fractions were determined to have the most complex composition on the basis of the number of tandem MS spectra acquired and peptides identified from database searching of each fraction. To improve throughput in the second stage of fractionation, the MSWIFT device was assembled in such a manner that two of the first stage fractions could be separated into three additional wells each (six fractions total). To carry this out, a gap fraction was added in the middle; therefore, seven true fractions resulted from the second stage separation. The gap fraction was added in order to evenly cut the second dimension fractions while retaining the anodic and cathodic membranes from the first stage separation. The MS/MS data collected from the contents of each well from the second stage of fractionation was database searched and the results are summarized in Figure 16. The number of peptides identified from the second stage fractionation of fractions two and three (Figure 16A) and those obtained from the second stage separation of fractions four and five (Figure 16B) are provided.

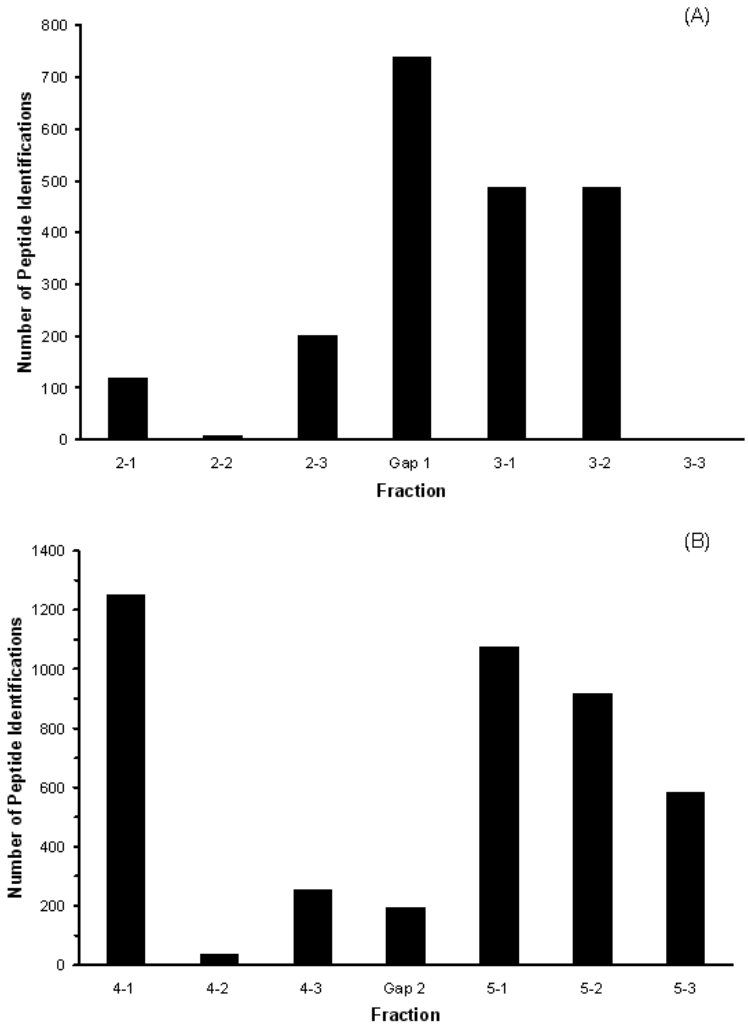

Figure 16. Number of peptides identified from the second stage of fractionation of *N. crassa* tryptic peptides. Results from peptides collected from the second and third fractions (pH 4.3-6.6) further separated are in the top panel (A) and peptides collected from the fourth and fifth fractions (pH 6.6-9.5) are provided in the bottom panel (B). The numbering system used for each fraction is based on the fraction number from the first stage, followed by the resulting fraction number in the second stage separation. A gap was used in order to distribute each first stage sample into three distinct fractions.

In order to determine if the second stage of fractionation has analytical utility for bottom-up proteomic strategies, the number of peptides identified was compared. Since the 'gap' fractions overlapped the pI ranges of the second and third fractions (as well as the fourth and fifth), the total number of peptides from fractions two and three were compared to the total number of peptides from the second stage analysis. The total number of peptides identified by combining fractions two and three is 2002 compared to 2038 from the second stage (seven fractions) results. A more dramatic increase is observed when comparing fractions four and five which had 1197 identifications to 4309 peptide identifications from the second stage analysis. To gain a better perspective on the benefits of performing the multi-stage separation, the number of distinct peptides was compared. A distinct peptide is defined as a peptide that can be directly related to a protein within a specific genome. Figure 17 contains a bar graph representing the number of distinct peptides and protein identifications in the single stage analysis and after performing the second stage analysis. Following initial fractionation and LC-MS/MS, 2558 distinct peptides were assigned corresponding to 672 identified proteins at the 95% confidence level. Database searching of the MS data collected from the first and second stages of separation results in 4075 distinct peptides and 731 high confidence (95% confidence level) proteins. A Venn diagram is provided in Figure 18 displaying the number of protein identifications obtained from the respective search. Only one protein identification was unique to the first stage separation which was the protein NCU04164T1 (conserved hypothetical protein). Conversely, 60 protein identifications were unique to the second stage of separation illustrating one advantage of performing

multiple stages of pI-based separations. Also note that for the proteins identified in both the single and dual stage fractionation, amino acid sequence coverage values and therefore confidence in assignments also greatly increased.

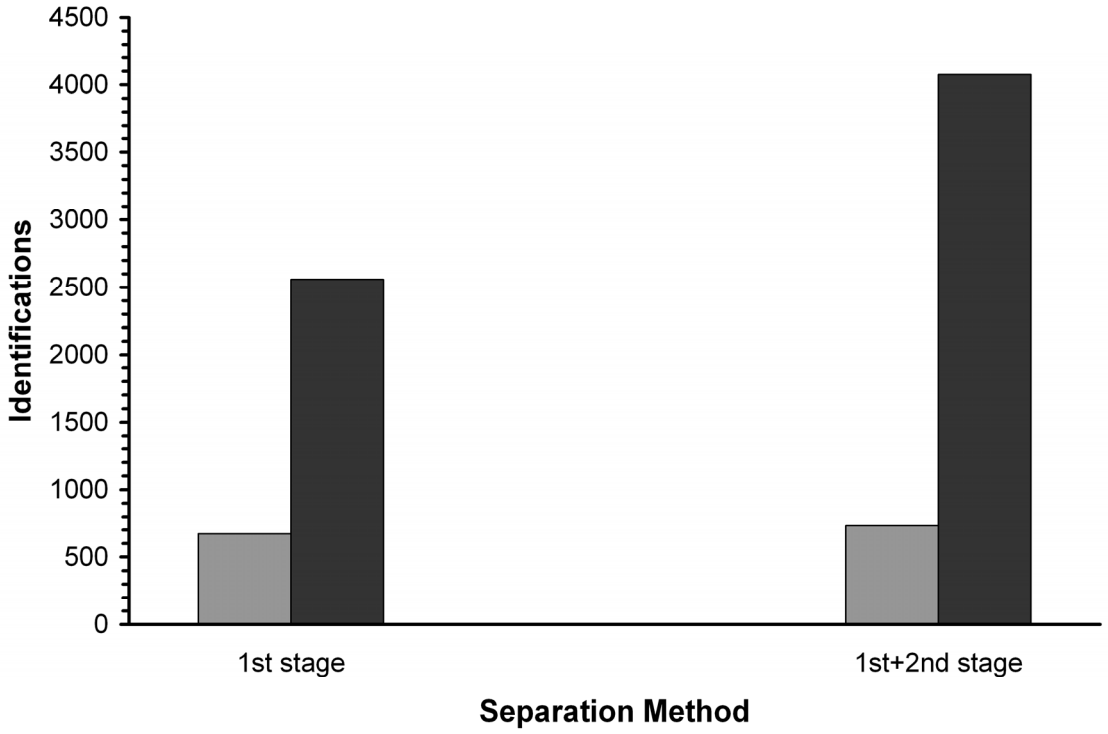

Figure 17. Bar graph representing the number of peptide (black bars) and protein (gray bars) identifications resulting from a single stage of MSWIFT fractionation versus incorporating a second stage of fractionation.

While only a small fraction of additional proteins were identified from the second stage, the amino acid sequence coverage significantly increased for several proteins. Take for example, fumarate hydratase (NCU10008T0) for which coverage increased from 10.5% to 15% and eukaryotic translation initiation factor 3 110kDa subunit (NCU00040T0) for which coverage nearly doubled from 6.6% to 12.6 %. The 6% increase corresponds to approximately 66 additional amino acids (*ca*. 6 peptides) being identified assuming that the average amino acid mass is 100 Da and the average peptide length is 10 amino acids. Therefore, performing the dual stage separation has provided additional protein identifications and increased amino acid sequence coverage for protein assignments resulting in higher confidence identifications.

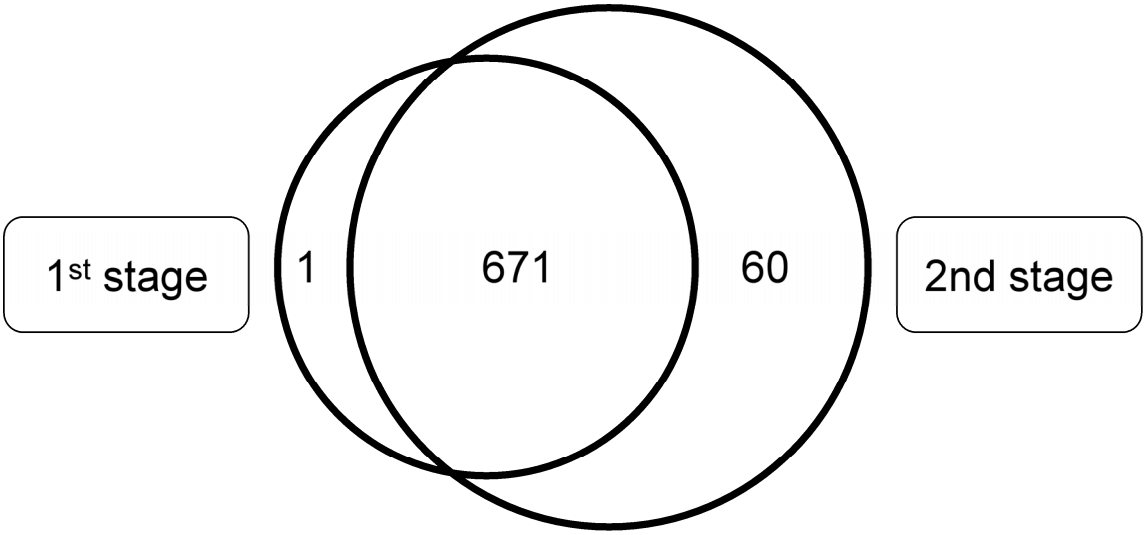

Figure 18. Venn diagram representing the total number of proteins identified from the analysis of *Neurospora crassa* tryptic peptides. Also, the number of unique proteins identified from each separation method is provided.

CONCLUSIONS

The first large scale proteomic profiling study of the model fungus *Neurospora crassa* is presented. Initial experiments incorporated pI-based fractionation using the MSWIFT as an efficient separation device prior to LC-MS/MS analysis where several hundred proteins were identified. As a means to identify additional peptides and proteins - and therefore increase the depth of proteome coverage - a new experimental platform has been introduced. Namely, two stages of peptide fractionation were performed using MSWIFT which resulted in an increase in the number of total peptides, distinct peptides and high confidence protein assignments. Finally, we have compared the protein identifications from only a single stage of pI-based separations to data from the first and second stage where an additional 65 protein identifications were made. To achieve even more protein identifications additional analyses of the concentrated contents of the second stage compartments are needed in order to detect low abundance peptides which in turn may correspond to low abundance proteins.

CHAPTER IV

STUDIES OF HISTIDINE AS AN ALTERANTIVE BUFFER FOR TYPTIC DIGESTION AND ISOELECTRIC TRAPPING FRACTIONATION IN BOTTOM-UP PROTEOMICS

INTRODUCTION

Isoelectric point (pI)-based separation techniques, and specifically isoelectric trapping (IET), are useful for the separation of peptides and proteins in the absence of carrier ampholytes. In IET, buffering membranes are used to create a step-wise pH gradient in a compartmentalized setup referred to as a multi-compartment electrolyzer (MCE).[65,72,102,103] During electrophoresis, ampholytes migrate until they reach a compartment in which the pH values of the buffering membranes at the anodic and cathodic side of the compartment bracket the pI values of the peptides. Thus, the ampholyte is 'trapped' into a compartment based on its pI.

Several analytical-scale MCEs have been introduced and utilized for proteomic applications [45,48,65,66] including our in-house developed device termed membrane separated wells for isoelectric focusing and trapping (MSWIFT).[56] We have demonstrated that the MSWIFT is an efficient pre-fractionation device that can be used to separate peptides, followed by MS and reversed phase LC-MS/MS for bottom-up proteomic studies.[101] One advantage of the MSWIFT is higher power loads can be applied compared to the commercially available analytical IEF and IET devices. The benefit to applying high electric field strength is a reduction in separation time.

However, regardless of the device, the conductivity of the sample inherently affects the results of the separation. Recently, Mann and coworkers[52] described a proteomics approach to analyze yeast peptides using the OFFGEL™ Fractionator (Agilent Technologies). The authors note that 'salt concentration is critical' and that 'buffering conditions with 50 mM ammonium bicarbonate resulted in failure of the IEF.' These observations could be explained by the conductivity of the sample since successful peptide fractionation was observed using 4-(2-hydroxyethyl)-1-piperazineethane sulfonic acid (HEPES) buffer which has a significantly lower conductivity. Therefore, sample preparation is extremely crucial to consider when employing electrophoretic separations. Low conductivity buffers have been used for capillary zone electrophoresis,[104-106] including histidine,[107, 108] carrier ampholytes,[109] and isoelectric buffers for IET separations.[53]

The analysis of biological samples incorporating electrophoretic methods can be plagued by the buffers and sample preparation methods typically performed. That is, many samples require high concentrations of buffers and salts or detergents to maintain stability[110] which, in turn, are detrimental to the electrophoretic separation. Downstream analysis using MS can also be plagued by interferences from these additives.[111] In this work we investigate the effect of traditional sample preparation methods using ammonium bicarbonate as the protein digestion and separation buffer using the MSWIFT device followed by matrix assisted laser desorption/ionization (MALDI) MS analysis. We then compare these results to those obtained using a lower conductivity ampholytic buffer, histidine.

EXPERIMENTAL SECTION

All chemicals were purchased from Sigma-Aldrich (St. Louis, MO), unless otherwise noted. HPLC grade methanol and isopropanol was purchased from EMD Chemicals Inc. (Gibbstown, NJ). Sequencing grade trypsin was purchased from Promega (Madison, WI). All experiments were performed with 18MΩ water (ddH_2O) purified using a purification unit from Barnstead International (Dubuque, IA). All chemicals were used as received without further purification.

Membrane Separated Wells for Isoelectric Focusing and Trapping (MSWIFT)

Details outlining the design and assembly of the MSWIFT have been previously described.[55, 56] Briefly, the main housing of the MSWIFT was built using polycarbonate equipped with an aluminum heat sink. Alumina separation compartments were assembled serially and contained up to 200 μL of sample solution. Poly(vinyl-alcohol) based buffering membranes with tunable pH values were synthesized in-house.[41-43] The anode compartment contained 3 mM methanesulfonic acid whereas 3 mM sodium hydroxide was used as the cathode buffer. Samples were separated at 5W constant power. Theoretical pI values were calculated using the compute pI/MW tool from ExPASy.[79] Theoretical conductivity and buffering capacity values were obtained from Peakmaster v.5.2. [112] Solution conductivity measurements were performed using a Model 145A Conductivity Meter (Thermo Orion, Waltham, MA) equipped with a MI-900 Series conductivity electrode (Microelectrodes Inc, Bedford, NH).

Proteolytic Digestion and Sample Preparation

Ten micrograms of bovine serum albumin was dissolved in 10 μL of either 5 mM histidine or 25 mM ammonium bicarbonate. The protein was denatured thermally at 90 °C for ten minutes and allowed to cool to room temperature. Trypsin (Promega, Madison, WI) was added at a ratio of 1:50 (w/w) and the solutions were incubated at 37 °C overnight.

A mixture containing 10 μg each of the following five proteins: bovine serum albumin, apo-transferrin, α_{s1}-casein, ribonuclease A, and cytochrome C was dissolved in 200 μL of either 10 mM histidine or 25 mM ammonium bicarbonate. The protein mixture was reduced and denatured with 5 mM tris(2-carboxyethyl)phosphine at 60 °C for 1 hour. Alkylation was performed by the addition of 2 mM methyl methanethiosulfonate and incubated at room temperature for ten minutes. Trypsin was added at a ratio of 1:50 (w/w) enzyme: protein ratio and the solution was incubated at 37 °C overnight. The digest solution was then distributed into all MSWIFT wells for initial studies. For the separation time course, the digest solution was loaded in the pH 6.8-7.6 well. The contents of each well were mixed via pipette then a 1 μL aliquot was taken for MALDI-MS analysis. The contents of each well were analyzed at 1, 3, 5, 10, 20, 30 and 45 min.

MALDI-MS and MALDI-MS/MS

All MALDI-MS experiments were performed using a 4700 Proteomics Analyzer MALDI-TOF/TOF (Applied Biosystems, Foster City, CA). The MS data were acquired

using the reflectron detector in positive ion mode (700-4500 Da) with internal calibration. Collision induced dissociation tandem MS spectra were acquired using air at the medium pressure setting and at 1 kV of collision energy. All MS and MS/MS data were searched against the SwissProt protein sequence database using the GPS Explorer (Applied Biosystems) software with an in-house license of MASCOT (V 2.1).[83] Database searching parameters were as follows; taxonomy, Metazoa; precursor mass tolerance, 100 ppm; enzyme, trypsin; missed cleavages, one; and variable modifications, MMTS (C), oxidation (M). Protein assignments were made at the 99.990% confidence interval calculated by the GPS Explorer software taking into account the MASCOT score for each peptide. Peptide assignments were made with a MASCOT ion score cut off of ≥20.

RESULTS AND DISCUSSION

Proteolytic digestion using trypsin is advantageous for proteomic analysis because of the unique features of tryptic peptides. Namely, peptides resulting from proteolytic cleavage end in a C-terminal arginine or lysine and typically have molecular weights ranging from 700-3000 Da making mass spectrometry-based proteomics ideal for these mixtures. Traditional protocols for trypsin digestion utilize buffers in high concentrations and at physiological pH to optimize tryptic digestion. Histidine is an ideal alternative for tryptic digestion because it is an isoelectric buffer with a solution pH value of ~ 7.5 at low mM concentrations thus, providing the initial motivation behind this work. Therefore, we sought out to develop a method incorporating histidine as a

sample buffer compatible with tryptic digestion. Additionally, since histidine has low conductivity, our second aim was to utilize the histidine buffer system for quick electrophoretic separations.

Initial experiments were aimed at investigating the tryptic digestion efficiency in histidine buffer and comparing the results to those typically obtained with ammonium bicarbonate, a traditional buffer used for proteolytic digestion. Figure 19 contains representative MALDI mass spectra for the tryptic digestion of bovine serum albumin performed in 25 mM ammonium bicarbonate (Figure 19A) and 5 mM histidine (Figure 19B). The ion signals labeled with an asterisks denote tryptic peptides from albumin that have been confirmed by peptide mass mapping. The amino acid sequence coverage obtained from these digests are 52% in ammonium bicarbonate and 56% in histidine buffer indicating that digestion in histidine is just as efficient as in the more commonly used ammonium bicarbonate buffer. Trypsin digestion relies on pH and temperature for optimal activity; therefore, since the ammonium bicarbonate and histidine buffer solutions are both within the optimal pH range and the protein was digested at 37°C, the mass spectra of the digests are expected to look similar. Experiments performed in our laboratory on more complex systems (*i.e.,* cell lysates) have utilized histidine as the sample buffer and digestion buffer for successful tryptic digestion (data not shown).

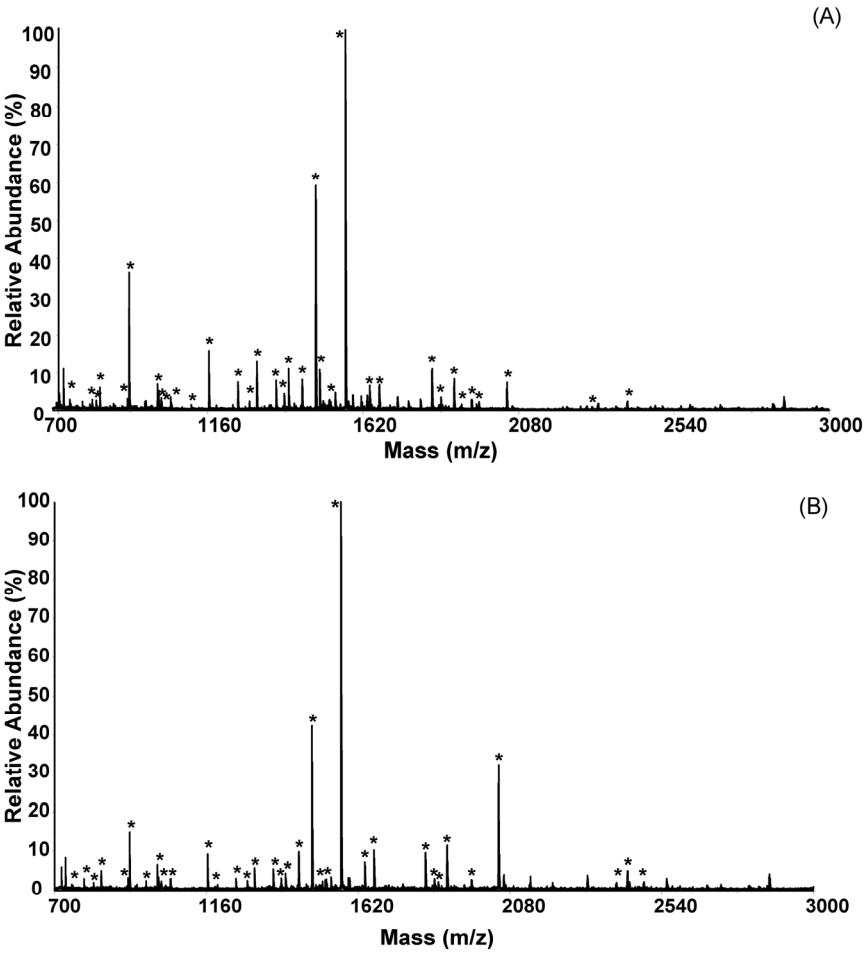

Figure 19. MALDI mass spectrum of a tryptic digestion of bovine serum albumin (10 μg) in (A) 25 mM ammonium bicarbonate and (B) 5 mM histidine. Amino acid sequence coverage values were 52% for ammonium bicarbonate buffer digestion compared to 56% for histidine buffer digestion. Peaks denoted with an asterisks correspond to peptides from bovine serum albumin confirmed by peptide mass mapping. The theoretical conductivities for these buffer solutions are 0.26 S/m for 25 mM ammonium bicarbonate and 6.1E-4 S/m for 5 mM histidine.

Once we determined that tryptic digestion could be successfully performed using histidine as the buffer, we chose to analyze a mixture of tryptic peptides from five standard proteins using isoelectric trapping in the MSWIFT device followed by MALDI mass spectrometry analysis. Our hypothesis is that separations performed in a higher conductivity buffer (ammonium bicarbonate in this case) would result in less efficient separations that take longer compared to those in the low conductivity buffer, histidine. That is, for separations performed in multi-compartmental electrolyzers such as the MSWIFT, the conductivity of the solution in a particular well will dictate the effective field strength for that well (*i.e.,* high conductivity will result in a low field strength). The mathematical derivations outlining the advantages of using low conductivity buffers for electrophoresis have been previously described.[105]

For comparison, a mixture of five standard proteins was subjected to tryptic digestion in either ammonium bicarbonate or histidine buffer. In each case, the mixture was distributed evenly across all compartments in the MSWIFT device and IET was carried out. Figure 20 is a plot of the tandem MS confirmed peptides that are identified in each compartment either separated in ammonium bicarbonate buffer (Figure 20B). Notice in the top figure (ammonium bicarbonate buffer) that fraction 5 (pH 7.6-9.5) possesses several points that correspond to peptides that do not have pI values that fall between the pH values of the membranes used in the experiment. Similarly, much

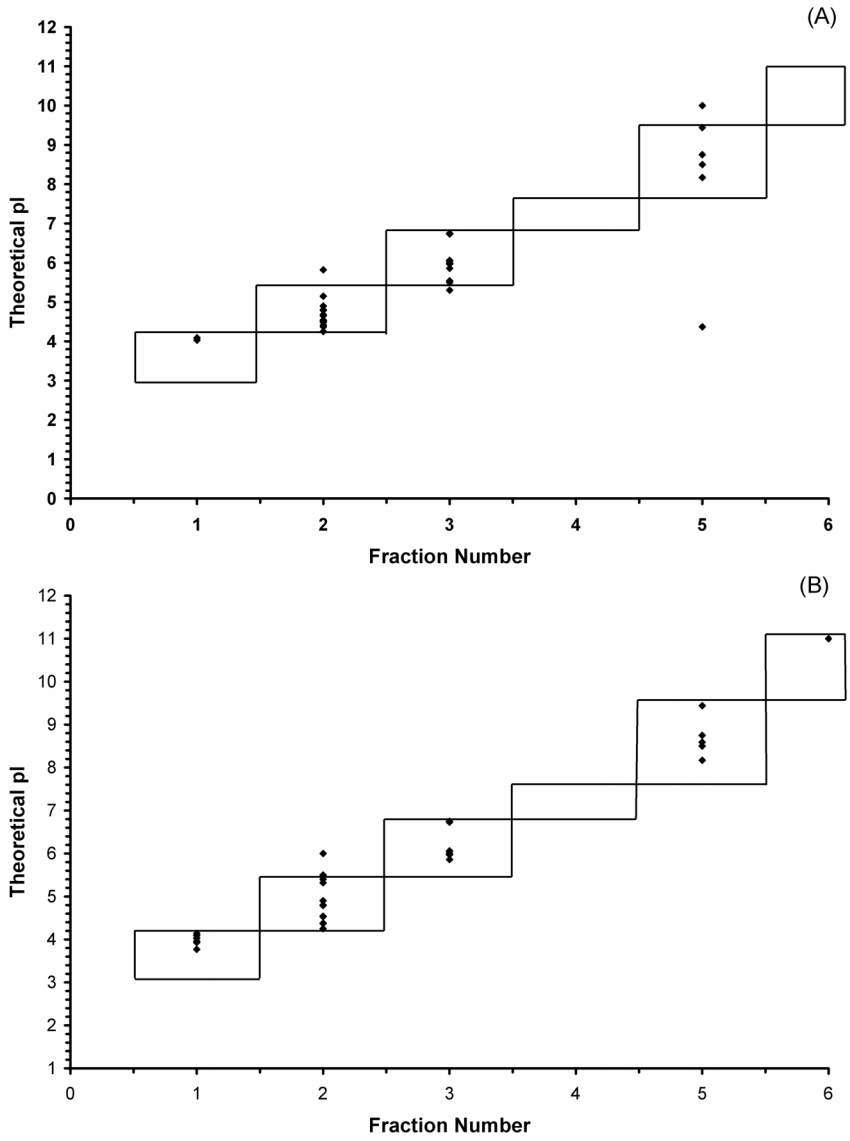

Figure 20. Plot of tandem-MS confirmed (≥ 20 ion score) tryptic peptides from a MSWIFT separation of a mixture of five proteins. Each assigned peptide is plotted as the theoretical pI value versus the observed fraction number. Peptides identified from ammonium bicarbonate buffer solution (A) and histidine buffer solution (B) are provided. Boxes outline the pH values of the buffering membranes used in the separation.

more of this incomplete separation has been observed at even higher concentrations of ammonium bicarbonate (data not shown). Conversely, incomplete separation has not been seen in with the histidine buffer.

To confirm that the high conductivity of the solution was truly the reason why outlier peptides were observed in the fifth fraction, we measured the solution conductivity in each compartment after the IET separation. Figure 21 contains a plot of the measured conductivity from the ammonium bicarbonate separation (squares) and the histidine separation (circles). Clearly, in the fifth fraction, the conductivity of the solution is much higher in the ammonium bicarbonate experiment than in the histidine experiment. Therefore, owing to the conductivity, the field strength across that compartment is very low, causing peptide migration out of the well to be very slow, supporting the reason for the observation in Figure 20.

The most significant advantage of using a low conductivity buffer for IET is the reduction in separation time required for most samples. To illustrate this concept, we performed a time course study of the five-protein mixture digest using the MSWIFT. The digest was loaded in the fourth separation well of MSWIFT and aliquots were taken at various time points and analyzed using MALDI-MS. Figure 22A contains the MALDI mass spectrum of the solution in the fourth separation well (pH 6.8 and 7.6 buffering membranes) after 3 minutes of separation of the digestion mixture prepared in ammonium bicarbonate. Observed in the spectra are several ion signals corresponding to tryptic peptides from the five proteins. The theoretical pI values are provided for each of the assigned peptides. Comparing the spectrum to the same sample separated in

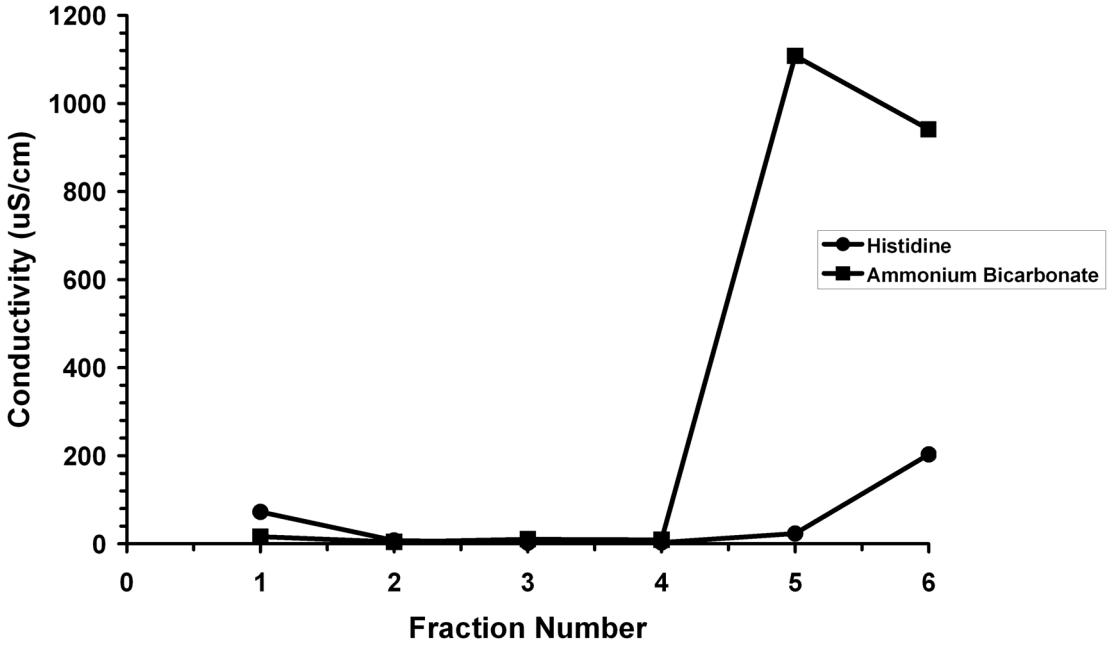

Figure 21. Typical plot of conductivity measured in each fraction after 30 minutes of IET separation of a tryptic digest of bovine serum albumin prepared in histidine or ammonium bicarbonate buffers using the MSWIFT device.

histidine (Figure 22B), the histidine separation occurs at a much faster rate. That is, the complexity of the spectrum taken after three minutes of separation in histidine is less than that of the same sample taken after three minutes of separation in ammonium bicarbonate buffer. The MALDI mass spectra acquired after 3, 10 and 30 minutes of separation are also provided for each buffer solution in Figure 23. Clearly, peptide migration after 10 minutes is nearly complete in the histidine sample (right panel, middle) compared to the high number of ion signals observed in the ammonium

bicarbonate spectrum (left panel, middle). These observations further confirm that under ideal sample conditions (*e.g.,* histidine buffer); peptide migration in the MSWIFT can be very rapid.

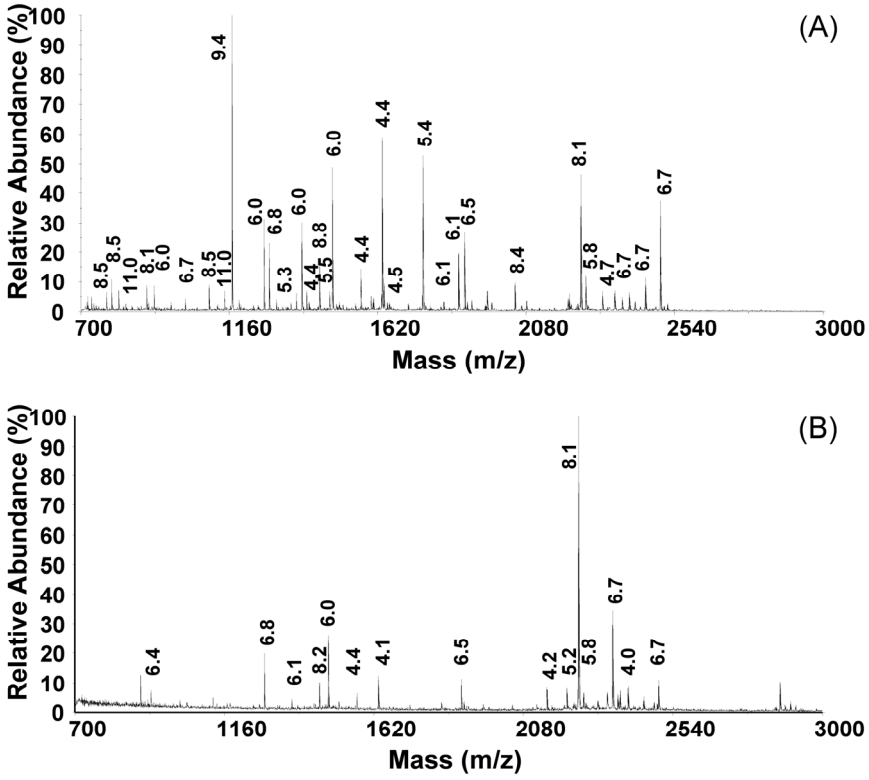

Figure 22. MALDI mass spectra taken from a MSWIFT separation time course study using a mixture of five proteins digested with trypsin. The spectra below are taken from an aliquot of the solution in the separation well bracketed by pH 6.8 and 7.6 (loading fraction) buffering membranes after 3 minutes of separation in the ammonium bicarbonate buffer (A) and histidine buffer (B). Peaks are labeled with their calculated pI values.

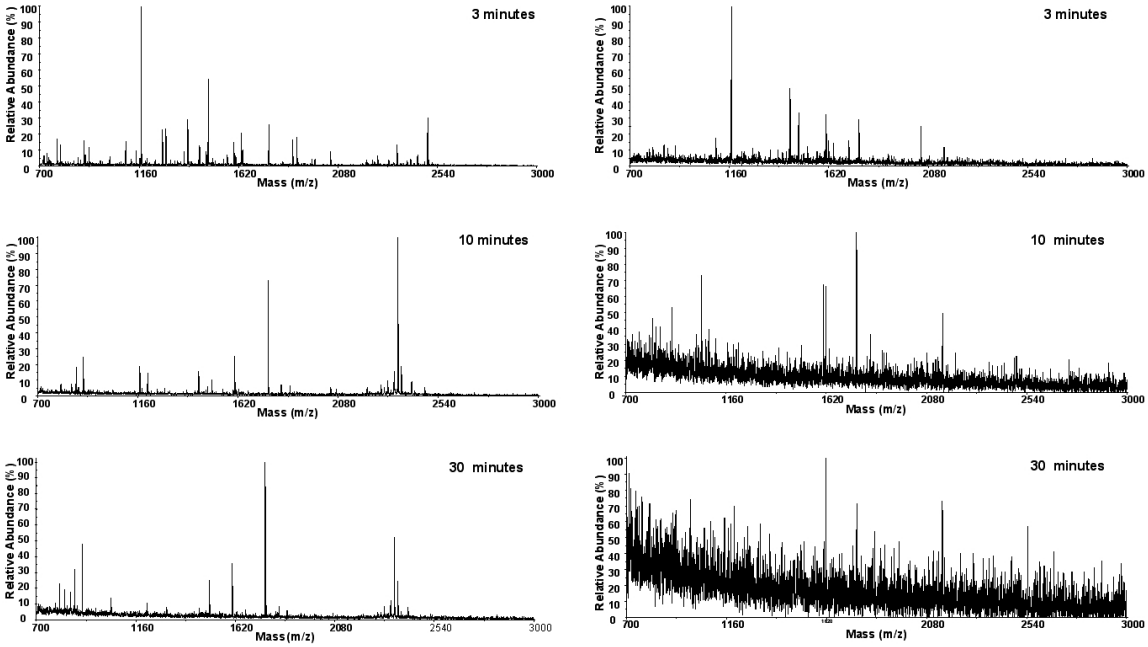

Figure 23. MALDI mass spectra taken from the loading fraction of a time course study of the separation of a five protein mixture tryptic digestion using MSWIFT. The time course data was collected using a digest prepared in ammonium bicarbonate buffer (left panel) and in histidine buffer (right panel).

To confirm that peptides migrating out of the loading compartment are being trapped in the proper fraction, the MALDI mass spectrum taken for the adjacent well (pH 5.4-6.8) at the three minute time point is also provided (Figure 24). The top spectrum (Figure 24A) was taken from the ammonium bicarbonate buffer separation whereas the bottom spectrum (Figure 24B) was taken from the histidine buffer separation. The number of peptide ion signals is much greater in the histidine separation suggesting that more peptides are being transported out of the loading well and are migrating into the more acidic fractions. Additionally, the pI values of the tryptic

peptides observed in the histidine separation are typically more acidic than those observed in the ammonium bicarbonate separation for the same fraction. This may suggest that the very acidic peptides (highly charged at neutral to basic pH) are moving much quicker than the peptides whose pI values are closer to the pH values of the membranes that bracket the loading well. Conversely, the peptide ions in the spectrum taken from the histidine separation contain several peptides that belong in that particular well and some more acidic peptides. One interesting peptide ion signal was observed at m/z 2249.00. This peptide was observed in the MALDI spectrum of the digests performed in both buffers as Figure 24B. We have assigned this to the cytochrome c peptide ^{10}IFVQKCAQCHTVEK^{23} with the heme bound. The heme is known to covalently bind at amino acid residues 15 and 18 which are included within this tryptic peptide fragment.[113] The $[M+H]^+$ calculated for this peptide sequence is 1633.81 and the difference between the observed mass and theoretical is 615.19 Da. The mass difference corresponds to the mass of the heme with and Fe (III) as previously reported.[114] Additionally, we have performed tandem MS experiments on this peptide to confirm the assignment. The theoretical pI value for this peptide is 8.1. However, the attached heme moiety changes the isoelectric point of the peptide owing to its acidic nature.[115] This example of the heme containing peptides demonstrates an additional advantage to using pI-based separation techniques for peptide analysis. In the case of typical data processing (via a database) this peak would likely be omitted from the results as an assignment could not be clearly made based on the parameters set by the user. However,

by manual inspection of the MS and MS/MS data collected for this peptide, clearly an assignment can be made utilizing estimated pI, accurate mass and the isotope pattern.

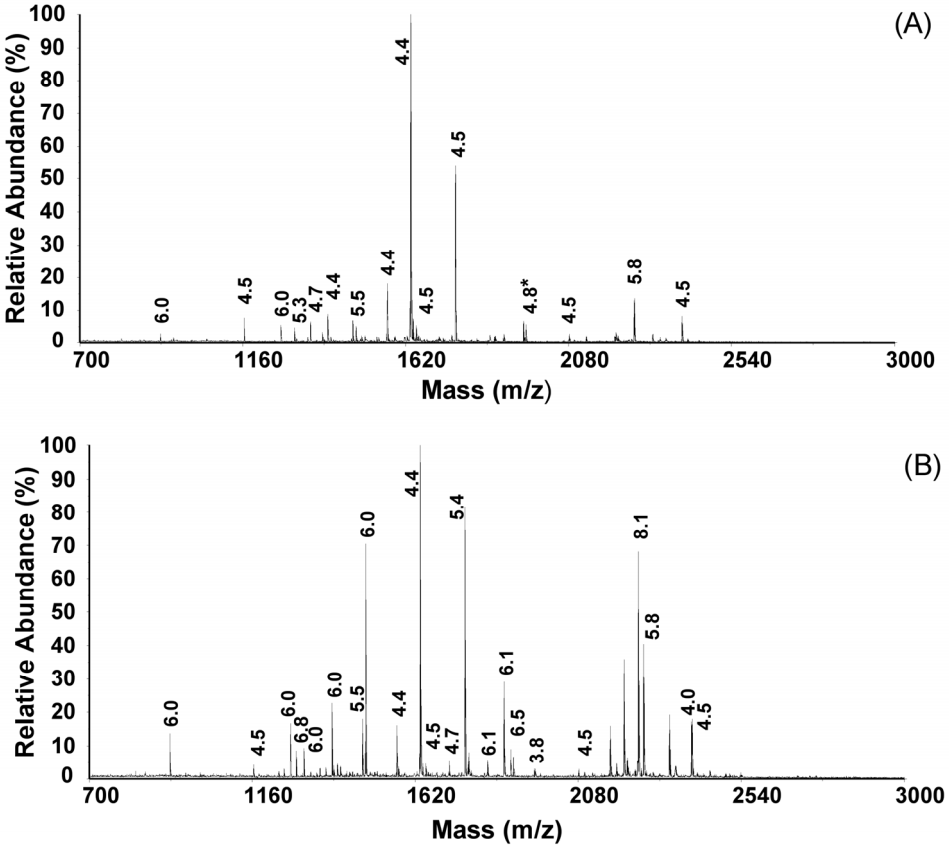

Figure 24. MALDI mass spectrum taken from a time course study using a mixture of five proteins digested with trypsin. The spectra are taken from an aliquot of the solution in the separation well bracketed by pH 5.4 and 6.8 buffering membranes after 3 minutes of the separation in the ammonium bicarbonate buffer (A) and histidine buffer (B). Peaks are labeled with their calculated pI values.

CONCLUSIONS

In this work we have successfully used histidine as a buffer for tryptic digestion of a single protein and for a complex mixture of proteins. Amino acid sequence coverage values do not seem to be compromised suggesting that the utility of histidine as digestion buffer is comparable to that of ammonium bicarbonate. Smearing of peptides during IET separations was observed in experiments with high concentrations of ammonium bicarbonate buffer thus leading us to believe that conductivity in the loading well is affecting the separation. Additionally, we performed pI based separations using the MSWIFT device followed by MALDI-MS/MS analysis to compare the separation efficiency between the histidine and ammonium bicarbonate buffers. Histidine buffer is an excellent choice for quick IET separations without spectral interference or reduction in the quality of the separation.

.

CHAPTER V

USING HISTIDINE BUFFER FOR PROTEOMICS: COUPLING MSWIFT FRACTIONATION AND CAPILLARY ELECTROPHORESIS-MASS SPECTROMETRY FOR HIGH THROUGHPUT PROTEOMIC ANALYSES

INTRODUCTION

Electrophoretic methods provide quick and efficient separation of peptides and proteins for mass spectrometry (MS) –based proteomics studies.[116-118] Migration under an electric field based on molecular weight, charge-to-size ratio or isoelectric point (pI) provides several options for peptide and protein separations. Arguably, the most widely utilized electrophoretic method in proteomics is sodium dodecylsulfate- polyacrylamide gel electrophoresis (SDS-PAGE). Several studies have reported the successful use of SDS-PAGE followed by trypsin digestion and MS analysis (termed GeLC-MS) for protein identification.[21,22] However, several researchers are now incorporating other electrophoretic methods prior to MS analysis into proteomic studies which provide quicker separations and require less sample handling.[26,119,120]

Isoelectric trapping (IET) separations performed in multi-compartmental electrolyzers (MCEs) without the use of carrier ampholytes provide an alternative means for pI-based separations. A relatively new IET device that performs high throughput separations that are MS compatible named membrane separated wells for isoelectric focusing and trapping (MSWIFT) was recently described.[56,120] The MSWIFT device was designed to overcome limitations associated with other such devices, while

elimination of carrier ampholytes allows for reduced sample cleanup procedures. We have described advantages of using MSWIFT for mass spectrometry-based bottom-up proteomic studies,[120] in addition to developing a new sample preparation method using histidine as an isoelectric sample buffer which is compatible with tryptic digestion. Samples prepared in histidine separate rapidly in MSWIFT owing to the low conductivity of this buffer relative to that of more traditional buffers (*e.g.,* Tris, HEPES, ammonium bicarbonate, etc.).[121]

Capillary electrophoresis (CE) coupled with mass spectrometry (CE-MS) has emerged as a powerful tool for proteomics[122] and biomarker discovery.[123-125] We have recently shown the added analytical utility of charge-state specific trends revealed in two-dimensional plots of log (μ^{eff}) versus log (MW) for CE-MALDI-MS data of proteolytic protein digests.[119] These charge-specific trends indicate the number of basic residues in each peptide along a trendline. Therefore, using two-dimensional plots collected from CE-MS experiments, the in-solution charge state can be used as an indication for the presence of charge state altering modifications or as added information to assist in peptide and/or protein identification.

In this work, the MSWIFT device is used for high-throughput pI-based separations followed by CE-MS analysis. Additionally, we incorporate the histidine sample preparation method as previously described which assists in quick and efficient separations both in the MSWIFT and in CE. This method allows us to obtain estimated pI values along with solution charge state information from two-dimensional CE-MS plots which can be used to assist with peptide and protein assignment. Proof-of-concept

experiments performed on tryptic peptides from standard protein mixtures and ribosomal proteins isolated from *Escherichia coli* demonstrate the benefit of performing two-dimensions of separation in a quick, high-throughput manner. Incorporation of a multi-separation scheme (using MSWIFT and CE) allows for improved peptide and protein identification in proteomic studies of complex mixtures while solution charge state information and estimated pI values assist in high confidence peptide assignments.

EXPERIMENTAL SECTION

All chemicals were purchased from Sigma-Aldrich (St. Louis, MO), unless otherwise noted. HPLC grade methanol and isopropanol were purchased from EMD Chemicals Inc. (Gibbstown, NJ). Formic acid (99%) was acquired from Acros Organics (Morris Plains, NJ). Sequencing grade trypsin was purchased from Promega (Madison, WI). All experiments were performed with 18MΩ water (ddH_2O) obtained using a purification unit from Barnstead International (Dubuque, IA). All chemicals were used as received without further purification.

Membrane Separated Wells for Isoelectric Focusing and Trapping (MSWIFT)

Details outlining the design and assembly of the MSWIFT have been described.[55, 56] The alumina separation compartments of the MSWIFT were assembled serially and contained up to 200 μL of sample solution. Poly(vinyl-alcohol) based buffering membranes with tunable pH values were synthesized in-house.[41-43] The anolyte was 3 mM methanesulfonic acid, whereas the catholyte was 3 mM sodium hydroxide.

Typical separation times ranged from 45-60 minutes at 5W constant power. Theoretical pI values were calculated using the compute pI/MW tool from ExPASy.[79]

Proteolytic Digestion and Sample Preparation

A mixture containing 10 μg each of the following five proteins: bovine serum albumin, apo-transferrin, α_{s1}-casein, ribonuclease A, and cytochrome C was dissolved in 200 μL of either 10 mM histidine or 25 mM ammonium bicarbonate. The protein mixture was reduced and denatured with 5 mM tris(2-carboxyethyl)phosphine at 60 °C for 1 hour. Alkylation was performed by the addition of 2 mM methyl methanethiosulfonate and incubation of the mixture at room temperature for ten minutes. Trypsin was added at a 1:50 (w/w) enzyme to protein ratio and the solution was incubated at 37 °C overnight. The pH values of the membranes used for this experiment were: 2.9, 4.2, 5.4, 6.8, 7.6, 9.5, and 11.0. The contents of each well were mixed via pipette, then a 1 μL aliquot was taken for MALDI-MS analysis.

70S ribosomes were isolated from *E. coli* using a standard protocol.[80] Ribosomal RNA was removed by acid precipitation (1% v/v TFA) followed by centrifugation. One hundred micrograms of soluble proteins were then precipitated using six-fold excess volumes of cold acetone. The protein pellet was re-suspended in 5 mM histidine buffer followed by tryptic digestion (1:100 enzyme to protein ratio) at 37 °C overnight. Following digestion the protein solution was thermally denatured at 60°C for 1 hr. The protein solution was then allowed to digest for an additional 3 hrs with a subsequent aliquot of trypsin as previously described.[81] The pH values of the buffering membranes

used for this separation were: 2.9, 4.7, 5.4, 6.8, 7.5, 8.4, and 11.0. The sample was loaded in the well bracketed by pH 7.5 and 8.4 buffering membranes. The resulting MSWIFT fractions were concentrated 10-fold and re-suspended in 0.5 mM histidine buffer for CE-MS analysis.

CE-MALDI

A layer of 5-mg mL^{-1} α-cyano-4-hydroxycinnamic acid (CHCA) was applied onto the MALDI plate prior to the CE separations using an x-y-z translation stage (ProBot, LC Packings, Sunnyvale, CA). CHCA was dissolved in 12:7:1 MeOH:ddH_20:IPA (v/v/v) with 10-mM dihydrogen ammonium phosphate and doped with 50-fmol μL^{-1} bradykinin fragment (2-9) (PPGFSPFR) and 150-fmol μL^{-1} ACTH fragment (18-39) (RPVKVYPNGAEDESAEAFPLEF) as internal calibrants. The CHCA matrix solution was infused through a fused-silica capillary at 1.0 μL min^{-1} with a 5 second spotting interval to prepare a 30 row by 30 column array (900 total spots). MALDI plates were used for CE fraction collection using a sheath liquid composed of 50:50 MeOH: 250 mM FA (0.5 μl min^{-1} flow rate) as the overlayer.

CE separations were carried out on a 70-cm (50 μm i.d., 360 μm o.d.) fused-silica capillary (Polymicro Technologies, Phoenix, AZ) with 200-nm UV detection at 50 cm on a homebuilt apparatus. The cathodic end capillary tip was interfaced to a ProBot (LC Packings, Sunnyvalve, CA) as previously described.[119] The CE capillary was coated with a neutral linear polyacrylamide dynamic coating (Ultratrol LN, Target Discovery, Palo Alto, CA). The background electrolyte consisted of 250-mM formic

acid at pH 2.20. Sample stacking injections were performed by injecting at 2.0 psi for 20 seconds, corresponding to 65 nl injection volumes. Separations were performed at a potential of +25 kV, using a 30-kV high-voltage power supply (Gamma High-Voltage Research, Ormond Beach, FL). UV electropherograms were collected using a homebuilt virtual instrument interface in the LabView 7.1 (National Instruments, Austin, TX) environment. CE fractions were collected using the ProBot with 10 second spotting intervals.

MALDI-MS and MALDI-MS/MS

All MALDI-MS experiments were performed using a 4700 Proteomics Analyzer MALDI-TOF/TOF (Applied Biosystems, Foster City, CA). The MS data were acquired using the reflectron detector in positive ion mode (700-4500 Da) with internal calibration. Collision induced dissociation tandem MS spectra were acquired using air at the medium pressure setting and at 1 kV of collision energy. All MS and MS/MS data were searched against the SwissProt protein sequence database using the GPS Explorer (Applied Biosystems) software with an in-house license of MASCOT (v 2.1).[83]. Database searching parameters were as follows; taxonomy, Metazoa; precursor mass tolerance, 50 ppm; enzyme, trypsin; missed cleavages, one; and variable modifications, MMTS I, oxidation (M). Database searches performed for the ribosome data included the same parameters with the exception of the taxonomy being *Escherichia coli*. Peptide identification was considered with a MASCOT ion score of 20 or greater. Protein

identifications were made at the 99.990% confidence level as calculated by the GPS Explorer software taking into account the MASCOT score for each peptide.

RESULTS AND DISCUSSION

For complex mixtures, such as whole cell lysates where hundreds to thousands of proteins are present, multiple separation techniques are required in order to analyze low abundance proteins which are typically the analytes of interest. To achieve this, we chose to couple, off-line, fractions collected from the MSWIFT device which provides pI-based separations with CE-MALDI-MS while also utilizing the histidine sample preparation method previously described. Incorporating the histidine sample preparation and a two-dimension electrophoretic separation scheme results in rapid separation of analytes that can be analyzed using MS in a high-throughput manner. A schematic of the general experimental scheme is provided in Figure 25.

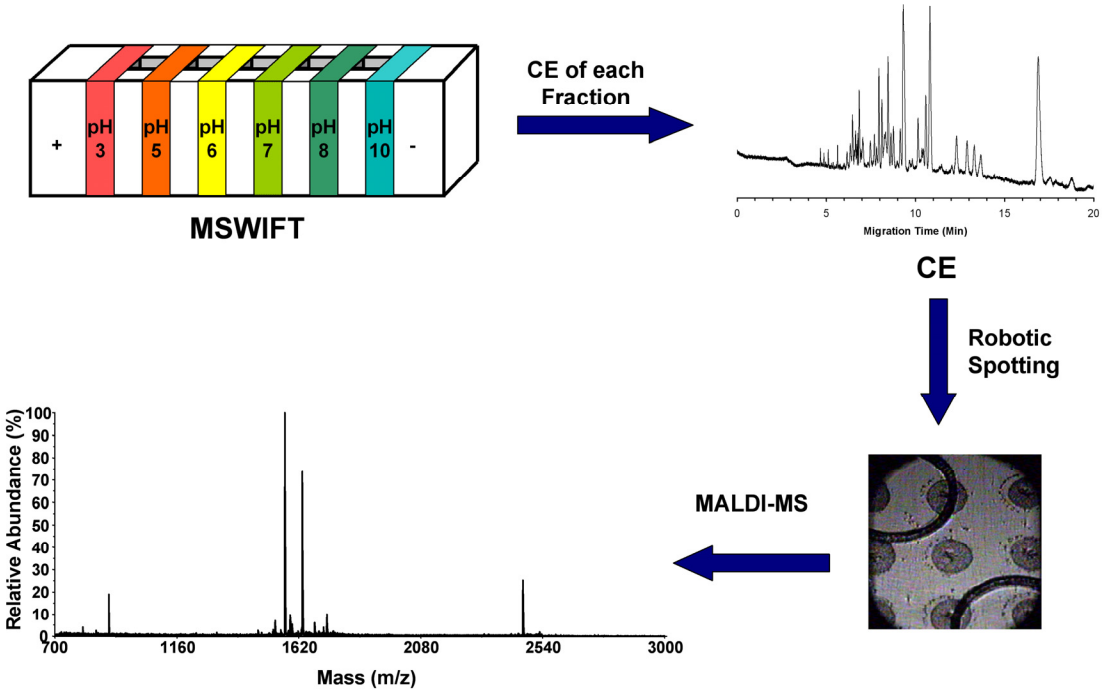

Figure 25. Experimental scheme for the MSWIFT-CE-MS analysis of tryptic peptides. Peptides are first separated based on pI using the MSWIFT, followed by CE separation of the contents of each MSWIFT well. The eluent from the CE is directly spotted onto a MALDI target plate via a robotic spotting device and each spot is interrogated to obtain MS and MS/MS data.

To initially evaluate the effectiveness of coupling MSWIFT fractionation with CE-MS, their orthogonality must be considered. Orthogonality ensures that the separation achieved in the first dimension is not lost in the second dimension.[91] A similar study reported that separation by an IEF device (OFFGEL^{TM}) followed by CE results in 43% orthognality and, for comparison, the commonly used SCX-RPLC coupling has an orthognality of 47% without the use of mass spectrometric detection.[126]

However, it should be noted that the number of fractions collected from MSWIFT is lower than those collected from the OFFGEL^{TM}, thereby potentially reducing the orthognality slightly. Since the MSWIFT device is capable of holding a variable number of wells, the same configuration could be repeated using MSWIFT and given that data points were observed in roughly the same number of bins, the orthognality would be considered equivalent. Furthermore, we chose to investigate the distribution of pI and MW and charge stage in a tryptic digest of a standard protein to ensure that coupling the two methods would be advantageous for tryptic peptide fractionation. Figure 26 contains a plot of molecular weight vs. theoretical pI (Figure 26a) for an *in silico* digest of bovine serum albumin considering one missed cleavage This plot indicates that there is a distribution of pI values across the digest and that the high pI peptides tend to cluster in the low MW range. However, the majority of the tryptic peptides possess acidic pI values similar to findings obtained in our laboratory and those previously reported for *Escherichia coli*.[88] Performing CE-MALDI MS is valuable owing to the added dimension of information that can be obtained (*i.e.,* in-solution charge state). The solution charge state of peptides can be determined based on the charge-state trendlines that are observed when plotting log (μ^{eff}) versus log (MW). The resulting charge-state trendlines can be incorporated as validation criteria for peptide identification; specifically, when tandem MS data is poor or not available. Figure 26b contains a plot of theoretical pI versus predicted in-solution charge state for a tryptic digest of bovine serum albumin at pH 2.2 to consider whether coupling the techniques would be valuable to proteomic analysis. The distribution of theoretical pI values over charge states 1-5

further confirms that coupling these two methods is advantageous for proteomic studies. In addition to using estimated pI information obtained from MSWIFT fractionation, including charge state information from CE-MS can result in increased confidence of peptide assignment.

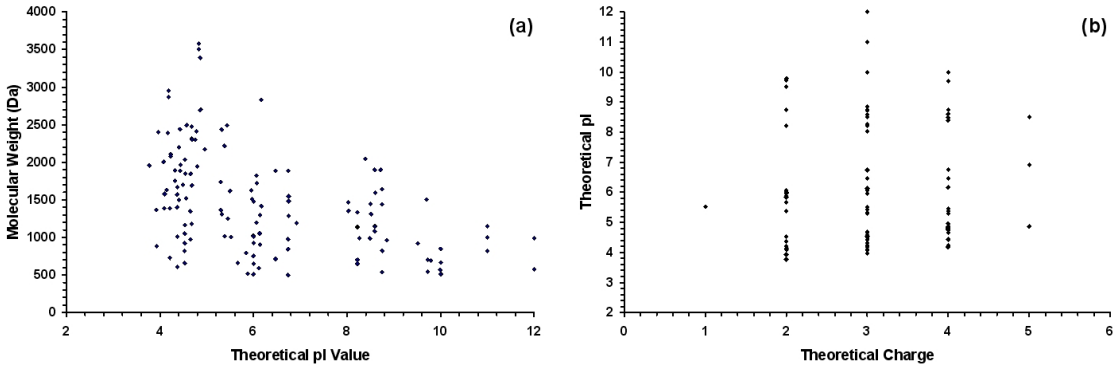

Figure 26. Plot of molecular weight versus theoretical pI value (a) and plot of theoretical pI value versus in solution charge at pH 2.2 (b) for an *in silico* tryptic digestion of bovine serum albumin from molecular weight 500-4000 Da allowing for one missed cleavage.

Initial proof-of-concept experiments using MSWIFT for pI-based fractionation followed by CE-MALDI-MS/MS analysis were performed using a mixture of tryptically derived peptides from a standard mixture of five proteins. The first step was to confirm that MSWIFT fractionation was occurring properly. Figure 27 is a plot of the theoretical pI value versus fractionation number from the MSWIFT fractionation of this standard

mixture. Peptides that have been confirmed by tandem MS experiments are represented in the fraction number in which they were observed.

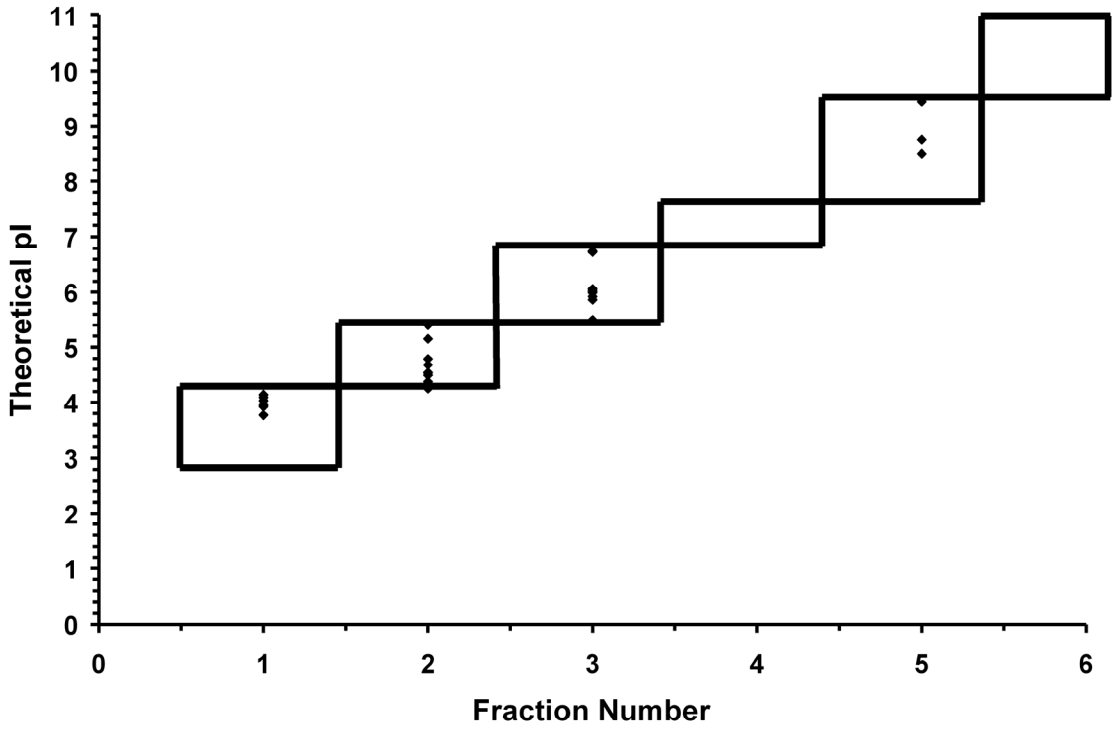

Figure 27. Plot of theoretical pI versus fraction number for tryptic peptides confirmed by tandem MS data from the separation of a tryptic digest of five standard proteins using the MSWIFT device. Peptides with the same theoretical pI value observed in the same well are represented as a single point.

Following confirmation that the pI-based fractionation was successful, aliquots from each MSWIFT fraction were subjected to CE-MALDI-MS/MS analysis for further separation. Incorporating the histidine sample preparation method not only assists in rapid separation in the MSWIFT, but also allows for higher sample loads using sample stacking methods for CE owing to the low conductivity of the sample buffer.[127] Figure 28 contains a representative two-dimensional plot obtained from the CE separation of the pH 5.4-6.8 MSWIFT fraction. Distinct charge state trends are observed in the data corresponding to +2, +3, and +4 charged. Several examples are provided of tandem MS confirmed peptides which possess theoretical pI values that fall between the pH values of the buffering membranes used in the MSWIFT and also fall on the correct trend lines corresponding to the respective solution charge states at pH 2.2.

To further analyze whether coupling these two separation methods is advantageous for proteomic profiling studies, the protein identification data obtained from database searching was compared among each technique. Table 4 contains a summary of the number of tandem MS confirmed peptides and the corresponding amino acid sequence identified for each protein in the mixture. Note that while only five standard proteins were used, α_{S1}-casein contains a high abundance contaminant (α_{S2}-casein). Therefore, corresponding peptides and this protein were also identified. Take for example, the protein bovine serum albumin (ALBU_BOVIN). MSWIFT separation

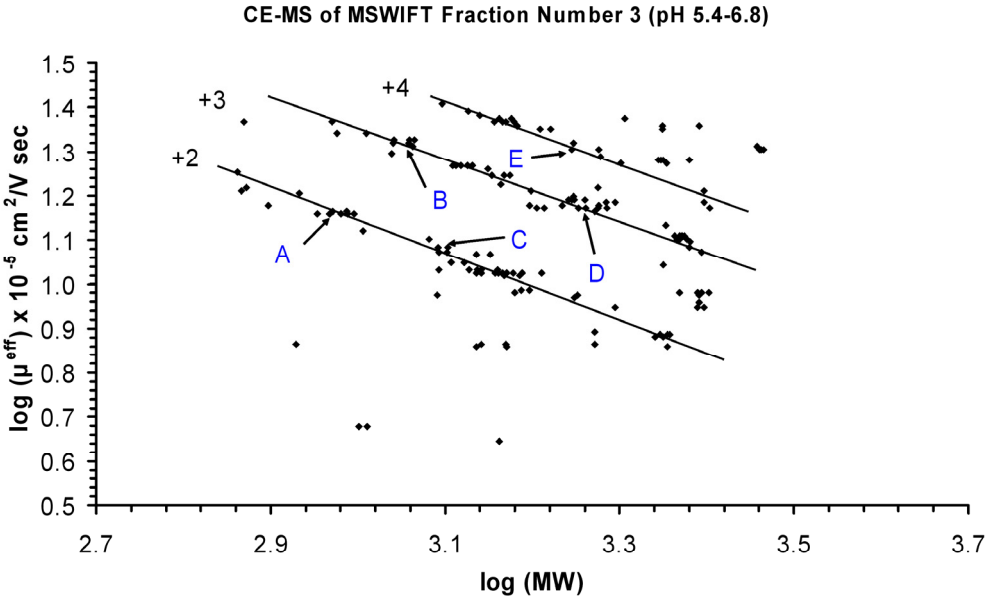

Label	Peptide Sequence	$[M+H]^+_{obs}$	Mass Error	pI (a)	q (b)	Modification	Protein ID
			ppm				
A	^{161}YLYEIA***R***^{167}	927.49	-5	6.00	2		ALBU_BOVIN
B	^{460}CCT***K***PESE***R***^{468}	1144.42	2	6.13	3	MMTS (2)	ALBU_BOVIN
C	^{106}YLGYLEQLL***R***^{115}	1267.70	-1	6.00	2		CASA1_BOVIN
D	^{508}***R***PCFSALTPDETYVP***K***^{523}	1823.90	-1	6.06	3		ALBU_BOVIN
E	^{300}D***K***PDNFQLFQSP***H***G***K***^{314}	1757.86	-1	6.75	4	MMTS(1)	TRFE_BOVIN

a - Theoretical pI values calculated using ExPASy pI/MW calculator
b - Measured charge state determined from 2D CE-MS plot

Figure 28. Representative plot of MSWIFT-CE-MS data obtained from the analysis of a tryptic digest of five proteins. By plotting log (μ^{eff}) versus log (MW), trendlines can be observed corresponding to the in-solution charge state of the peptide at pH 2.2. Several peptides (denoted A-E) are provided as examples in which the theoretical pI values and charge state agree with experimentally determined values.

only followed by MALDI-MS/MS analysis results in 32% amino acid sequence coverage compared to 46% obtained from CE-MALDI-MS/MS. Coupling these two methods increases the sequence coverage almost two-fold to 63%. Similar trends are observed with each of the other standard proteins with the exception of ribonuclease A (RNAS1_BOVIN). The slight decrease in the sequence coverage for this protein may be owing to an increase in the number of overall signals observed in the mass spectrum, thereby excluding one or two peptides from tandem MS analysis. Alternatively, poor tandem MS quality may also account for this slight decrease. Alternately, ribonulcease A has very few tryptic sites therefore a decrease in only one peptide being detecting could result in a significant loss in amino acid sequence coverage. Regardless, a general trend in the increased number of peptides identified and amino acid sequence coverage is observed.

Following initial proof of concept experiments, we sought to apply this experimental scheme to a more complex mixture. The analysis of tryptic peptides from ribosomal proteins is ideal owing to their inherent properties. *Escherichia coli* ribosomes (70S subunit) contain 56 proteins spanning 3-30 kDa and possess large numbers of arginine and lysine residues.[128] First, we performed MALDI-MS/MS analysis of a

Table 4. Summary of protein identification data for a five protein mixture tryptically digested and subjected to MSWIFT-MS only, CE-MS only, and MSWIFT-CE-MS analysis. The total number of peptide assignments and amino acid sequence coverage values are provided for each standard protein and each method.

MSWIFT MS

Protein ID	Peptides	Seq. Cov. (%)
ALBU_BOVIN	18	32
TRFE_BOVIN	14	27
CYC_HORSE	6	52
CASA1_BOVIN	5	33
CASA2_BOVIN	1	4
RNAS1_BOVIN	5	58

CE-MS

Protein ID	Peptides	Seq. Cov. (%)
ALBU_BOVIN	26	46
TRFE_BOVIN	20	38
CYC_HORSE	8	56
CASA1_BOVIN	6	40
CASA2_BOVIN	N/A	N/A
RNAS1_BOVIN	4	54

MSWIFT CE-MS

Protein ID	Peptides	Seq. Cov. (%)
ALBU_BOVIN	45	63
TRFE_BOVIN	44	64
CYC_HORSE	13	68
CASA1_BOVIN	11	44
CASA2_BOVIN	8	27
RNAS1_BOVIN	4	46

ribosomal protein tryptic digest without any separation which resulted in the identification of 12 ribosomal proteins. MSWIFT-MALDI-MS/MS yields 20 proteins compared to 27 proteins identified from CE-MALDI-MS/MS alone. Finally, by coupling the two techniques, we were able to identify 33 ribosomal proteins, clearly

showing an increase in the number of protein identifications compared to those obtained from a single fractionation step or no fractionation. From these experiments we have demonstrated that pI-based fractionation methods are compatible with CE separation in the second dimension followed by MALDI-MS/MS analysis. Similar work performed by Girault *et al.* shows that coupling these two electrophoretic methods and MS can be an alternative to LC-MS analysis.[126] To illustrate the type of information that can be obtained from this two dimensional separation experiment, Figure 29a contains the two-dimensional plot obtained from CE-MALDI analysis of the pH 2.9 – 4.7 fraction collected from MSWIFT. Several distinct trendlines can be observed corresponding to the +1, +2, and +3 in-solution charge states. A few examples are provided (Figure 29b) such as the tryptic peptide ^{20}QYDINEAIALL***K***^{31} labeled D in the plot from the protein L1 observed at m/z 1390.73 that has a theoretical pI value of 4.37 and calculated charge of +2. The theoretical pI value falls between the pH values of the buffering membranes and the predicted charge of +2 is correct considering the protonation of the N-terminus and the C-terminal lysine residue. Peptides similar in both mass and pI can be further separated on the basis of different charge states. For example, the ribosomal L24 tryptic peptide ^{7}***R***DDEVIVLTG***K***^{17} (m/z 1244.68, pI 4.56) denoted as A falls on the +3 trendline, while ^{110}ALEEAGAEVEV***K***^{121} (m/z 1244.62, pI 4.09) from the L7/L12 ribosomal complex is located on the +2 trendline. These two peptides would require greater than 22,000 mass spectral resolution to completely resolve their 0.06 Da mass difference. Note that only MSWIFT fraction 1 contains +1 charge state peptides which could be a peptide with a charge altering modification (*e.g.,* sulfation, phosphorylation

or acetylation) or the C-terminus of the protein. The +1 charge state peptides ^{79}FISIEAE^{85} (m/z 808.37, pI 4.24) and ^{135}SM(ox)GLVVED^{142} (m/z 865.38, pI 4.03) correspond to the C-terminal peptides from the ribosomal proteins L27 and L11, respectively. Overall, the added MSWIFT CE-MS separation scheme provides accurate mass measurement, estimated pI range, and the in-solution charge state which increases the confidence of peptide identification and therefore protein identification and also increases the number of peptide identifications, resulting in increased amino acid sequence coverage values for those proteins which are identified.

Here we show the use of a low conductivity buffer (*e.g.,* histidine) which assists in pI-based and charge to size – based separations. While histidine was sufficient for these experiments, several properties must be considered. For example, the buffering capacity of 10 mM histidine is 1.1 mM compared to 3.6 mM for 25 mM ammonium bicarbonate illustrating a limitation to this method.

(a)

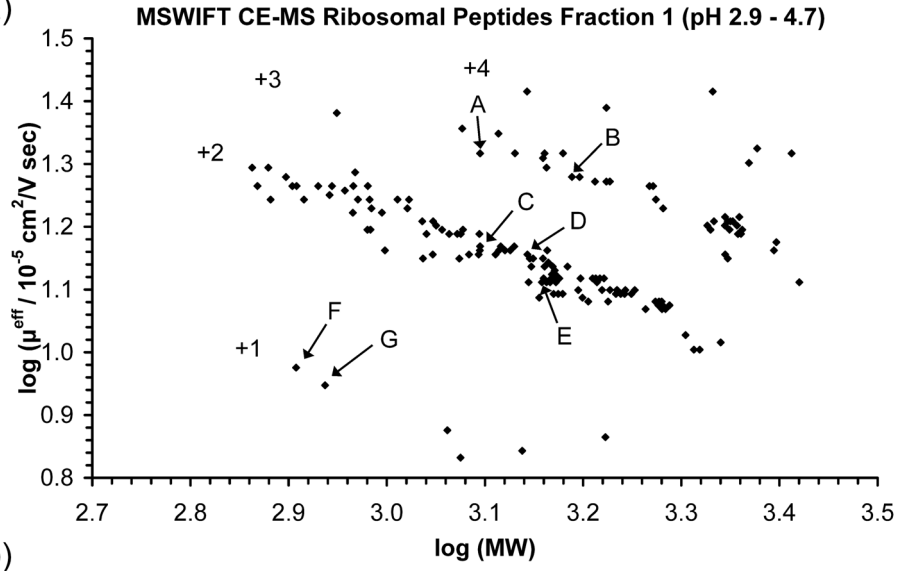

(b)

Label	Peptide Sequence	Protein	$[M+H]^+_{obs}$	t_m	pI (a)	q (b)	$\log(\mu^{eff})$	log(m/z)
A	^{7}***R***DDEVIVLTG***K***^{17}	L24	1244.678	12.17	4.56	3	1.317	3.095
B	^{18}S***H***DALTAVTSLSVD***K***^{32}	L32	1543.769	13.00	5.19	3	1.279	3.189
C	^{110}ALEEAGAEVEV***K***^{121}	L7/L12	1244.622	15.67	4.09	2	1.169	3.095
D	^{20}QYDINEAIALL***K***^{31}	L1	1390.733	16.00	4.37	2	1.156	3.143
E	^{56}DGYADGWAQAGTA***R***^{69}	L6	1438.649	17.17	4.21	2	1.112	3.158
F	^{79}FISIEAE^{85}	L27	808.370	21.00	4.24	1	0.976	2.908
G	^{135}SM(ox)GLVVED^{142}	L11	865.375	21.83	4.03	1	0.948	2.937

a - Theoretical pI values calculated using ExPASy pI/MW Calculator: http://us.expasy.org/cgi-bin/pi_tool
b - Measured charge state determined from 2D CE-MS plot

Figure 29. (a) Typical 2D plot of $\log(\mu^{eff})$ versus log(MW) for CE-MS data obtained from MSWIFT fraction 1 (pH range 2.9 – 4.7). (b) Table summarizing proteolytic peptides labeled along each in-solution charge-state trendline. The peptide amino acid sequence, ribosomal protein, observed m/z values, migration time t_m, theoretical pI, measured charge state (q), log (μ^{eff}) and log(MW) are given for each peptide.

Secondly, downstream processing, such as affinity chromatography (e.g., nickel column) could be affected. In any case, these experiments highlight the importance of buffer selection and how separations can be improved when considering buffer composition. Moreover, following proteolytic digestion performed in histidine, electrophoretic separation methods can be easily performed owing to the low conductivity of the buffer and sample stacking can be easily achieved which improves the sample loading capacity in CE. Peptide information that can be obtained from both electrophoretic methods can further be used to increase peptide assignment confidence and coupling also increases the number of protein identifications that can be made by increasing the overall peak capacity.

CONCLUSIONS

In this work we have successfully used histidine as a buffer for tryptic digestion of simple protein mixtures and for complex protein mixtures. Additionally, MSWIFT fractionation and CE separation are compared for bottom-up proteomic analysis and have also been coupled to improve protein sequence coverage. The two-dimensional separation scheme is orthogonal; therefore compromises in either separation mode are not necessary. Peptides with similar pI values but different in-solution charge states (owing to the number of basic residues) are distinctly identified in two-dimensional CE-MS plots of $\log(\mu^{eff})$ vs. log (MW). By incorporating these two separation techniques, estimated pI and charge state values are obtained to further aid in protein identification.

This method provides an alternative to the more commonly used chromatographic techniques allowing for high-throughput analyses.

CHAPTER VI

CONCLUSIONS

MSWIFT FRACTIONATION FOR BOTTOM-UP PROTEOMICS

Isoelectric Point-Based Fractionation Using MSWIFT

In this work, data is presented to illustrate that a small-scale isoelectric point fractionation device, MSWIFT, is an MS-compatible fractionation device whose solutions from each compartment can be analyzed directly by mass spectrometry or can be subjected to LC-MS/MS analysis. Proof-of-concept experiments performed with standard peptide mixtures confirm pI-based fractionation, MS compatibility and also demonstrate an advantage of fractionation namely, decreasing ion suppression effects that are commonly observed for complex mixtures. The MSWIFT device has also been used for pre-fractionation of tryptic peptides from a yeast cell lysate where resulting fractions were subjected to LC-MS/MS analysis. A total of 593 protein identifications were obtained from a single analysis.

Multi-Stage Fractionation for Proteomics

MSWIFT can also be utilized in multi-stage separation platforms (IET^n) as was illustrated in preliminary experiments using yeast tryptic peptides. Subjecting the protein digest to pI-based fractionation allowed for distribution of tryptic peptides across six fractions. An aliquot from the second fraction (pH 4.0-5.4) was then subjected LC-MS/MS analysis followed by additional fractionation of the remaining solution. The

three resulting fractions from the second-stage fractionation were then analyzed using LC-MS/MS. The number of identified unique peptides doubled by performing the second stage of fractionation and the number of protein identifications increased from 112 to 177. This preliminary data led us to perform a large-scale analysis utilizing this IET^n experimental scheme.

Following the successful multi-stage separation experiment performed on yeast tryptic peptides, the experimental platform was utilized for the first large-scale proteomic profiling study of the fungus *Neurospora crassa*. MSWIFT-LC-MS/MS analysis of *N. crassa* tryptic peptides resulted in identification of 2558 unique peptides and 672 proteins. Performing the second stage of fractionation followed by LC-MS/MS increased the number of peptides and proteins identified to 4075 and 731 respectively. This experimental platform proved to be advantageous and does not discriminate considering the majority (all but one) of proteins in the first stage were also identified from searching the second stage. This initial study clearly provides an indication of the *N. crassa* proteins that are expressed at high or moderate levels. Further experimentation is required in order to provide a more complete report on the total number of expressed proteins.

Sample Preparation and Separation in Histidine Buffer

To improve electrophoretic separations, a new sample preparation method has been introduced by incorporating a low conductivity buffer, histidine into the work-flow. Histidine is an isoelectric buffer with a pH ~7.5 at low millimolar concentrations. Tryptic digests performed in histidine compared to the more traditional buffer ammonium bicarbonate buffer are comparable for standard proteins. More complex mixtures such as ribosomal proteins and whole cell lysates have also been successfully digested using the histidine buffer. To illustrate the advantage of using low conductivity buffers, a fractionation time-course study was performed on a tryptic digest of five standard proteins. Compared to using ammonium bicarbonate, the peptides prepared in histidine migrate out of the loading well of MSWIFT much quicker. Also, the peptides isolated in the adjacent well are very acidic for the ammonium bicarbonate buffer compared to the neutral peptides expected in the well as found with the histidine buffer suggesting that peptides are migrating and being trapped faster with histidine as sample buffer.

Coupling MSWIFT and CE Separation for Bottom-up Proteomics

An additional advantage to the histidine buffer sample preparation method and MSWIFT fractionation is to be able to couple MSWIFT fractionations with capillary electrophoresis (CE) – MS/MS. Two-dimensional plots of $\log(\mu^{eff})$ versus log(MW) from CE-MALDI MS data results in charge state trend lines corresponding to the in-solution charge state of the peptides under the separation conditions used during CE.

This added information can assist with peptide identification and provide indications for peptide modifications such as phosphorylation, methylation, oxidation and disulfide bonding. By coupling MSWIFT fractions with CE-MS/MS analysis, peptide pI and in-solution charge state can be utilized to assist with peptide assignment, particularly when tandem MS data is poor or not available. To demonstrate the utility of coupling these two techniques, tryptic peptides from standard proteins and ribosomal proteins were analyzed where an increase in the number of ribosomal protein identifications was obtained when coupling the two techniques compared to performing each separation individually followed by MALDI-MS/MS analysis. Therefore, utilizing histidine sample preparation improves the MSWIFT separation, CE sample stacking ability and coupling the two methods provides a feasible means for performing high throughput mass spectrometry-based proteomic studies.

REFERENCES

(1) Anderson, N. L.; Anderson, N. G. *Molecular & Cellular Proteomics* **2002**, *1*, 845-867.

(2) Karas, M.; Hillenkamp, F. *Analytical Chemistry* **1988**, *60*, 2299-2301.

(3) Fenn, J. B.; Mann, M.; Meng, C. K.; Wong, S. F.; Whitehouse, C. M. *Science* **1989**, *246*, 64-71.

(4) Aebersold, R.; Mann, M. *Nature* **2003**, *422*, 198-207.

(5) Wehr, T. *Lc Gc North America* **2006**, *24*, 1004-+.

(6) McLafferty, F. W. *Science* **1981**, *214*, 280-287.

(7) Loo, J. A.; Edmonds, C. G.; Smith, R. D. *Science* **1990**, *248*, 201-204.

(8) Kelleher, N. L. *Analytical Chemistry* **2004**, *76*, 196A-203A.

(9) Tang, H. Y.; Ali-Khan, N.; Echan, L. A.; Levenkova, N.; Rux, J. J.; Speicher, D. W. *Proteomics* **2005**, *5*, 3329-3342.

(10) Wu, S.; Lourette, N. M.; Tolic, N.; Zhao, R.; Robinson, E. W.; Tolmachev, A. V.; Smith, R. D.; Pasa-Tolic, L. *Journal of Proteome Research* **2009**, *8*, 1347-1357.

(11) Strader, M. B.; VerBerkmoes, N. C.; Tabb, D. L.; Connelly, H. M.; Barton, J. W.; Bruce, B. D.; Pelletier, D. A.; Davison, B. H.; Hettich, R. L.; Larimer, F. W.; Hurst, G. B. *Journal of Proteome Research* **2004**, *3*, 965-978.

(12) Waanders, L. F.; Hanke, S.; Mann, M. *Journal of the American Society for Mass Spectrometry* **2007**, *18*, 2058-2064.

(13) Righetti, P. G.; Castagna, A.; Herbert, B.; Reymond, F.; Rossier, J. S. *Proteomics* **2003**, *3*, 1397-1407.

(14) Malmstrom, J.; Lee, H.; Aebersold, R. *Current Opinion in Biotechnology* **2007**, *18*, 378-384.

(15) Washburn, M. P.; Wolters, D.; Yates, J. R. *Nature Biotechnology* **2001**, *19*, 242-247.

(16) McDonald, W. H.; Ohi, R.; Miyamoto, D. T.; Mitchison, T. J.; Yates, J. R. *International Journal of Mass Spectrometry* **2002**, *219*, 245-251.

(17) Cantin, G. T.; Yi, W.; Lu, B. W.; Park, S. K.; Xu, T.; Lee, J. D.; Yates, J. R. *Journal of Proteome Research* **2008**, *7*, 1346-1351.

(18) Gilar, M.; Olivova, P.; Daly, A. E.; Gebler, J. C. *Journal of Separation Science* **2005**, *28*, 1694-1703.

(19) Dowell, J. A.; Vander Heyden, W.; Li, L. *Journal of Proteome Research* **2006**, *5*, 3368-3375.

(20) Boersema, P. J.; Divecha, N.; Heck, A. J. R.; Mohammed, S. *Journal of Proteome Research* **2007**, *6*, 937-946.

(21) Pernemalm, M.; Orre, L. M.; Lengqvist, J.; Wikstrom, P.; Lewensohn, R.; Lehtio, J. *Journal of Proteome Research* **2008**, *7*, 2712-2722.

(22) Kristjansdottir, K.; Wolfgeher, D.; Lucius, N.; Angulo, D. S.; Kron, S. J. *Journal of Proteome Research* **2008**, *7*, 2812-2824.

(23) Wu, C. C.; MacCoss, M. J. *Current Opinion in Molecular Therapeutics* **2002**, *4*, 242-250.

(24) O'Farrell, P. H. *The Journal of Biological Chemistry* **1975**, *250*, 4007-4021.

(25) Rosenfeld, J.; Capdevielle, J.; Guillemot, J. C.; Ferrara, P. *Analytical Biochemistry* **1992**, *203*, 173-179.

(26) Tran, J. C.; Doucette, A. A. *Analytical Chemistry* **2008**, *80*, 1568-1573.

(27) Tran, J. C.; Doucette, A. A. *Analytical Chemistry* **2009**, *81*, 6201-6209.

(28) Vellaichamy, A.; Tran, J. C.; Catherman, A. D.; Lee, J. E.; Kellie, J. F.; Sweet, S. M. M.; Zamdborg, L.; Thomas, P. M.; Ahlf, D. R.; Durbin, K. R.; Valaskovic, G. A.; Kelleher, N. L. *Analytical Chemistry*, *82*, 1234-1244.

(29) Lee, J. E.; Kellie, J. F.; Tran, J. C.; Tipton, J. D.; Catherman, A. D.; Thomas, H. M.; Ahlf, D. R.; Durbin, K. R.; Vellaichamy, A.; Ntai, I.; Marshall, A. G.; Kelleher, N. L. *Journal of the American Society for Mass Spectrometry* **2009**, *20*, 2183-2191.

(30) Righetti, P. G.; Simo, C.; Sebastiano, R.; Citterio, A. *Electrophoresis* **2007**, *28*, 3799-3810.

(31) Sebastiano, R.; Simo, C.; Mendieta, M. E.; Antonioli, P.; Citterio, A.; Cifuentes, A.; Peltre, G.; Righetti, P. G. *Electrophoresis* **2006**, *27*, 3919-3934.

(32) Rovida, E.; Gelfi, C.; Morelli, A.; Righetti, P. G. *Journal of Chromatography* **1986**, *363*, 159-171.

(33) Righetti, P. G.; Bossi, A. *Analytica Chimica Acta* **1998**, *372*, 1-19.

(34) Sluyterman, L. A. A.; Elgersma, O. *Journal of Chromatography* **1978**, *150*, 17-30.

(35) Bjellqvist, B.; Ek, K.; Righetti, P. G.; Gianazza, E.; Gorg, A.; Westermeier, R.; Postel, W. *Journal of Biochemical and Biophysical Methods* **1982**, *6*, 317-339.

(36) Righetti, P. G. *Immobilized pH Gradients: Theory and Methodology*; Elseiver: Amsterdam, 1990.

(37) Righetti, P. G.; Wenisch, E.; Faupel, M. *Journal of Chromatography* **1989**, *475*, 293-309.

(38) Anderson, L.; Anderson, N. G. *Proceedings of the National Academy of Sciences of the United States of America* **1977**, *74*, 5421-5425.

(39) Gygi, S. P.; Corthals, G. L.; Zhang, Y.; Rochon, Y.; Aebersold, R. *Proceedings of the National Academy of Sciences of the United States of America* **2000**, *97*, 9390-9395.

(40) Martin, A. J. P.; Hampson, F.: US, 1981; Vol. 4,243,507.

(41) Lalwani, S.; Shave, E.; Fleisher, H. C.; Nzeadibe, K.; Busby, M. B.; Vigh, G. *Electrophoresis* **2004**, *25*, 2128-2138.

(42) Lalwani, S.; Shave, E.; Vigh, G. *Electrophoresis* **2004**, *25*, 3323-3330.

(43) Fleisher, H. C.; Vigh, G. *Electrophoresis* **2005**, *26*, 2511-2519.

(44) Fleisher-Craver, H. C.; Vigh, G. *Electrophoresis* **2008**, *29*, 4247-4256.

(45) Tran, J. C.; Doucette, A. A. *Journal of Proteome Research* **2008**, *7*, 1761-1765.

(46) Zilberstein, G.; Korol, L.; Righetti, P. G.; Bukshpan, S. *Analytical Chemistry* **2007**, *79*, 8624-8630.

(47) Tan, A. M.; Pashkova, A.; Zang, L.; Foret, F.; Karger, B. L. *Electrophoresis* **2002**, *23*, 3599-3607.

(48) Ros, A.; Faupel, M.; Mees, H.; van Oostrum, J.; Ferrigno, R.; Reymond, F.; Michel, P.; Rossier, J. S.; Girault, H. H. *Proteomics* **2002**, *2*, 151-156.

(49) Michel, P. E.; Reymond, F.; Arnaud, I. L.; Josserand, J.; Girault, H. H.; Rossier, J. S. *Electrophoresis* **2003**, *24*, 3-11.

(50) Heller, M.; Michel, P. E.; Morier, P.; Crettaz, D.; Wenz, C.; Tissot, J. D.; Reymond, F.; Rossier, J. S. *Electrophoresis* **2005**, *26*, 1174-1188.

(51) Horth, P.; Miller, C. A.; Preckel, T.; Wenz, C. *Molecular & Cellular Proteomics* **2006**, *5*, 1968-1974.

(52) Hubner, N. C.; Ren, S.; Mann, M. *Proteomics* **2008**, *8*, 4862-4872.

(53) Shave, E.; Vigh, G. *Electrophoresis* **2004**, *25*, 381-387.

(54) EsteveRomero, J. S.; Bossi, A.; Righetti, P. G. *Electrophoresis* **1996**, *17*, 1242-1247.

(55) Lim, P. Dissertation, Texas A&M University, College Station, 2006.

(56) Lim, P.; North, R.; Vigh, G. *Electrophoresis* **2007**, *28*, 1851-1859.

(57) Kolin, A. *Journal of Chemical Physics* **1954**, *22*, 1628-1629.

(58) Svensson, H. *Acta Chemica Scandinavica* **1961**, *15*, 325-341.

(59) Jensen, P. K.; Pasa-Tolic, L.; Anderson, G. A.; Horner, J. A.; Lipton, M. S.; Bruce, J. E.; Smith, R. D. *Analytical Chemistry* **1999**, *71*, 2076-2084.

(60) Heller, M.; Michel, P.; Morier, P.; Crettaz, D.; Wenz, C.; Tissot, J. D.; Reymond, F.; Rossier, J. S. *Electrophoresis* **2005**, *26*, 1174-1188.

(61) Righetti, P. G.; Bossi, A.; Wenisch, E.; Orsini, G. *Journal of Chromatography B* **1997**, *699*, 105-115.

(62) Anderson, N. L.; Anderson, N. G. *Electrophoresis* **1991**, *12*, 883-906.

(63) Henzel, W. J.; Billeci, T. M.; Stults, J. T.; Wong, S. C.; Grimley, C.; Watanabe, C. *Proceedings of the National Academy of Sciences of the United States of America* **1993**, *90*, 5011-5015.

(64) Gorg, A.; Weiss, W.; Dunn, M. J. *Proteomics* **2004**, *4*, 3665-3685.

(65) Righetti, P. G.; Barzaghi, B.; Luzzana, M.; Manfredi, G.; Faupel, M. *Journal of Biochemical and Biophysical Methods* **1987**, *15*, 189-198.

(66) Zuo, X.; Speicher, D. W. *Analytical Biochemistry* **2000**, *284*, 266-278.

(67) Ramachandran, P.; Boontheung, P.; Xie, Y. M.; Sondej, M.; Wong, D. T.; Loo, J. A. *Journal of Proteome Research* **2006**, *5*, 1493-1503.

(68) Han, M. J.; Herlyn, M.; Fisher, A. B.; Speicher, D. W. *Electrophoresis* **2008**, *29*, 695-705.

(69) Myung, J.-K.; Lubec, G. *Journal of Proteome Research* **2008**, *5*, 1267-1275.

(70) Michel, P. E.; Crettaz, D.; Morier, P.; Heller, M.; Gallot, D.; Tissot, J. D.; Reymond, F.; Rossier, J. S. *Electrophoresis* **2006**, *27*, 1169-1181.

(71) Herbert, B.; Righetti, P. G. *Electrophoresis* **2000**, *21*, 3639-3648.

(72) Martin, A. J. P.; Hampson, F. *Journal of Chromatography* **1978**, *159*, 101-110.

(73) Ogle, D.; Ho, A.; Gibson, T.; Rylatt, D.; Shave, E.; Lim, P.; Vigh, G. *Journal of Chromatography A* **2002**, *979*, 155-161.

(74) Waller, L. N.; Shores, K.; Knapp, D. R. *Journal of Proteome Research* **2008**, *7*, 4577-4584.

(75) Manadas, B.; English, J. A.; Wynne, K. J.; Cotter, D. R.; Dunn, M. J. *Proteomics* **2009**, *9*, 5194-5198.

(76) de Godoy, L. M. F.; Olsen, J. V.; Cox, J.; Nielsen, M. L.; Hubner, N. C.; Frohlich, F.; Walther, T. C.; Mann, M. *Nature* **2008**, *455*, 1251-U1260.

(77) Lengqvist, J.; Uhlen, K.; Lehtio, J. *Proteomics* **2007**, *7*, 1746-1752.

(78) Chenau, J.; Michelland, S.; Sidibe, J.; Seve, M. *Proteome Science* **2008**, *6*.

(79) Gasteiger, E.; Gattiker, A.; Hoogland, C.; Ivanyi, I.; Appel, R. D.; Bairoch, A. *Nucleic Acids Research* **2003**, *31*, 3784-3788.

(80) Staeheli.T; Maglot, D.; Monro, R. E. *Cold Spring Harbor Symposia on Quantitative Biology* **1969**, *34*, 39-&.

(81) Rosas-Acosta, G.; Russell, W. K.; Deyrieux, A.; Russell, D. H.; Wilson, V. G. *Molecular & Cellular Proteomics* **2005**, *4*, 56-72.

(82) Bradford, M. M. *Analytical Biochemistry* **1976**, *72*, 248-254.

(83) Perkins, D. N.; Pappin, D. J. C.; Creasy, D. M.; Cottrell, J. S. *Electrophoresis* **1999**, *20*, 3551-3567.

(84) Knochenmuss, R.; Stortelder, A.; Breuker, K.; Zenobi, R. *Journal of Mass Spectrometry* **2000**, *35*, 1237-1245.

(85) Cargile, B. J.; Stephenson, J. L. *Analytical Chemistry* **2004**, *76*, 267-275.

(86) Breci, L.; Hattrup, E.; Keeler, M.; Letarte, J.; Johnson, R.; Haynes, P. A. *Proteomics* **2005**, *5*, 2018-2028.

(87) Cargile, B. J.; Talley, D. L.; Stephenson, J. L. *Electrophoresis* **2004**, *25*, 936-945.

(88) Cargile, B. J.; Sevinsky, J. R.; Essader, A. S.; Stephenson, J. L.; Bundy, J. L. *Journal of Biomolecular Techniques* **2005**, *16* 181-189.

(89) Gevaert, K.; Van Daame, P.; Ghesquiere, B.; Impens, F.; Martens, L.; Helsens, K.; Vandekerckhove, J. *Proteomics* **2007**, *7*, 2698-2718.

(90) Wilkins, M. R.; Gasteiger, E.; Sanchez, J. C.; Bairoch, A.; Hochstrasser, D. F. *Electrophoresis* **1998**, *19*, 1501-1505.

(91) Blumberg, L.; Klee, M. *Journal of Chromatography A* **2010**, *1217*, 99-103.

(92) Matis, M.; Zakelj-Mavric, M.; Peter-Katalinic, J. *Proteomics* **2005**, *5*, 67-75.

(93) Bruneau, J. M.; Magnin, T.; Tagat, E.; Legrand, R.; Bernard, M.; Diaquin, M.; Fudali, C.; Latge, J. P. *Electrophoresis* **2001**, *22*, 2812-2823.

(94) Bhadauria, V.; Zhao, W. S.; Wang, L. X.; Zhang, Y.; Liu, J. H.; Yang, J.; Kong, L. A.; Peng, Y. L. *Microbiological Research* **2007**, *162*, 193-200.

(95) D'Ambrosio, C.; Arena, S.; Scaloni, A.; Guerrier, L.; Boschetti, E.; Mendieta, M. E.; Citterio, A.; Righetti, P. G. *Journal of Proteome Research* **2008**, *7*, 3461-3474.

(96) Galagan, J. E.; Calvo, S. E.; Borkovich, K. A.; Selker, E. U.; Read, N. D.; Jaffe, D.; FitzHugh, W.; Ma, L. J.; Smirnov, S.; Purcell, S.; Rehman, B.; Elkins, T.; Engels, R.; Wang, S. G.; Nielsen, C. B.; Butler, J.; Endrizzi, M.; Qui, D. Y.; Ianakiev, P.; Pedersen, D. B.; Nelson, M. A.; Werner-Washburne, M.; Selitrennikoff, C. P.; Kinsey, J. A.; Braun, E. L.; Zelter, A.; Schulte, U.; Kothe, G. O.; Jedd, G.; Mewes, W.; Staben, C.; Marcotte, E.; Greenberg, D.; Roy, A.;

Foley, K.; Naylor, J.; Stabge-Thomann, N.; Barrett, R.; Gnerre, S.; Kamal, M.; Kamvysselis, M.; Mauceli, E.; Bielke, C.; Rudd, S.; Frishman, D.; Krystofova, S.; Rasmussen, C.; Metzenberg, R. L.; Perkins, D. D.; Kroken, S.; Cogoni, C.; Macino, G.; Catcheside, D.; Li, W. X.; Pratt, R. J.; Osmani, S. A.; DeSouza, C. P. C.; Glass, L.; Orbach, M. J.; Berglund, J. A.; Voelker, R.; Yarden, O.; Plamann, M.; Seller, S.; Dunlap, J.; Radford, A.; Aramayo, R.; Natvig, D. O.; Alex, L. A.; Mannhaupt, G.; Ebbole, D. J.; Freitag, M.; Paulsen, I.; Sachs, M. S.; Lander, E. S.; Nusbaum, C.; Birren, B. *Nature* **2003**, *422*, 859-868.

(97) Gan, X.; Arita, K.; Isono, S.; Kitakawa, M.; Yoshin, K.; Yonezawa, K.; Kato, A.; Inoue, H.; Isono, K. *Fems Microbiology Letters* **2006**, *254*, 157-164.

(98) Schmitt, S.; Prokisch, H.; Schlunck, T.; Camp, D. G.; Ahting, U.; Waizenegger, T.; Scharfe, C.; Meitinger, T.; Imhof, A.; Neupert, W.; Oefner, P. J.; Rapaport, D. *Proteomics* **2006**, *6*, 72-80.

(99) Baker, C. L.; Kettenbach, A. N.; Loros, J. J.; Gerber, S. A.; Dunlap, J. C. *Molecular Cell* **2009**, *34*, 354-363.

(100) Shimizu, M.; Wariishi, H. *Fems Microbiology Letters* **2005**, *247*, 17-22.

(101) Cologna, S. M., Russell, W.K., Lim, P.J., Vigh, G., Russell, D.H. *Submitted* **2010**.

(102) Faupel, M.; Barzaghi, B.; Gelfi, C.; Righetti, P. G. *Journal of Biochemical and Biophysical Methods* **1987**, *15*, 147-161.

(103) Wenger, P.; Dezuanni, M.; Javet, P.; Gelfi, C.; Righetti, P. G. *Journal of Biochemical and Biophysical Methods* **1987**, *14*, 29-43.

(104) Hjerten, S. L., Jia-Li; States, U., Ed.: US, 1995, pp 15.

(105) Hjerten, S.; Valtcheva, L.; Elenbring, K.; Liao, J. L. *Electrophoresis* **1995**, *16*, 584-594.

(106) Bossi, A.; Olivieri, E.; Castelletti, L.; Gelfi, C.; Hamdan, M.; Righetti, P. G. 1999; 71-82.

(107) Gelfi, C.; Mauri, D.; Perduca, M.; Stellwagen, N. C.; Righetti, P. G. *Electrophoresis* **1998**, *19*, 1704-1710.

(108) Gelfi, C.; Perego, M.; Righetti, P. G.; Cainarca, S.; Firpo, S.; Ferrari, M.; Cremonesi, L. *Clinical Chemistry* **1998**, *44*, 906-913.

(109) Fullarto.Jr; Kenny, A. J. *Biochemical Journal* **1970**, *116*, 147-&.

(110) Ahmad, F.; Bigelow, C. C. *Journal of Protein Chemistry* **1986**, *5*, 355-367.

(111) Börnsen, K. O. *Influence of Salts, Buffers, Detergents, Solvents,and Matrices on MALDI-MS Protein Analysis in Complex Mixtures*, 2000.

(112) Bos, G., 2009; Vol. 2009.

(113) Bairoch, A.; Consortium, U.; Bougueleret, L.; Altairac, S.; Amendolia, V.; Auchincloss, A.; Argoud-Puy, G.; Axelsen, K.; Baratin, D.; Blatter, M. C.; Boeckmann, B.; Bolleman, J.; Bollondi, L.; Boutet, E.; Quintaje, S. B.; Breuza, L.; Bridge, A.; Decastro, E.; Ciapina, L.; Coral, D.; Coudert, E.; Cusin, I.; Delbard, G.; Dornevil, D.; Roggli, P. D.; Duvaud, S.; Estreicher, A.; Famiglietti, L.; Feuermann, M.; Gehant, S.; Farriol-Mathis, N.; Ferro, S.; Gasteiger, E.; Gateau, A.; Gerritsen, V.; Gos, A.; Gruaz-Gumowski, N.; Hinz, U.; Hulo, C.; Hulo, N.; James, J.; Jimenez, S.; Jungo, F.; Junker, V.; Kappler, T.; Keller, G.;

Lachaize, C.; Lane-Guermonprez, L.; Langendijk-Genevaux, P.; Lara, V.; Lemercier, P.; Le Saux, V.; Lieberherr, D.; Lima, T. D.; Mangold, V.; Martin, X.; Masson, P.; Michoud, K.; Moinat, M.; Morgat, A.; Mottaz, A.; Paesano, S.; Pedruzzi, I.; Phan, I.; Pilbout, S.; Pillet, V.; Poux, S.; Pozzato, M.; Redaschi, N.; Reynaud, S.; Rivoire, C.; Roechert, B.; Schneider, M.; Sigrist, C.; Sonesson, K.; Staehli, S.; Stutz, A.; Sundaram, S.; Tognolli, M.; Verbregue, L.; Veuthey, A. L.; Yip, L.; Zuletta, L.; Apweiler, R.; Alam-Faruque, Y.; Antunes, R.; Barrell, D.; Binns, D.; Bower, L.; Browne, P.; Chan, W. M.; Dimmer, E.; Eberhardt, R.; Fedotov, A.; Foulger, R.; Garavelli, J.; Golin, R.; Horne, A.; Huntley, R.; Jacobsen, J.; Kleen, M.; Kersey, P.; Laiho, K.; Leinonen, R.; Legge, D.; Lin, Q.; Magrane, M.; Martin, M. J.; O'Donovan, C.; Orchard, S.; O'Rourke, J.; Patient, S.; Pruess, M.; Sitnov, A.; Stanley, E.; Corbett, M.; di Martino, G.; Donnelly, M.; Luo, J.; van Rensburg, P.; Wu, C.; Arighi, C.; Arminski, L.; Barker, W.; Chen, Y. X.; Hu, Z. Z.; Hua, H. K.; Huang, H. Z.; Mazumder, R.; McGarvey, P.; Natale, D. A.; Nikolskaya, A.; Petrova, N.; Suzek, B. E.; Vasudevan, S.; Vinayaka, C. R.; Yeh, L. S.; Zhang, J. *Nucleic Acids Research* **2009**, *37*, D169-D174.

(114) Yang, F.; Bogdanov, B.; Strittmatter, E. F.; Vilkov, A. N.; Gritsenko, M.; Shi, L.; Elias, D. A.; Ni, S. S.; Romine, M.; Pasa-Tolic, L.; Lipton, M. S.; Smith, R. D. *Journal of Proteome Research* **2005**, *4*, 846-854.

(115) Das, D. K.; Medhi, O. K. *Journal of Inorganic Biochemistry* **1998**, *70*, 83-90.

(116) Fang, X. P.; Balgley, B. M.; Lee, C. S. *Electrophoresis* **2009**, *30*, 3998-4007.

(117) Rabilloud, T.; Vaezzadeh, A. R.; Potier, N.; Lelong, C.; Leize-Wagner, E.; Chevallet, M. *Mass Spectrometry Reviews* **2009**, *28*, 816-843.

(118) Lee, J.; Soper, S. A.; Murray, K. K. *Journal of Mass Spectrometry* **2009**, *44*, 579-593.

(119) Williams, B. J.; Russell, W. K.; Russell, D. H. *Analytical Chemistry* **2007**, *79*, 3850-3855.

(120) Cologna, S. M. R., W.K.; Lim, P.J.; Vigh, G.; Russell, D.H. *Journal of the American Society for Mass Spectrometry* **Submitted**.

(121) Cologna, S. M. W., B.J.; Russell, W.K.; Vigh, G.; Russell, D.H. **In Preparation**.

(122) Simpson, D. C.; Smith, R. D. *Electrophoresis* **2005**, *26*, 1291-1305.

(123) Theodorescu, D.; Fliser, D.; Wittke, S.; Mischak, H.; Krebs, R.; Walden, M.; Ross, M.; Eltze, E.; Bettendorf, O.; Wulfing, C.; Semjonow, A. *Electrophoresis* **2005**, *26*, 2797-2808.

(124) Wittke, S.; Mischak, H.; Walden, M.; Kolch, W.; Radler, T.; Wiedemann, K. *Electrophoresis* **2005**, *26*, 1476-1487.

(125) Zurbig, P.; Renfrow, M. B.; Schiffer, E.; Novak, J.; Walden, M.; Wittke, S.; Just, I.; Pelzing, M.; Neususs, C.; Theodorescu, D.; Root, K. E.; Ross, M. M.; Mischak, H. *Electrophoresis* **2006**, *27*, 2111-2125.

(126) Busnel, J. M.; Lion, N.; Girault, H. H. *Analytical Chemistry* **2007**, *79*, 5949-5955.

(127) Shihabi, Z. K. *Journal of Chromatography A* **2000**, *902*, 107-117.

(128) Arnold, R. J.; Reilly, J. P. *Analytical Biochemistry* **1999**, *269*, 105-112.

APPENDIX A

TABLE SUMMARY OF PROTEIN IDENTIFICATIONS FROM THE MSWIFT FRACTIONATION AND LC-MS/MS ANALYSIS OF YEAST

Rank	Gene Name	Accession Number	Protein MW	Protein pI	Peptide Count	Total Ion Score	Total Ion Score C.I. %	Best Ion Score
1	PGK1	YCR012W	44711	7.11	38	2588	100.000	168
2	CDC19	YAL038W	54510	7.56	43	2453	100.000	147
3	SSA1	YAL005C	69615	5.00	38	2409	100.000	144
4	SSA2	YLL024C	69427	4.95	39	2387	100.000	186
5	ENO1	YGR254W	46787	6.16	33	2365	100.000	241
6	ENO2	YHR174W	46885	5.67	33	2343	100.000	241
7	HSC82	YMR186W	80850	4.78	39	1886	100.000	119
8	EFT1	YOR133W	93230	5.92	41	1881	100.000	134
9	SSB1	YDL229W	66561	5.32	36	1853	100.000	157
10	SSB2	YNL209W	66554	5.37	37	1832	100.000	157
11	TDH3	YGR192C	35724	6.46	29	1747	100.000	207
12	HSP82	YPL240C	81356	4.84	33	1712	100.000	119
13	TDH2	YJR009C	35824	6.46	25	1575	100.000	139
14	PDC1	YLR044C	61457	5.80	25	1481	100.000	115
15	HSP104	YLL026W	101972	5.31	44	1410	100.000	89
16	FBA1	YKL060C	39596	5.51	19	1382	100.000	211
17	TDH1	YJL052W	35728	8.29	24	1345	100.000	135
18	PGI1	YBR196C	61261	6.00	25	1292	100.000	132
19	GPM1	YKL152C	27592	8.81	21	1195	100.000	143
20	SSA4	YER103W	69609	5.03	26	1190	100.000	186

21	TKL1	YPR074C	73760	6.51	26	1160	100.000	181
22	FAS2	YPL231W	206818	5.32	48	1107	100.000	108
23	DDR48	YMR173W	46207	4.22	16	1027	100.000	192
24	TEF1	YPR080W	50001	9.14	23	953	100.000	148
25	HSP60	YLR259C	60714	5.23	27	862	100.000	119
26	SSA3	YBL075C	70504	5.05	21	826	100.000	134
27	SSC1	YJR045C	70585	5.48	23	776	100.000	86
28	TPI1	YDR050C	26779	5.74	14	759	100.000	119
29	YEF3	YLR249W	115872	5.73	26	715	100.000	92
30	TIF1	YKR059W	44669	5.02	15	712	100.000	149
31	ADH1	YOL086C	36826	6.21	16	709	100.000	111
32	STI1	YOR027W	66224	5.45	25	696	100.000	153
33	FAS1	YKL182W	228547	5.64	38	685	100.000	108
34	MET6	YER091C	85807	6.07	28	667	100.000	74
35	HXK1	YFR053C	53705	5.28	20	632	100.000	178
36	SSE1	YPL106C	77318	5.12	24	617	100.000	73
37	RPL5	YPL131W	33694	6.36	15	613	100.000	177
38	ACO1	YLR304C	85315	8.17	19	606	100.000	127
39	URA2	YJL130C	244972	5.59	42	579	100.000	79
40	RPL3	YOR063W	43730	10.29	18	574	100.000	142
41	GLK1	YCL040W	55342	5.80	16	573	100.000	161
42	ACT1	YFL039C	41663	5.44	16	549	100.000	102
43	HXK2	YGL253W	53908	5.16	17	546	100.000	74
44	TFP1	YDL185W	118562	5.83	30	545	100.000	104
45	SSZ1	YHR064C	58202	4.94	16	537	100.000	125
46	SAH1	YER043C	49094	5.83	18	535	100.000	79
47	ADK1	YDR226W	24240	5.98	16	513	100.000	108
48	ADE17	YMR120C	65223	6.12	18	510	100.000	90
49	IPP1	YBR011C	32280	5.36	14	503	100.000	126
50	OYE2	YHR179W	44983	6.13	17	490	100.000	83
51	RPL8B	YLL045C	28094	10.02	13	487	100.000	79

52	PFK1	YGR240C	107903	5.98	22	480	100.000	120
53	SOD1	YJR104C	15845	5.62	9	463	100.000	100
54	RPL8A	YHL033C	28107	10.04	13	459	100.000	79
55	PFK2	YMR205C	104552	6.23	24	457	100.000	56
56	GND1	YHR183W	53509	6.19	15	457	100.000	108
57	RPL13B	YMR142C	22511	11.08	10	452	100.000	139
58	RPL2B	YIL018W	27392	11.10	12	449	100.000	94
59	SHM2	YLR058C	52186	6.98	14	448	100.000	106
60	ALD6	YPL061W	54380	5.31	19	445	100.000	60
61	RPL4A	YBR031W	39068	10.64	12	430	100.000	148
62	PAB1	YER165W	64304	5.71	15	419	100.000	102
63	HSP12	YFL014W	11686	5.22	8	409	100.000	95
64	RPS4A	YJR145C	29392	10.09	15	404	100.000	85
65	ADE13	YLR359W	54476	6.01	15	403	100.000	98
66	ERG10	YPL028W	41703	7.01	12	386	100.000	104
67	BMH2	YDR099W	31042	4.82	13	380	100.000	87
68	CPR1	YDR155C	17380	6.90	8	379	100.000	78
69	RPS8B	YER102W	22476	10.67	11	373	100.000	89
70	BFR1	YOR198C	54606	9.18	15	369	100.000	118
71	RPP0	YLR340W	33696	4.75	8	362	100.000	127
72	CYS4	YGR155W	55987	6.25	13	357	100.000	65
73	HSP26	YBR072W	23865	5.31	10	356	100.000	77
74	CDC60	YPL160W	124063	5.61	16	351	100.000	64
75	TSA1	YML028W	21576	5.03	5	331	100.000	101
76	GUS1	YGL245W	80792	7.21	18	329	100.000	80
77	STM1	YLR150W	29977	9.66	10	326	100.000	85
78	RPS24B	YIL069C	15319	10.51	11	326	100.000	67
79	CIT1	YNR001C	53327	8.23	13	325	100.000	78
80	MMF1	YIL051C	15898	9.30	6	319	100.000	90
81	HOM6	YJR139C	38478	6.86	9	318	100.000	116
82	RPL15A	YLR029C	24407	11.38	7	314	100.000	78

83	SSE2	YBR169C	77573	5.46	22	306	100.000	73
84	BMH1	YER177W	30073	4.82	13	304	100.000	72
85	TAL1	YLR354C	37013	6.09	16	300	100.000	81
86	ECM10	YEL030W	70042	5.93	13	300	100.000	86
87	BBC1	YJL020C	128218	5.17	17	299	100.000	56
88	RPL12A	YEL054C	17812	9.43	9	288	100.000	106
89	VMA2	YBR127C	57713	4.95	11	287	100.000	83
90	RPL26B	YGR034W	14226	10.47	11	283	100.000	61
91	UBA1	YKL210W	114195	4.97	13	281	100.000	71
92	RPL19A	YBR084C-A	21691	11.35	10	276	100.000	67
93	RPS7A	YOR096W	21609	9.83	9	276	100.000	91
94	RPS5	YJR123W	25023	8.63	12	272	100.000	109
95	ZUO1	YGR285C	48990	8.18	14	270	100.000	75
96	PMI40	YER003C	48158	5.66	12	270	100.000	104
97	RPL27A	YHR010W	15522	10.36	7	267	100.000	75
98	GRE1	YPL223C	19014	4.55	6	265	100.000	146
99	GLT1	YDL171C	237952	6.15	24	264	100.000	62
100	EFB1	YAL003W	22613	4.30	8	264	100.000	56
101	RPL15B	YMR121C	24407	11.38	7	263	100.000	78
102	RPS1B	YML063W	28795	10.02	13	256	100.000	57
103	TPM1	YNL079C	23527	4.58	12	255	100.000	83
104	HEF3	YNL014W	115796	5.87	13	254	100.000	92
105	RPS14B	YJL191W	14641	10.54	7	254	100.000	64
106	VAS1	YGR094W	125691	6.52	17	253	100.000	48
107	ARC1	YGL105W	42058	7.69	7	250	100.000	114
108	CYC1	YJR048W	12174	9.47	5	249	100.000	148
109	HIS4	YCL030C	87666	5.17	15	247	100.000	61
110	RPL17B	YJL177W	20539	10.92	7	246	100.000	79
111	DPS1	YLL018C	63476	6.16	16	244	100.000	47
112	WTM1	YOR230W	48353	5.18	14	244	100.000	77

113	CPR6	YLR216C	42045	5.83	9	243	100.000	68
114	ILV5	YLR355C	44341	9.10	13	240	100.000	66
115	TSL1	YML100W	122941	6.17	18	239	100.000	67
116	ADE16	YLR028C	65242	6.12	8	238	100.000	62
117	ABP1	YCR088W	65536	4.59	9	236	100.000	72
118	EDE1	YBL047C	150692	4.61	12	235	100.000	84
119	RPL17A	YKL180W	20537	10.92	7	234	100.000	67
120	SAM2	YDR502C	42229	5.18	11	232	100.000	115
121	HOM2	YDR158W	39519	6.27	11	231	100.000	46
122	RPS0B	YLR048W	27945	4.69	7	228	100.000	68
123	ZEO1	YOL109W	12582	5.43	7	228	100.000	65
124	AHP1	YLR109W	19103	5.01	5	228	100.000	133
125	RPL7A	YGL076C	27621	10.15	6	227	100.000	110
126	RPS1A	YLR441C	28726	10.00	10	226	100.000	57
127	CDC48	YDL126C	91939	4.82	16	223	100.000	35
128	NPL3	YDR432W	45380	5.38	11	223	100.000	66
129	PIL1	YGR086C	38326	4.54	10	217	100.000	55
130	RPG1	YBR079C	110276	5.97	23	215	100.000	41
131	RTC3	YHR087W	12002	5.05	5	215	100.000	98
132	GLN4	YOR168W	93075	8.56	16	214	100.000	49
133	DYN1	YKR054C	471049	5.90	39	214	100.000	27
134	RPL26A	YLR344W	14225	10.57	10	212	100.000	48
135	RPS25B	YLR333C	12002	10.32	4	211	100.000	115
136	RHR2	YIL053W	27929	5.35	11	209	100.000	67
137	ADE12	YNL220W	48249	8.15	4	205	100.000	103
138	RPL10	YLR075W	25345	10.03	7	204	100.000	71
139	SCP160	YJL080C	134727	5.64	18	204	100.000	44
140	EMI2	YDR516C	55886	5.88	8	201	100.000	93
141	SIS1	YNL007C	37567	9.02	9	200	100.000	64
142	RPS21A	YKR057W	9740	5.76	6	198	100.000	63
143	UGP1	YKL035W	55953	6.98	15	197	100.000	39

144	SAM1	YLR180W	41792	5.04	8	194	100.000	115
145	SEN1	YLR430W	252339	8.78	32	194	100.000	23
146	GPH1	YPR160W	103211	5.41	14	193	100.000	44
147	EGD1	YPL037C	17010	6.10	5	192	100.000	104
148	RPL28	YGL103W	16711	10.62	6	190	100.000	56
149	MDN1	YLR106C	558959	4.90	42	186	100.000	15
150	PYK2	YOR347C	55161	6.43	10	185	100.000	83
151	RPS3	YNL178W	26486	9.42	12	185	100.000	43
152	RPS17A	YML024W	15779	10.51	6	184	100.000	94
153	HSP78	YDR258C	91280	8.17	20	183	100.000	38
154	ADE5,7	YGL234W	86014	5.08	16	182	100.000	34
155	ADH2	YMR303C	36709	6.26	6	180	100.000	60
156	RPS9B	YBR189W	22285	10.09	8	179	100.000	76
157	TEF4	YKL081W	46491	7.63	9	178	100.000	66
158	RPS27A	YKL156W	8874	9.37	5	178	100.000	88
159	PDC6	YGR087C	61542	5.80	7	177	100.000	65
160	TOM1	YDR457W	373949	5.06	38	177	100.000	18
161	RPS23B	YPR132W	16028	10.73	8	176	100.000	64
162	KAP123	YER110C	122525	4.54	6	175	100.000	60
163	MLP2	YIL149C	195022	5.80	35	175	100.000	24
164	IDP1	YDL066W	48160	8.84	13	175	100.000	49
165	HTS1	YPR033C	59915	7.55	13	174	100.000	68
166	RPS21B	YJL136C	9754	5.76	6	171	100.000	63
167	YNL247W	YNL247W	87476	6.40	8	170	100.000	66
168	SAC6	YDR129C	71728	5.30	15	170	100.000	49
169	RPL20B	YOR312C	20424	10.30	7	170	100.000	56
170	YDL124W	YDL124W	35538	5.84	10	169	100.000	74
171	PDI1	YCL043C	58191	4.38	9	166	100.000	51
172	HYP2	YEL034W	17103	4.81	2	165	100.000	92
173	RPS20	YHL015W	13899	9.52	4	165	100.000	73
174	SHP1	YBL058W	46959	4.89	7	164	100.000	75

175	EGD2	YHR193C	18698	4.84	6	163	100.000	87
176	DUG1	YFR044C	52838	5.43	7	163	100.000	82
177	RPS6A	YPL090C	26980	10.44	8	163	100.000	48
178	PDC5	YLR134W	61873	5.99	11	162	100.000	54
179	YPR117W	YPR117W	285724	8.44	35	162	100.000	16
180	IRA1	YBR140C	350758	6.13	28	162	100.000	17
181	TRA1	YHR099W	432905	6.11	35	162	100.000	18
182	UTP20	YBL004W	287379	6.59	25	161	100.000	17
183	CAM1	YPL048W	47058	8.43	8	161	100.000	66
184	LEU1	YGL009C	85741	5.61	13	158	100.000	43
185	THR4	YCR053W	57439	5.46	14	158	100.000	41
186	RPS19A	YOL121C	15907	9.61	5	158	100.000	51
187	YIL080W	YIL080W	181575	9.31	25	156	100.000	32
188	RPL36A	YMR194W	11117	11.60	6	155	100.000	70
189	TIF4631	YGR162W	107036	5.80	13	154	100.000	62
190	RIB4	YOL143C	18544	6.06	5	152	100.000	44
191	GLN1	YPR035W	41679	5.92	5	152	100.000	55
192	ADE3	YGR204W	102141	6.37	15	151	100.000	34
193	YHB1	YGR234W	44618	5.86	7	150	100.000	73
194	RPL16B	YNL069C	22235	10.54	9	150	100.000	42
195	SGT2	YOR007C	37195	4.68	11	150	100.000	31
196	MEC1	YBR136W	273169	8.54	25	149	100.000	27
197	YLR422W	YLR422W	221422	7.88	25	149	100.000	17
198	SRS2	YJL092W	134223	8.86	25	148	100.000	17
199	ADO1	YJR105W	36350	4.99	6	148	100.000	88
200	ADE6	YGR061C	148811	5.15	13	147	100.000	30
201	ASN2	YGR124W	64552	5.53	10	146	100.000	40
202	RPL40B	YKR094C	14545	9.87	6	146	100.000	57
203	SPT16	YGL207W	118557	4.99	15	146	100.000	44
204	SPT6	YGR116W	168188	4.89	14	145	100.000	94
205	RPL32	YBL092W	14762	11.17	8	145	100.000	32

206	YMR226C	YMR226C	29140	6.34	6	145	100.000	90
207	MYO1	YHR023W	223498	6.06	28	142	100.000	14
208	HOR2	YER062C	27796	5.80	9	141	100.000	47
209	KRS1	YDR037W	67915	5.78	10	141	100.000	66
210	ARG4	YHR018C	51956	5.47	10	140	100.000	91
211	UGA1	YGR019W	52913	6.34	7	138	100.000	101
212	BNR1	YIL159W	156754	8.05	20	138	100.000	21
213	THS1	YIL078W	84467	6.59	18	137	100.000	34
214	ERG13	YML126C	54979	8.36	9	137	100.000	67
215	CYR1	YJL005W	227692	6.88	25	137	100.000	17
216	DED81	YHR019C	62168	5.60	10	137	100.000	53
217	SMC6	YLR383W	127930	7.21	19	136	100.000	23
218	RPL11A	YPR102C	19707	9.92	7	135	100.000	33
219	KAR2	YJL034W	74422	4.79	10	135	100.000	82
220	YMR099C	YMR099C	33934	5.75	6	135	100.000	54
221	LSB3	YFR024C-A	49314	7.66	8	134	100.000	81
222	MLS1	YNL117W	62751	6.72	11	134	100.000	32
223	YHR080C	YHR080C	149588	8.75	20	133	100.000	13
224	TMA17	YDL110C	16761	4.58	5	133	100.000	67
225	MDH1	YKL085W	35628	8.46	7	133	100.000	64
226	ARO1	YDR127W	174645	5.89	15	133	100.000	36
227	OLA1	YBR025C	44146	7.05	9	132	100.000	57
228	RPS11A	YDR025W	17738	10.79	9	132	100.000	43
229	RPL18A	YOL120C	20551	11.70	10	132	100.000	37
230	CYS3	YAL012W	42516	6.06	6	131	100.000	43
231	GLC3	YEL011W	81064	5.76	10	131	100.000	31
232	PGM2	YMR105C	63049	6.18	14	131	100.000	30
233	RAD50	YNL250W	152475	5.78	21	130	100.000	23
234	GVP36	YIL041W	36647	4.91	8	129	100.000	63
235	FUM1	YPL262W	53118	8.48	9	129	100.000	67

236	NET1	YJL076W	128454	7.56	21	129	100.000	22
237	RPL31A	YDL075W	12945	9.99	4	129	100.000	43
238	INO80	YGL150C	171349	5.52	23	129	100.000	17
239	RPL25	YOL127W	15748	10.11	7	128	100.000	54
240	COF1	YLL050C	15891	5.05	2	128	100.000	87
241	ACC1	YNR016C	250197	5.89	30	128	100.000	13
242	HRP1	YOL123W	59613	5.42	8	128	100.000	80
243	PMA2	YPL036W	102107	4.91	14	127	100.000	29
244	SPO71	YDR104C	145090	9.22	18	126	100.000	23
245	ECM29	YHL030W	210299	6.16	21	126	100.000	27
246	YBT1	YLL048C	189043	8.26	22	126	100.000	15
247	SER3	YER081W	51161	5.36	5	126	100.000	49
248	ECM16	YMR128W	144864	5.98	21	125	100.000	27
249	HBT1	YDL223C	113548	5.92	16	124	100.000	26
250	SNT2	YGL131C	163098	8.84	27	124	100.000	12
251	BCY1	YIL033C	47190	7.71	10	124	100.000	43
252	FRS1	YLR060W	67322	5.53	14	124	100.000	24
253	ZWF1	YNL241C	57486	5.92	8	124	100.000	43
254	PCK1	YKR097W	60944	5.93	9	123	100.000	46
255	RPO21	YDL140C	191491	5.42	23	123	100.000	22
256	YSP1	YHR155W	143493	8.36	14	123	100.000	27
257	CHC1	YGL206C	187117	5.11	18	123	100.000	35
258	ERR2	YPL281C	47298	5.15	5	122	100.000	100
259	YLR301W	YLR301W	27484	5.10	7	122	100.000	48
260	YRF1-6	YNL339C	210965	6.94	24	121	100.000	18
261	FUN12	YAL035W	112199	5.61	15	121	100.000	33
262	GCD11	YER025W	57829	6.37	10	120	100.000	63
263	RPS22A	YJL190C	14617	9.94	5	120	100.000	76
264	RPS22B	YLR367W	14617	9.94	5	120	100.000	76
265	YNL208W	YNL208W	20139	6.97	3	119	100.000	81
266	KEM1	YGL173C	175350	7.04	19	119	100.000	17

267	SEC27	YGL137W	99383	4.63	9	118	100.000	63
268	RPL31B	YLR406C	12959	9.99	5	118	100.000	43
269	POL2	YNL262W	255508	6.53	19	118	100.000	21
270	RPL23B	YER117W	14464	10.33	8	117	100.000	52
271	BNI1	YNL271C	219566	6.13	27	117	100.000	24
272	VPS13	YLL040C	357625	5.41	29	117	100.000	28
273	DAK1	YML070W	62168	5.25	9	116	100.000	35
274	ICL1	YER065C	62369	5.97	11	114	100.000	39
275	URA1	YKL216W	34779	5.80	6	114	100.000	51
276	USO1	YDL058W	206326	4.88	23	114	100.000	19
277	GLR1	YPL091W	53407	7.67	13	113	100.000	40
278	RPS7B	YNL096C	21621	9.92	6	113	100.000	72
279	YER067W	YER067W	18977	5.74	4	113	100.000	45
280	RPS16A	YMR143W	15838	10.26	6	113	100.000	37
281	YRF1-5	YLR467W	203652	7.59	23	112	100.000	18
282	TEL1	YBL088C	321364	6.52	25	112	100.000	22
283	DNF1	YER166W	177686	5.73	21	112	100.000	16
284	TMA19	YKL056C	18729	4.41	3	112	100.000	66
285	LEU4	YNL104C	68366	5.70	12	111	100.000	20
286	HFA1	YMR207C	241634	8.18	22	110	100.000	20
287	SEC53	YFL045C	29045	5.14	9	110	100.000	46
288	CYC7	YEL039C	12524	9.61	4	109	100.000	83
289	TRP5	YGL026C	76578	6.05	6	109	100.000	48
290	GRS1	YBR121C	75364	5.71	14	109	100.000	31
291	SSK2	YNR031C	180414	5.61	17	109	100.000	22
292	YDJ1	YNL064C	44643	5.95	5	109	100.000	74
293	SKT5	YBL061C	77019	9.30	13	109	100.000	21
294	GCN2	YDR283C	190075	5.98	23	109	100.000	18
295	VPS15	YBR097W	166254	6.29	22	108	100.000	14
296	PEP4	YPL154C	44471	4.70	4	108	100.000	56
297	ALA1	YOR335C	107211	5.36	15	108	100.000	28

298	BAT1	YHR208W	43569	9.01	6	108	100.000	55
299	ADR1	YDR216W	150846	6.27	18	107	100.000	17
300	ARO80	YDR421W	108138	5.92	18	107	100.000	23
301	YJL225C	YJL225C	197441	7.47	22	107	100.000	18
302	TAO3	YIL129C	269687	5.95	19	106	100.000	12
303	TIF3	YPR163C	48493	5.17	12	106	100.000	42
304	ALD4	YOR374W	56688	6.31	8	106	100.000	39
305	OYE3	YPL171C	44892	5.40	5	105	100.000	68
306	IRA2	YOL081W	351446	6.59	22	105	100.000	13
307	RPT1	YKL145W	51950	5.32	6	105	100.000	64
308	MGM1	YOR211C	99116	7.28	18	105	100.000	17
309	YFR016C	YFR016C	137616	4.40	20	105	100.000	15
310	BUD3	YCL014W	184605	5.84	21	105	100.000	13
311	RPO41	YFL036W	152952	8.92	19	105	100.000	13
312	YKL215C	YKL215C	140340	6.32	14	104	100.000	25
313	RAV1	YJR033C	154835	8.48	19	103	100.000	20
314	BRR2	YER172C	246031	5.34	19	102	100.000	17
315	GCV2	YMR189W	114379	6.83	11	102	100.000	36
316	ARC35	YNR035C	39542	6.33	7	102	100.000	37
317	STH1	YIL126W	156646	6.30	17	102	100.000	25
318	SEC31	YDL195W	138618	5.49	7	102	100.000	60
319	TIF34	YMR146C	38731	5.41	5	102	100.000	81
320	PRP22	YER013W	129929	7.79	15	101	100.000	18
321	ACS2	YLR153C	75444	6.21	13	101	100.000	21
322	TPS3	YMR261C	118761	5.94	15	101	100.000	34
323	YGR109W-B	YGR109W-B	178308	8.98	19	101	100.000	32
324	TRR1	YDR353W	34216	5.69	5	100	100.000	70
325	ATP2	YJR121W	54760	5.52	10	100	100.000	35
326	YPR1	YDR368W	34733	6.62	5	100	100.000	50
327	LYS1	YIR034C	41439	9.18	5	100	100.000	77

328	YFR006W	YFR006W	61714	5.78	10	100	100.000	26
329	CRN1	YLR429W	72509	5.64	11	100	100.000	25
330	DUR1,2	YBR208C	201705	5.45	15	99	100.000	15
331	DHR2	YKL078W	82661	9.06	19	99	100.000	13
332	FPR1	YNL135C	12150	5.72	5	99	100.000	55
333	RRP5	YMR229C	193016	5.86	11	99	100.000	28
334	VIP1	YLR410W	129674	8.77	24	99	100.000	12
335	RPN10	YHR200W	29729	4.73	5	98	100.000	78
336	FAB1	YFR019W	257290	8.54	21	98	100.000	12
337	UBI4	YLL039C	42800	7.00	7	98	100.000	57
338	SUB2	YDL084W	50278	5.34	13	98	100.000	23
339	ARP3	YJR065C	49511	5.57	9	98	100.000	27
340	SES1	YDR023W	53276	5.80	6	97	100.000	42
341	LTE1	YAL024C	163050	6.05	17	97	100.000	19
342	MCM4	YPR019W	104938	5.85	19	97	100.000	12
343	JNM1	YMR294W	43580	4.84	13	97	100.000	23
344	LEU9	YOR108W	67158	6.31	13	96	100.000	20
345	VMA5	YKL080W	44161	6.22	7	96	100.000	37
346	HRQ1	YDR291W	123471	6.22	19	95	100.000	34
347	MSH1	YHR120W	109340	8.91	19	95	100.000	18
348	RPL16A	YIL133C	22187	10.48	5	95	100.000	42
349	PMA1	YGL008C	99556	4.96	12	95	100.000	29
350	SRV2	YNL138W	57486	5.48	7	95	100.000	36
351	SBA1	YKL117W	24066	4.46	4	95	100.000	53
352	YRF1-4	YLR466W	156269	6.83	19	95	100.000	18
353	MIP1	YOR330C	143411	8.95	24	94	100.000	10
354	RAD9	YDR217C	148306	5.20	15	94	100.000	47
355	SEC3	YER008C	154599	5.34	15	94	100.000	17
356	SER33	YIL074C	51156	5.98	7	94	100.000	35
357	TAF2	YCR042C	161369	5.46	12	93	100.000	38
358	ARO2	YGL148W	40813	7.66	9	93	100.000	57

359	ADE1	YAR015W	34582	5.66	7	93	100.000	37
360	MBF1	YOR298C-A	16394	10.61	9	92	100.000	27
361	RPA135	YPR010C	135656	7.56	12	92	100.000	25
362	RPL1A	YPL220W	24470	9.73	4	92	100.000	51
363	AGC1	YPR021C	104239	8.08	11	92	100.000	22
364	CTT1	YGR088W	64543	6.09	7	92	100.000	38
365	SPA2	YLL021W	163043	5.07	18	92	100.000	17
366	MSR1	YHR091C	73647	9.41	12	91	100.000	25
367	GAL10	YBR019C	78146	5.66	6	91	100.000	44
368	ULS1	YOR191W	184291	7.32	15	91	100.000	25
369	CPA2	YJR109C	123838	5.18	9	91	100.000	20
370	TIF5	YPR041W	45233	4.95	5	91	100.000	67
371	RPL37B	YDR500C	9862	11.79	7	91	100.000	36
372	RAT1	YOR048C	115861	6.37	13	91	100.000	22
373	RPS2	YGL123W	27433	10.44	6	90	100.000	58
374	IDP3	YNL009W	47826	9.24	4	90	100.000	49
375	PRK1	YIL095W	90976	9.63	13	90	100.000	26
376	COR1	YBL045C	50197	6.77	8	90	100.000	48
377	NTH1	YDR001C	85825	7.61	10	90	100.000	45
378	DBP2	YNL112W	60962	8.90	11	90	100.000	49
379	BLM10	YFL007W	245840	5.58	16	90	100.000	22
380	TOR2	YKL203C	281390	7.25	24	89	100.000	12
381	GIN4	YDR507C	129779	9.22	20	89	100.000	9
382	RPS26A	YGL189C	13496	10.76	5	89	100.000	40
383	APE2	YKL157W	105518	7.89	17	88	100.000	19
384	CCH1	YGR217W	234449	8.63	20	88	100.000	12
385	HER1	YOR227W	139372	8.98	18	88	100.000	13
386	LSP1	YPL004C	38048	4.62	10	88	100.000	39
387	SGS1	YMR190C	163735	5.93	16	88	100.000	17
388	YLL066C	YLL066C	135561	8.12	19	88	100.000	15

389	ASN1	YPR145W	64429	5.73	10	88	100.000	19
390	WRS1	YOL097C	49319	6.35	5	88	100.000	61
391	DED1	YOR204W	65512	7.67	9	87	100.000	49
392	GCN1	YGL195W	296513	5.16	16	87	100.000	16
393	YGR027W-B	YGR027W-B	198534	8.30	13	87	100.000	21
394	PSK1	YAL017W	152236	5.48	12	87	100.000	15
395	DIP2	YLR129W	106276	5.69	14	87	100.000	17
396	YPL260W	YPL260W	62742	5.00	6	87	100.000	60
397	TOR1	YJR066W	280962	6.81	21	87	100.000	8
398	RPB2	YOR151C	138663	6.09	20	87	100.000	10
399	APE3	YBR286W	60100	5.13	6	86	100.000	58
400	PXL1	YKR090W	79398	5.08	15	86	100.000	22
401	GUA1	YMR217W	58445	6.05	10	86	100.000	22
402	SLA2	YNL243W	108928	5.31	10	86	100.000	21
403	MOT1	YPL082C	209844	6.13	17	86	100.000	18
404	RPL35A	YDL191W	13901	10.58	7	85	100.000	28
405	FAA1	YOR317W	77817	7.53	10	85	100.000	21
406	LYS2	YBR115C	155248	5.63	14	85	100.000	14
407	YLR419W	YLR419W	162943	9.16	16	84	100.000	15
408	DNF3	YMR162C	188200	6.32	18	84	100.000	15
409	GIP4	YAL031C	86582	9.72	7	84	100.000	30
410	YKL105C	YKL105C	125517	5.52	12	84	100.000	14
411	THO2	YNL139C	183816	7.55	14	84	100.000	18
412	DDP1	YOR163W	21559	8.27	6	84	100.000	59
413	RIF1	YBR275C	217824	6.13	16	84	100.000	32
414	MSH6	YDR097C	139992	5.58	14	84	100.000	27
415	APC1	YNL172W	196020	5.66	17	84	100.000	15
416	PKH2	YOL100W	121585	9.65	17	83	100.000	23
417	SPP41	YDR464W	161500	8.93	14	83	100.000	19
418	BEM2	YER155C	245278	8.53	22	83	100.000	14

419	SAC3	YDR159W	149475	8.97	17	83	100.000	15
420	MLC1	YGL106W	16434	4.55	6	83	100.000	59
421	FMP27	YLR454W	303287	8.19	18	83	100.000	11
422	CTR9	YOL145C	124578	5.99	14	83	100.000	20
423	CSF1	YLR087C	338044	5.63	19	83	100.000	11
424	KIC1	YHR102W	116989	8.12	14	83	100.000	27
425	POL3	YDL102W	124512	8.23	18	83	100.000	20
426	STT4	YLR305C	214471	7.25	18	82	100.000	17
427	SPC110	YDR356W	111714	6.65	21	82	100.000	13
428	PSA1	YDL055C	39541	5.95	4	82	100.000	50
429	CAB3	YKL088W	65198	4.91	8	82	100.000	42
430	CLU1	YMR012W	145076	5.99	13	82	100.000	27
431	TFC3	YAL001C	132026	9.38	10	82	100.000	20
432	BCK1	YJL095W	164094	9.50	15	82	100.000	17
433	VMA13	YPR036W	54382	5.95	8	82	100.000	34
434	UBP2	YOR124C	146264	5.08	15	82	100.000	15
435	MET17	YLR303W	48642	5.97	4	81	100.000	38
436	TRK1	YJL129C	140986	8.64	17	81	100.000	17
437	MYO4	YAL029C	169237	7.52	20	81	100.000	11
438	PRT1	YOR361C	88074	5.71	9	81	100.000	31
439	HUL4	YJR036C	103391	9.04	15	80	100.000	15
440	ECM21	YBL101C	123534	6.43	18	80	100.000	12
441	YEL077C	YEL077C	143002	6.79	15	80	100.000	18
442	YDR341C	YDR341C	69481	6.32	9	80	100.000	25
443	PNC1	YGL037C	24978	5.81	2	80	100.000	52
444	SAL1	YNL083W	55711	9.03	12	80	100.000	14
445	PRB1	YEL060C	69579	5.94	6	80	100.000	38
446	PRX1	YBL064C	29477	8.97	6	80	100.000	50
447	ELP3	YPL086C	63617	9.11	14	80	100.000	18
448	SUA7	YPR086W	38176	8.85	13	79	100.000	28
449	TAZ1	YPR140W	44160	8.80	10	79	100.000	16

450	YER138C	YER138C	198439	8.14	12	79	100.000	21
451	NQM1	YGR043C	37230	5.99	4	79	100.000	38
452	TPS1	YBR126C	56113	5.71	6	79	100.000	24
453	TFC4	YGR047C	120154	5.14	14	79	100.000	13
454	PKH1	YDR490C	86198	9.26	12	79	100.000	15
455	BPH1	YCR032W	250713	6.04	16	79	100.000	19
456	URB1	YKL014C	203159	6.97	18	79	100.000	30
457	ECM32	YER176W	126892	9.45	14	79	100.000	15
458	ELM1	YKL048C	72105	8.36	11	79	100.000	15
459	RAD26	YJR035W	124451	7.11	15	78	100.000	13
460	ECM5	YMR176W	162598	6.39	16	78	100.000	15
461	PYC2	YBR218C	130085	6.06	12	78	100.000	18
462	DCS1	YLR270W	40744	5.85	6	78	100.000	40
463	YRA1	YDR381W	24940	11.33	8	78	100.000	31
464	YMR031C	YMR031C	93288	5.99	12	78	100.000	20
465	TRM1	YDR120C	64012	9.19	12	78	100.000	11
466	RNR4	YGR180C	40029	5.11	9	78	100.000	29
467	GDB1	YPR184W	174861	5.48	8	78	100.000	20
468	NTF2	YER009W	14444	4.50	3	78	100.000	45
469	MCM5	YLR274W	86357	5.50	15	77	100.000	27
470	HAL5	YJL165C	95396	8.63	15	77	100.000	15
471	INP51	YIL002C	108362	6.29	11	77	100.000	24
472	RPS18B	YML026C	17027	10.27	7	77	100.000	28
473	MCM7	YBR202W	94815	5.14	11	77	100.000	24
474	YIL092W	YIL092W	70962	9.15	13	77	100.000	18
475	PBI2	YNL015W	8585	6.28	3	77	100.000	46
476	PYC1	YGL062W	130018	5.84	10	77	100.000	18
477	GAD1	YMR250W	65948	6.15	11	77	100.000	42
478	JIP4	YDR475C	98630	9.59	17	77	100.000	12
479	HRK1	YOR267C	85642	6.87	16	77	100.000	11
480	BUB1	YGR188C	117795	6.28	11	77	100.000	22

481	GAL11	YOL051W	120235	9.81	15	76	100.000	14
482	CFT1	YDR301W	153309	5.62	18	76	100.000	13
484	TYS1	YGR185C	43992	8.57	6	76	100.000	31
485	MYO2	YOR326W	180567	5.95	16	76	100.000	12
486	YMR086W	YMR086W	105810	9.72	20	75	100.000	9
487	MRN1	YPL184C	68621	5.61	9	75	100.000	30
488	NEO1	YIL048W	130136	6.02	13	75	100.000	16
489	RPA190	YOR341W	186314	6.65	17	75	100.000	11
490	ARO8	YGL202W	56143	5.68	7	75	100.000	26
491	GRE3	YHR104W	37095	6.60	8	75	100.000	26
492	LSC2	YGR244C	46871	7.09	10	75	100.000	22
493	NPT1	YOR209C	48988	6.44	12	75	100.000	30
494	FAR11	YNL127W	109724	5.43	13	75	100.000	20
495	FAA3	YIL009W	77897	9.10	7	75	100.000	23
496	VMR1	YHL035C	180811	8.73	12	75	100.000	26
497	SIN3	YOL004W	174731	5.39	12	74	100.000	26
498	RRP12	YPL012W	137422	6.61	13	74	100.000	22
499	RIM1	YCR028C-A	15377	7.93	2	74	100.000	74
500	NBA1	YOL070C	55889	5.65	13	74	100.000	21
501	KIP3	YGL216W	91034	6.66	14	74	100.000	10
502	RPL24A	YGL031C	17603	11.28	6	74	100.000	33
503	FOL1	YNL256W	93061	6.02	10	74	100.000	21
504	YEL047C	YEL047C	50812	5.93	7	74	100.000	30
505	PET127	YOR017W	93350	9.31	17	74	100.000	15
506	NUT1	YGL151W	128714	5.00	9	74	100.000	17
507	GPD2	YOL059W	49391	6.60	6	73	100.000	32
508	ESC8	YOL017W	82137	6.48	12	73	100.000	12
509	PUS7	YOR243C	76955	7.61	13	73	100.000	12
510	RPS13	YDR064W	17018	10.44	6	73	100.000	34
511	ATG9	YDL149W	115331	5.66	7	73	100.000	22

512	LIA1	YJR070C	36142	4.78	4	73	100.000	32
513	TCB3	YML072C	170970	6.69	10	73	100.000	38
514	KEL1	YHR158C	131014	5.21	15	72	100.000	28
515	NUM1	YDR150W	312838	5.26	20	72	100.000	13
516	NUP133	YKR082W	133237	5.00	13	72	100.000	12
517	BOI1	YBL085W	109229	9.13	17	72	100.000	7
518	STE11	YLR362W	80671	6.74	11	72	100.000	15
519	GDE1	YPL110C	137928	6.31	10	72	100.000	21
520	DNL4	YOR005C	108446	8.65	11	72	100.000	34
521	RNR2	YJL026W	46118	5.14	10	72	100.000	19
522	GCS1	YDL226C	39272	5.65	8	72	100.000	26
523	FKS1	YLR342W	214712	6.84	13	72	100.000	14
524	NCP1	YHR042W	76724	5.03	10	72	100.000	15
525	PGM1	YKL127W	63072	6.82	7	72	100.000	30
526	VTC3	YPL019C	96494	6.96	12	72	100.000	19
527	YBR085C-A	YBR085C-A	9399	5.22	2	72	100.000	68
529	MDS3	YGL197W	166971	7.75	22	72	100.000	8
530	SEC18	YBR080C	84004	8.03	9	71	100.000	22
531	YER160C	YER160C	198446	8.68	13	71	100.000	20
532	DNF2	YDR093W	182504	5.84	18	71	100.000	10
533	DBP10	YDL031W	113088	9.29	18	71	100.000	10
534	URC2	YDR520C	88592	8.15	10	71	100.000	16
535	TIF6	YPR016C	26441	4.54	4	71	100.000	51
536	RPL9B	YNL067W	21644	9.66	4	71	100.000	35
537	YMR050	YMR050C	198432	8.75	12	71	100.000	20
538	PRP6	YBR055C	104164	8.20	14	71	100.000	23
539	YGR161C-D	YGR161C-D	198436	8.60	12	71	100.000	20
540	RAD54	YGL163C	101690	9.15	12	71	100.000	15
541	HPT1	YDR399W	25175	5.46	3	71	100.000	60

542	IRC3	YDR332W	78497	9.01	14	70	100.000	13
543	UTP10	YJL109C	199956	6.11	14	70	100.000	12
544	SNU114	YKL173W	113969	5.67	15	70	100.000	27
545	VPS54	YDR027C	101457	5.95	8	70	100.000	17
546	SCC2	YDR180W	170994	6.40	17	70	100.000	13
547	SIP1	YDR422C	91015	6.10	13	70	100.000	10
548	ADE4	YMR300C	56683	5.90	10	70	100.000	25
549	NOT3	YIL038C	94346	5.46	11	70	100.000	13
550	YML133C	YML133C	155455	8.32	17	70	100.000	15
551	UBR1	YGR184C	224696	5.33	14	70	100.000	10
552	NOP14	YDL148C	94244	6.95	11	69	100.000	16
553	HAP1	YLR256W	166003	7.02	14	69	100.000	28
554	DBP1	YPL119C	67875	8.96	12	69	100.000	12
555	TRK2	YKR050W	101022	9.58	10	69	100.000	28
556	LYS21	YDL131W	48564	5.88	7	69	100.000	31
557	ESP1	YGR098C	187326	8.47	10	69	100.000	25
558	BIR1	YJR089W	108600	6.06	15	69	100.000	14
559	ARO3	YDR035W	41044	7.04	6	69	100.000	26
560	KES1	YPL145C	49461	5.73	4	69	100.000	28
561	RFC1	YOR217W	94844	9.25	15	69	100.000	10
562	ATP1	YBL099W	58582	9.06	8	68	100.000	19
564	SQS1	YNL224C	86896	5.47	18	68	100.000	9
565	ADH3	YMR083W	40344	8.65	7	68	100.000	45
566	GAL4	YPL248C	99340	6.79	12	68	100.000	12
567	NUP192	YJL039C	191415	5.19	11	68	100.000	20
568	MON2	YNL297C	186718	5.50	12	68	100.000	11
569	PNT1 S	YOR266W	48903	9.49	6	68	100.000	25
570	IRC8	YJL051W	91200	6.18	7	68	100.000	20
571	PMC1	YGL006W	130778	7.16	15	68	100.000	11
572	UPC2	YDR213W	100277	5.67	13	68	100.000	11
573	HIR3	YJR140C	191560	5.85	15	68	100.000	9

574	CAT8	YMR280C	160385	9.13	15	68	100.000	12
575	YMR124W	YMR124W	105849	6.44	11	68	100.000	18
576	SAK1	YER129W	126794	8.87	9	68	100.000	13
577	SIR1	YKR101W	76884	9.12	7	68	100.000	36
578	BUD2	YKL092C	126584	8.90	16	67	100.000	12
579	IMD3	YLR432W	56549	7.04	6	67	100.000	24
580	HIR1	YBL008W	93831	6.72	13	67	100.000	16
581	RPS29B	YDL061C	6723	10.07	6	67	100.000	39
582	GPD1	YDL022W	42842	5.30	5	67	100.000	49
583	MTC1	YJL123C	53445	4.50	5	67	100.000	41
584	YME1	YPR024W	81721	6.64	13	67	100.000	15
585	INP52	YNL106C	133248	8.79	12	67	100.000	12
586	DSS1	YMR287C	110752	9.11	9	67	100.000	24
587	VPS8	YAL002W	144871	5.58	12	67	100.000	12
588	YTA7	YGR270W	157310	5.07	14	67	100.000	14
589	BAS1	YKR099W	89550	8.11	9	67	100.000	19
590	GPA1	YHR005C	54042	7.51	9	66	100.000	17
591	SGF73	YGL066W	72834	9.03	7	66	100.000	31
592	MSS116	YDR194C	76221	9.07	13	66	100.000	21
593	NMA111	YNL123W	110812	5.63	12	66	100.000	13
594	TRM5	YHR070W	56479	9.00	9	66	100.000	16
595	CPR5	YDR304C	25311	5.35	5	66	100.000	50
596	IRC5	YFR038W	96905	5.92	12	66	100.000	22
597	DNA2	YHR164C	171587	6.11	17	66	100.000	8
598	RTF1	YGL244W	65828	5.26	9	66	100.000	27
599	YTA12	YMR089C	93218	7.22	12	66	100.000	16
600	TRP3	YKL211C	53456	6.45	5	66	100.000	25
601	HSP31	YDR533C	25654	5.26	3	66	100.000	48
602	MEF1	YLR069C	84520	6.42	9	66	100.000	13
603	IML2	YJL082W	82483	6.22	11	66	100.000	12
605	SGD1	YLR336C	102789	5.73	10	66	100.000	25

606	SWC3	YAL011W	72469	9.18	11	66	100.000	20
607	SIR3	YLR442C	111291	6.02	14	66	100.000	13
608	ORC5	YNL261W	55254	5.66	6	65	100.000	28
609	BPT1	YLL015W	176762	7.69	13	65	100.000	17
610	PLC1	YPL268W	100484	9.20	10	65	100.000	19
611	RPL6A	YML073C	19949	10.10	5	65	100.000	32
612	RPH1	YER169W	90155	9.17	11	65	100.000	16
613	AI1	Q0050	96016	9.89	13	65	100.000	11
614	MCM6	YGL201C	112908	5.03	13	65	100.000	18
615	LYS9	YNR050C	48887	5.10	6	65	100.000	39
616	PRP8	YHR165C	279328	6.86	18	65	100.000	13
617	SET5	YHR207C	60509	6.03	11	65	100.000	14
618	NPR1	YNL183C	85937	8.61	10	65	100.000	16
619	PRP2	YNR011C	99751	8.57	9	64	100.000	23
620	YNL054W-B	YNL054W-B	198075	8.68	12	64	100.000	20
621	YDR026C	YDR026C	66311	9.33	13	64	100.000	15
622	SOF1	YLL011W	56754	9.42	12	64	100.000	12
623	ATG2	YNL242W	178303	5.62	15	64	100.000	13
624	YDR539W	YDR539W	56128	5.72	11	64	100.000	15
625	IQG1	YPL242C	172722	9.04	12	64	100.000	21
626	PTK2	YJR059W	91344	8.97	14	64	100.000	10
627	UFD2	YDL190C	109836	5.52	12	64	100.000	9
628	SWR1	YDR334W	174422	5.86	10	64	100.000	27
629	PSE1	YMR308C	120954	4.61	9	64	100.000	26
630	PMD1	YER132C	195263	7.79	17	64	100.000	11
631	IRC24	YIR036C	28786	6.00	5	64	100.000	38
632	SEC7	YDR170C	226745	4.68	15	64	100.000	8
633	YPL216W	YPL216W	128052	7.04	13	64	100.000	15
634	FAR10	YLR238W	54059	9.14	14	64	100.000	13
635	MSK1	YNL073W	66086	9.02	12	64	100.000	19

636	GSP2	YOR185C	24975	6.22	6	63	100.000	41
637	MLP1	YKR095W	218324	5.14	23	63	100.000	12
638	RIM15	YFL033C	196410	6.01	16	63	100.000	9
639	DIT2	YDR402C	56035	8.90	8	63	100.000	15
640	FSH1	YHR049W	27322	5.93	3	63	100.000	50
641	RSC2	YLR357W	102236	8.97	14	63	100.000	13
642	GAL1	YBR020W	57907	6.30	6	63	100.000	37
643	SEC17	YBL050W	32782	4.96	6	63	100.000	23
644	TCO89	YPL180W	88792	7.85	9	63	100.000	15
645	GRC3	YLL035W	72213	5.91	14	63	100.000	10
646	YGR126W	YGR126W	25830	5.95	2	63	100.000	52
647	YJL113W	YJL113W	207580	8.24	17	62	100.000	15
648	CDC5	YMR001C	80980	9.06	9	62	100.000	18
649	DAL7	YIR031C	62754	6.05	12	62	100.000	12
650	IST1	YNL265C	34474	5.71	7	62	100.000	26
651	HCH1	YNL281W	17236	4.56	3	62	100.000	31
652	IRC20	YLR247C	180231	6.10	18	62	100.000	11
653	TYW1	YPL207W	89748	8.48	14	62	100.000	12
654	RFA1	YAR007C	70304	5.87	12	62	100.000	13
655	NRM1	YNR009W	27547	10.04	9	62	100.000	19
656	YNL010W	YNL010W	27463	5.28	2	62	100.000	59
657	RPO31	YOR116C	162199	8.50	17	62	100.000	7
658	ITC1	YGL133W	145553	5.50	18	62	100.000	8
659	UBR2	YLR024C	216639	5.93	17	62	100.000	12
660	MLH2	YLR035C	78199	8.31	14	62	100.000	15
661	HSL1	YKL101W	169489	9.35	14	62	100.000	12
662	POL4	YCR014C	67484	8.28	9	62	100.000	15
663	YER140W	YER140W	64753	9.79	10	62	100.000	22
664	YDR049W	YDR049W	72688	8.99	7	62	100.000	19
665	YOR019W	YOR019W	83315	9.74	10	62	100.000	22
666	LEU5	YHR002W	40799	9.61	8	62	100.000	20

667	YPL141C	YPL141C	97633	9.49	12	62	100.000	11
668	REV3	YPL167C	172848	8.85	14	61	100.000	8
669	PAN1	YIR006C	160169	5.17	11	61	99.999	14
670	RPS29A	YLR388W	6656	10.31	4	61	99.999	39
671	DIS3	YOL021C	113635	6.22	15	61	99.999	9
672	RET2	YFR051C	60590	5.06	6	61	99.999	21
673	RPL34B	YIL052C	13633	10.84	5	61	99.999	33
674	TOP2	YNL088W	164112	6.62	13	61	99.999	14
675	ARE2	YNR019W	73975	7.59	5	61	99.999	23
676	GUK1	YDR454C	20625	6.63	5	61	99.999	25
677	SIP18	YMR175W	8868	8.01	2	61	99.999	58
678	AIM9	YER080W	72369	8.71	12	61	99.999	14
679	PTH2	YBL057C	23114	5.26	8	61	99.999	13
680	PCA1	YBR295W	131755	7.59	11	61	99.999	15
681	GLO2	YDR272W	31307	5.82	3	61	99.999	53
682	SMC2	YFR031C	133845	6.83	14	61	99.999	10
683	APL2	YKL135C	81816	5.09	8	61	99.999	13
684	TOP3	YLR234W	74324	8.71	10	61	99.999	12
685	PIM1	YBL022C	127033	5.43	13	61	99.999	14
686	DEG1	YFL001W	50856	9.34	7	61	99.999	39
687	SMC3	YJL074C	141250	5.63	13	61	99.999	14
688	SLH1	YGR271W	224686	6.10	16	61	99.999	9
689	CDC15	YAR019C	110215	8.16	9	61	99.999	20
690	SMC1	YFL008W	141193	6.11	14	61	99.999	12
691	KEL2	YGR238C	99913	8.24	13	60	99.999	12
692	PFK26	YIL107C	93359	8.73	16	60	99.999	10
693	SCC4	YER147C	72094	7.97	7	60	99.999	14
694	BRE5	YNR051C	57639	9.15	10	60	99.999	23
695	ROM1	YGR070W	131309	9.17	13	60	99.999	15
696	MTC5	YDR128W	130864	5.61	12	60	99.999	23
697	RET1	YOR207C	129374	8.40	12	60	99.999	15

698	SMC4	YLR086W	162089	5.92	18	60	99.999	14
699	APL6	YGR261C	91550	5.57	10	60	99.999	11
700	PWP2	YCR057C	103919	4.94	12	60	99.999	11
701	STF2	YGR008C	9609	7.98	3	60	99.999	39
702	PRP21	YJL203W	33032	7.67	11	60	99.999	20
703	PHO81	YGR233C	133946	5.53	11	59	99.999	14
704	SBE2	YDR351W	98909	8.56	12	59	99.999	14
705	SBP1	YHL034C	32969	5.48	9	59	99.999	22
706	RPS12	YOR369C	15462	4.68	3	59	99.999	48
707	PPT1	YGR123C	57958	7.59	10	59	99.999	19
708	IES1	YFL013C	78704	5.06	11	59	99.999	23
709	YKR104W	YKR104W	34631	7.62	9	59	99.999	18
710	NTH2	YBR001C	89623	6.05	4	59	99.999	45
711	ALK2	YBL009W	76325	9.41	11	59	99.999	12
712	PKC1	YBL105C	131436	6.69	14	59	99.999	14
713	FUR1	YHR128W	24579	5.58	8	59	99.999	16
714	OSH3	YHR073W	113690	8.67	8	59	99.999	14
715	YER158C	YER158C	63672	9.86	9	59	99.999	11
716	AFG3	YER017C	84491	9.20	14	59	99.999	11
717	ENP2	YGR145W	81698	6.20	9	59	99.999	19
718	RTG2	YGL252C	65531	8.17	11	59	99.999	21
719	YEL025C	YEL025C	135982	8.41	10	59	99.999	14
720	RPL37A	YLR185W	9844	11.64	7	59	99.999	22
721	IML1	YJR138W	181835	8.89	16	59	99.999	12
722	LEU3	YLR451W	100090	5.78	8	59	99.999	25
723	SNT1	YCR033W	138313	9.17	15	59	99.999	9
724	YGR001C	YGR001C	28564	4.77	4	58	99.999	48
725	BOP2	YLR267W	66302	6.06	9	58	99.999	14
726	ADH6	YMR318C	39592	6.28	6	58	99.999	33
727	YJL049W	YJL049W	52817	5.23	6	58	99.999	20
728	DBP7	YKR024C	83256	9.33	12	58	99.999	10

729	AKL1	YBR059C	123913	7.38	12	58	99.999	9
730	SAD1	YFR005C	52134	6.68	8	58	99.999	18
731	SDC25	YLL016W	121885	5.93	10	58	99.999	13
732	LAT1	YNL071W	51786	7.60	6	58	99.999	19
733	MDM1	YML104C	129899	6.01	9	58	99.999	14
734	HEH2	YDR458C	76329	7.84	6	58	99.999	21
735	YLR211C	YLR211C	25959	5.56	6	58	99.999	23
736	PMR1	YGL167C	104504	5.47	11	58	99.999	9
737	GND2	YGR256W	53889	6.84	10	58	99.999	19
738	RAD27	YKL113C	43252	9.05	8	58	99.999	14
739	MCM3	YEL032W	107452	5.26	10	58	99.999	24
740	QCR2	YPR191W	40453	7.67	3	58	99.999	34
741	KOG1	YHR186C	177497	7.91	12	58	99.999	11
742	RGA1	YOR127W	112761	6.03	8	58	99.999	19
743	DRS1	YLL008W	84791	5.59	12	58	99.999	13
744	PTP3	YER075C	105185	6.76	7	58	99.999	18
745	NAM7	YMR080C	109362	6.06	14	58	99.999	10
746	SUI1	YNL244C	12304	7.77	4	58	99.999	45
747	EXO84	YBR102C	85485	7.99	14	58	99.999	14
748	SPG4	YMR107W	13172	6.29	7	58	99.999	19
749	PDR15	YDR406W	172145	8.18	10	58	99.999	16
750	SNQ2	YDR011W	168658	7.64	14	57	99.999	9
751	LAP2	YNL045W	77304	6.11	8	57	99.999	35
752	YPR204W	YPR204W	115083	6.33	15	57	99.999	10
753	POM152	YMR129W	151558	6.29	13	57	99.999	8
754	RLF2	YPR018W	70167	6.38	11	57	99.999	18
755	SPB1	YCL054W	96424	8.08	7	57	99.999	18
756	GSC2	YGR032W	216850	6.59	11	57	99.999	14
757	IRE1	YHR079C	126896	6.14	12	57	99.999	14
758	MIP6	YHR015W	75872	9.48	11	57	99.999	21
759	SSK22	YCR073C	152620	7.75	14	57	99.999	11

760	SPO75	YLL005C	102104	9.65	9	57	99.999	13
761	CIN1	YOR349W	116574	8.53	9	57	99.999	15
762	GPB2	YAL056W	98549	7.08	10	57	99.999	11
763	STB5	YHR178W	83420	8.78	7	57	99.999	16
764	NOP13	YNL175C	45639	9.28	7	57	99.999	28
765	ITT1	YML068W	54059	5.41	6	57	99.999	26
766	SFB3	YHR098C	103884	5.87	7	57	99.999	30
767	ACK1	YDL203C	69327	8.57	12	57	99.999	14
768	SSP120	YLR250W	27273	4.98	6	57	99.999	21
769	YML020W	YML020W	76091	8.05	9	57	99.999	17
770	PRP9	YDL030W	62990	6.07	12	57	99.999	23
771	TFG1	YGR186W	82144	5.58	12	57	99.999	10
772	IMH1	YLR309C	105162	5.52	13	57	99.999	13
773	RPL33A	YPL143W	12147	11.07	7	57	99.998	22
774	YOR1	YGR281W	166621	7.71	8	57	99.998	18
775	ENT3	YJR125C	45064	4.71	7	57	99.998	30
776	TEL2	YGR099W	78637	6.22	6	57	99.998	23
777	YNR034W-A	YNR034W-A	10775	8.93	5	57	99.998	31
778	SIP4	YJL089W	95945	6.11	7	57	99.998	21
779	AI2	Q0055	97945	9.67	12	56	99.998	18
780	CIC1	YHR052W	42504	8.80	6	56	99.998	23
781	AAT1	YKL106W	51762	9.06	6	56	99.998	20
782	PUT2	YHR037W	64395	6.54	8	56	99.998	22
783	GIP3	YPL137C	140804	7.09	16	56	99.998	9
784	SKI2	YLR398C	145967	6.31	10	56	99.998	16
785	NAP1	YKR048C	47855	4.23	5	56	99.998	32
786	BUD6	YLR319C	88762	7.62	14	56	99.998	10
787	TCM62	YBR044C	64218	9.05	8	56	99.998	19
788	BRE4	YDL231C	129643	9.11	12	56	99.998	11
789	RPL42A	YNL162W	12204	10.60	4	56	99.998	43

790	YGR130C	YGR130C	92643	4.96	10	56	99.998	8
791	BMS1	YPL217C	135487	6.39	11	56	99.998	11
792	CUE2	YKL090W	50842	6.69	7	56	99.998	20
793	NUP120	YKL057C	120372	5.03	7	56	99.998	28
794	MET5	YJR137C	161119	5.31	14	56	99.998	12
795	PST2	YDR032C	20953	5.46	2	56	99.998	54
796	XKS1	YGR194C	68277	6.38	8	56	99.998	16
797	GBP2	YCL011C	48699	5.95	10	56	99.998	18
798	AIM17	YHL021C	53102	7.21	3	56	99.998	45
799	YLR112W	YLR112W	15908	10.70	4	56	99.998	24
800	PDR5	YOR153W	170329	8.02	11	56	99.998	12
801	DCS2	YOR173W	40915	6.15	2	56	99.998	52
802	VMA7	YGR020C	13453	4.98	3	56	99.998	43
803	FCY1	YPR062W	17496	5.68	5	56	99.998	38
804	MNN1	YER001W	88474	6.79	9	56	99.998	16
805	ARF1	YDL192W	20516	6.75	5	56	99.998	33
806	CDC25	YLR310C	178981	6.67	14	56	99.998	10
807	YMC2	YBR104W	36532	9.33	9	56	99.998	14
808	SPO14	YKR031C	195083	7.26	20	56	99.998	8
809	LAP4	YKL103C	57057	5.55	7	55	99.998	24
810	PMS1	YNL082W	99293	5.92	12	55	99.998	8
811	STU2	YLR045C	100855	8.68	11	55	99.998	13
812	CDC9	YDL164C	84774	7.44	12	55	99.998	21
813	SAP155	YFR040W	114918	4.56	9	55	99.998	12
814	NOP2	YNL061W	69769	4.95	12	55	99.998	9
815	CAP1	YKL007W	30680	5.18	7	55	99.998	19
816	TOF2	YKR010C	86313	7.97	9	55	99.998	12
817	RGC1	YPR115W	120320	9.31	13	55	99.998	10
818	RNR3	YIL066C	97453	5.68	12	55	99.998	12
819	PET309	YLR067C	112574	9.34	13	55	99.998	9
820	TCB2	YNL087W	132426	8.65	9	55	99.998	15

821	AIP1	YMR092C	67284	5.36	8	55	99.998	23
822	EST2	YLR318W	102598	9.33	11	55	99.998	16
823	YBR138C	YBR138C	60422	7.98	9	55	99.998	14
824	NSR1	YGR159C	44509	4.88	7	55	99.998	33
825	NOG2	YNR053C	55454	9.52	9	55	99.998	15
826	STB2	YMR053C	97766	6.22	10	55	99.998	11
827	FUN30	YAL019W	128428	5.24	12	55	99.998	15
828	RTT10	YPL183C	114389	5.78	14	54	99.998	11
829	GSY2	YLR258W	80029	5.91	8	54	99.997	19
830	HUL5	YGL141W	105499	6.05	10	54	99.997	24
831	FRS2	YFL022C	57475	5.53	4	54	99.997	32
832	RPS15	YOL040C	15992	10.70	5	54	99.997	30
833	CRR1	YLR213C	47326	7.93	9	54	99.997	13
834	RDH54	YBR073W	107963	9.30	11	54	99.997	10
835	MSH3	YCR092C	116460	6.69	10	54	99.997	11
836	RSN1	YMR266W	107604	8.74	9	54	99.997	11
837	YCS4	YLR272C	132883	5.43	10	54	99.997	13
839	YOL036W	YOL036W	84301	9.25	10	54	99.997	14
840	KAR3	YPR141C	83952	8.83	12	54	99.997	16
841	YOR093C	YOR093C	186788	8.75	14	54	99.997	10
842	UBP9	YER098W	86190	7.07	8	54	99.997	19
843	GDH1	YOR375C	49539	5.56	7	54	99.997	20
844	CPR3	YML078W	19906	8.81	6	54	99.997	32
845	MYO3	YKL129C	142419	9.45	13	54	99.997	10
846	GYP1	YOR070C	73243	6.71	6	54	99.997	20
847	STO1	YMR125W	99955	4.81	5	54	99.997	37
848	INN1	YNL152W	46197	6.81	7	54	99.997	24
849	OSH2	YDL019C	145707	6.37	12	54	99.997	7
850	KIP2	YPL155C	78330	9.44	12	54	99.997	17
851	SIR4	YDR227W	151969	9.03	11	54	99.997	14
852	RGR1	YLR071C	123280	8.87	14	54	99.997	15

853	PSD2	YGR170W	129984	7.97	12	54	99.997	13
854	EPS1	YIL005W	81167	7.88	7	54	99.997	19
855	RGA2	YDR379W	113221	8.06	11	53	99.997	13
856	URA3	YEL021W	29221	6.91	4	53	99.997	45
857	SOL3	YHR163W	27767	5.32	6	53	99.997	17
858	NEW1	YPL226W	134247	5.61	9	53	99.997	10
859	YPR097W	YPR097W	122976	5.54	11	53	99.996	13
860	PDC2	YDR081C	103880	6.01	11	53	99.996	8
861	RAD30	YDR419W	71470	8.53	7	53	99.996	16
862	MPH1	YIR002C	113986	7.00	10	53	99.996	14
863	FOX2	YKR009C	98642	9.06	12	53	99.996	10
864	STP3	YLR375W	37694	9.37	6	53	99.996	23
865	ADE2	YOR128C	62300	6.92	9	53	99.996	14
866	RIO1	YOR119C	56087	6.13	7	53	99.996	16
867	RPL14A	YKL006W	15158	10.94	4	53	99.996	34
868	MVD1	YNR043W	44088	5.54	6	53	99.996	16
869	YTA6	YPL074W	85248	9.64	12	53	99.996	13
870	CNM67	YNL225C	67358	5.74	9	53	99.996	14
871	YOL098C	YOL098C	118318	4.92	6	53	99.996	17
872	ERG8	YMR220W	50423	6.03	7	53	99.996	24
873	YER184C	YER184C	91018	8.05	14	53	99.996	11
874	CIS1	YDR022C	22178	4.03	5	53	99.996	25
875	SCT1	YBL011W	85640	6.85	12	53	99.996	12
876	ZIP1	YDR285W	99974	6.40	9	53	99.996	18
877	EAF1	YDR359C	112433	9.10	8	53	99.996	14
878	VMA4	YOR332W	26455	5.33	8	53	99.996	16
879	MTR4	YJL050W	121978	5.96	9	52	99.996	21
880	NOP7	YGR103W	69834	5.48	10	52	99.996	19
881	URB2	YJR041C	135032	5.96	12	52	99.996	11
882	SYP1	YCR030C	96079	8.65	9	52	99.996	10
883	RRP3	YHR065C	55933	9.22	10	52	99.996	9

884	RMD8	YFR048W	75867	6.81	7	52	99.996	33
885	PDX3	YBR035C	26892	6.93	5	52	99.996	20
886	TAD3	YLR316C	37084	5.95	5	52	99.996	22
887	PES4	YFR023W	70798	9.48	9	52	99.996	10
888	RSP5	YER125W	91760	6.24	8	52	99.996	14
889	HES1	YOR237W	49474	6.72	6	52	99.996	27
890	EXO70	YJL085W	71249	7.12	8	52	99.996	12
891	RKR1	YMR247C	180072	5.34	11	52	99.996	12
892	VAC17	YCL063W	47814	8.68	7	52	99.996	20
893	PIF1	YML061C	97621	9.06	9	52	99.996	13
894	GEP3	YOR205C	63813	9.35	11	52	99.996	15
895	ALG8	YOR067C	67341	9.52	7	52	99.996	16
896	ILS1	YBL076C	122906	5.74	6	52	99.996	14
897	LYS20	YDL182W	47069	6.84	8	52	99.995	17
898	PET494	YNR045W	57452	9.13	10	52	99.995	16
899	LRS4	YDR439W	39330	9.54	4	52	99.995	23
900	HIS7	YBR248C	61030	5.34	6	52	99.995	30
901	GSH2	YOL049W	55781	5.50	5	52	99.995	28
902	CFT2	YLR115W	96194	7.51	10	52	99.995	19
903	PUF2	YPR042C	119435	8.94	8	52	99.995	11
904	APC9	YLR102C	30837	5.34	7	52	99.995	16
905	IKI3	YLR384C	152894	4.95	7	52	99.995	14
906	APL3	YBL037W	114940	8.81	11	52	99.995	15
907	MSH5	YDL154W	102144	5.11	10	51	99.995	17
908	CMP2	YML057W	68484	5.92	10	51	99.995	11
909	EXO1	YOR033C	80112	8.61	11	51	99.995	13
910	PDS5	YMR076C	146950	5.90	11	51	99.995	16
911	PHO8	YDR481C	62965	5.31	5	51	99.995	21
912	RAD53	YPL153C	91905	7.88	9	51	99.995	12
913	RAD5	YLR032W	133918	5.98	11	51	99.995	13
914	HMG2	YLR450W	115618	7.51	9	51	99.995	13

915	LPE10	YPL060W	47053	8.83	7	51	99.995	14
916	CHL1	YPL008W	98743	8.12	9	51	99.995	10
917	PFY1	YOR122C	13669	5.47	3	51	99.994	43
918	SAP1	YER047C	100270	8.99	12	51	99.994	10
919	VPS27	YNR006W	70930	5.18	10	51	99.994	11
920	TRE1	YPL176C	88699	4.81	9	51	99.994	17
921	PEP1	YBL017C	177665	4.75	17	51	99.994	7
922	GCV3	YAL044C	18781	4.69	4	51	99.994	23
923	ERG20	YJL167W	40458	5.32	4	51	99.994	34
924	RAV2	YDR202C	39991	5.95	7	51	99.994	17
925	POL1	YNL102W	166704	5.89	12	51	99.994	12
926	HRD3	YLR207W	95420	6.15	7	51	99.994	20
927	NOG1	YPL093W	74363	8.91	10	51	99.994	14
928	TRS130	YMR218C	128049	5.73	6	51	99.994	16
929	MDM20	YOL076W	92750	7.77	8	51	99.994	11
930	YGR125W	YGR125W	116897	7.01	8	51	99.994	13
931	RAD51	YER095W	42936	4.82	7	51	99.994	24
932	SNF2	YOR290C	193931	6.54	15	51	99.994	13
933	NUP159	YIL115C	158811	4.73	11	50	99.994	9
934	TRM3	YDL112W	164943	5.74	15	50	99.994	9
935	MSA1	YOR066W	68649	9.97	10	50	99.993	13
936	SLP1	YOR154W	67410	5.36	10	50	99.993	10
937	KAP120	YPL125W	119547	5.14	8	50	99.993	13
938	RPN3	YER021W	60355	5.37	8	50	99.993	26
939	RDR1	YOR380W	61249	7.93	8	50	99.993	19
940	SYF1	YDR416W	100166	5.17	12	50	99.993	9
941	ACE2	YLR131C	86581	8.47	12	50	99.993	16
942	SNF7	YLR025W	26970	4.66	6	50	99.993	26
943	SRC1	YML034W	95438	5.43	10	50	99.993	21
944	SKG3	YLR187W	114040	8.37	10	50	99.993	12
945	IOC4	YMR044W	55392	5.21	10	50	99.993	20

946	YMR160W	YMR160W	95038	6.41	8	50	99.993	15
947	RNA14	YMR061W	79910	5.62	10	50	99.993	11
948	FRA1	YLL029W	84871	6.40	14	50	99.993	8
949	MDG1	YNL173C	40254	5.69	5	50	99.992	31
950	PAH1	YMR165C	94973	4.85	8	50	99.992	10
951	UGO1	YDR470C	57435	6.64	8	50	99.992	18
952	STE6	YKL209C	144673	8.27	10	50	99.992	10
953	BOI2	YER114C	115618	8.80	13	50	99.992	11
954	MRPL3	YMR024W	43972	9.47	9	50	99.992	18
955	MIH1	YMR036C	63319	7.27	8	50	99.992	14
956	WAR1	YML076C	107493	7.51	9	50	99.992	11
957	SLX4	YLR135W	84310	4.87	12	49	99.992	10
958	FAL1	YDR021W	45185	9.09	8	49	99.992	8
959	SAP190	YKR028W	124985	4.33	8	49	99.992	16
960	CTF18	YMR078C	84321	8.54	10	49	99.992	11
961	DUG2	YBR281C	98010	5.33	6	49	99.992	16
962	TCB1	YOR086C	133493	6.74	13	49	99.992	9
963	REB1	YBR049C	91819	4.96	9	49	99.992	13
964	DML1	YMR211W	55277	5.14	10	49	99.992	14
965	DRS2	YAL026C	153748	5.37	8	49	99.992	17
966	PTK1	YKL198C	72016	9.05	15	49	99.992	11
967	ATG14	YBR128C	40427	9.33	9	49	99.991	20
968	CET1	YPL228W	61812	5.41	12	49	99.991	6
969	YJL132W	YJL132W	84413	5.84	5	49	99.991	24
970	COP1	YDL145C	135523	5.66	9	49	99.991	23
971	IDH1	YNL037C	39300	8.99	4	49	99.991	19
972	TUB2	YFL037W	50890	4.64	4	49	99.991	24
973	JEN1	YKL217W	69331	5.64	7	49	99.991	15
974	REG1	YDR028C	112548	4.89	15	49	99.991	15
975	CBP1	YJL209W	76123	9.58	8	49	99.991	16
976	DCD1	YHR144C	35623	8.16	10	49	99.991	14

977	SNF3	YDL194W	96658	5.22	6	49	99.991	16
978	AEP2	YMR282C	67480	9.57	10	49	99.991	16
979	YHR003C	YHR003C	48852	6.36	9	49	99.991	12
980	YMR291W	YMR291W	66178	6.51	8	49	99.990	14
981	YMR134W	YMR134W	27904	5.30	7	49	99.990	17
982	YDR109C	YDR109C	79111	6.37	8	49	99.990	10
983	EST1	YLR233C	81748	9.40	7	49	99.990	13
984	PEX25	YPL112C	44883	9.10	3	49	99.990	40
985	MUD2	YKL074C	60422	8.41	12	49	99.990	8
986	YHR218W	YHR218W	68807	8.86	9	49	99.990	15
987	PTP2	YOR208W	85814	9.10	8	49	99.990	14
988	TAH18	YPR048W	72282	8.71	9	48	99.990	9
989	YDR239C	YDR239C	86382	6.11	15	48	99.990	12

APPENDIX B

PROTEIN IDENTIFICATIONS FROM THE TWO-STAGE SEPARATION OF NEUROSPORA CRASSA TRYPTIC PEPTIDES

Rank	Accession #	Name	Peptides(95%)	Seq. Cov (%)
1	NCU01328T0	| NCU01328 | Neurospora crassa OR74A (finished) transketolase (translation) (687 aa)	29	36.7
2	NCU07700T0	| NCU07700 | Neurospora crassa OR74A (finished) colonial temperature-sensitive-3 (translation) (845 aa)	22	36.7
3	NCU07027T0	| NCU07027 | Neurospora crassa OR74A (finished) glycogen phosphorylase (translation) (888 aa)	22	33.3
4	NCU09602T0	| NCU09602 | Neurospora crassa OR74A (finished) heat shock protein 70-1 (translation) (647 aa)	19	37.8
5	NCU01680T0	| NCU01680 | Neurospora crassa OR74A (finished) plasma membrane ATPase-1 (translation) (921 aa)	16	21.7
6	NCU07914T0	| NCU07914 | Neurospora crassa OR74A (finished) phosphoglycerate kinase (translation) (419 aa)	16	35.9
7	NCU06512T0	| NCU06512 | Neurospora crassa OR74A (finished) methionine synthase (translation) (770 aa)	17	27.2
8	NCU00018T1	| NCU00018 | Neurospora crassa OR74A (finished) cell division control protein Cdc48 (translation) (825 aa)	16	26.8
9	NCU02514T0	| NCU02514 | Neurospora crassa OR74A (finished) ATPase-1 (translation) (552 aa)	15	35.8
10	NCU02136T0	| NCU02136 | Neurospora crassa OR74A (finished) transaldolase (translation) (301 aa)	17	52.0
11	NCU01528T0	| NCU01528 | Neurospora crassa OR74A (finished)	17	39.6

		glyceraldehyde-3-phosphate dehydrogenase-1 (translation) (339 aa)		
12	NCU02797T0	| NCU02797 | Neurospora crassa OR74A (finished) UTP-glucose-1-phosphate uridylyltransferase (translation) (522 aa)	16	29.4
13	NCU02366T0	| NCU02366 | Neurospora crassa OR74A (finished) aconitase (translation) (785 aa)	14	22.1
14	NCU10042T1	| NCU10042 | Neurospora crassa OR74A (finished) enolase (translation) (439 aa)	15	46.8
15	NCU02003T0	| NCU02003 | Neurospora crassa OR74A (finished) translation elongation factor-1 (translation) (461 aa)	19	35.9
16	NCU02075T0	| NCU02075 | Neurospora crassa OR74A (finished) heat shock protein 70 (translation) (586 aa)	14	27.5
17	NCU00355T0	| NCU00355 | Neurospora crassa OR74A (finished) catalase-3 (translation) (720 aa)	13	18.6
18	NCU07922T0	| NCU07922 | Neurospora crassa OR74A (finished) elongation factor 3 (translation) (1057 aa)	13	16.9
19	NCU05770T0	| NCU05770 | Neurospora crassa OR74A (finished) peroxidase/catalase 2 (translation) (754 aa)	14	27.5
20	NCU02505T0	| NCU02505 | Neurospora crassa OR74A (finished) succinate (translation) (1193 aa)	12	17.6
21	NCU09477T0	| NCU09477 | Neurospora crassa OR74A (finished) ADP, ATP carrier protein (translation) (314 aa)	14	37.4
22	NCU07807T1	| NCU07807 | Neurospora crassa OR74A (finished) fructose bisphosphate aldolase (translation) (363 aa)	13	33.2
23	NCU03100T0	| NCU03100 | Neurospora crassa OR74A (finished) 6-phosphogluconate dehydrogenase (translation) (493 aa)	12	29.5
24	NCU00489T0	| NCU00489 | Neurospora crassa OR74A (finished) cytoplasmic ribosomal protein-10 (translation) (263 aa)	11	66.4
25	NCU05554T0	| NCU05554 | Neurospora crassa OR74A (finished) 60S ribosomal protein L13 (translation) (215 aa)	11	56.5

26	NCU02181T0	| NCU02181 | Neurospora crassa OR74A (finished) 40S ribosomal protein S4 (translation) (262 aa)	12	41.8
27	NCU03826T0	| NCU03826 | Neurospora crassa OR74A (finished) elongation factor 1-gamma (translation) (409 aa)	11	29.9
28	NCU02930T0	| NCU02930 | Neurospora crassa OR74A (finished) conserved hypothetical protein (translation) (330 aa)	11	39.8
29	NCU05430T0	| NCU05430 | Neurospora crassa OR74A (finished) ATP synthase beta subunit (translation) (520 aa)	11	33.1
30	NCU04779T0	| NCU04779 | Neurospora crassa OR74A (finished) 60S ribosomal protein L8 (translation) (263 aa)	11	45.0
31	NCU09228T0	| NCU09228 | Neurospora crassa OR74A (finished) aminopeptidase 2 (translation) (972 aa)	12	18.2
32	NCU02580T0	| NCU02580 | Neurospora crassa OR74A (finished) fumarate reductase Osm1 (translation) (617 aa)	11	21.3
33	NCU03757T0	| NCU03757 | Neurospora crassa OR74A (finished) 60S ribosomal protein L4-A (translation) (362 aa)	13	43.2
34	NCU05269T1	| NCU05269 | Neurospora crassa OR74A (finished) heat shock protein 88 (translation) (708 aa)	10	17.7
35	NCU04923T0	| NCU04923 | Neurospora crassa OR74A (finished) Gld1 (translation) (332 aa)	11	34.1
36	NCU04899T0	| NCU04899 | Neurospora crassa OR74A (finished) malate dehydrogenase (translation) (337 aa)	11	46.4
37	NCU06843T0	| NCU06843 | Neurospora crassa OR74A (finished) 60S ribosomal protein L3 (translation) (393 aa)	13	29.9
38	NCU04142T0	| NCU04142 | Neurospora crassa OR74A (finished) heat shock protein 80 (translation) (706 aa)	9	24.0
39	NCU03565T0	| NCU03565 | Neurospora crassa OR74A (finished) ribosomal protein L26 (translation) (137 aa)	10	69.1
40	NCU07281T0	| NCU07281 | Neurospora crassa OR74A (finished) glucose-6-phosphate isomerase (translation) (562 aa)	11	23.7

41	NCU02566T0	| NCU02566 | Neurospora crassa OR74A (finished) alanyl-tRNA synthetase (translation) (962 aa)	10	18.6
42	NCU01452T0	| NCU01452 | Neurospora crassa OR74A (finished) 40S ribosomal protein S1 (translation) (257 aa)	9	41.4
43	NCU07307T0	| NCU07307 | Neurospora crassa OR74A (finished) fatty acid synthase beta subunit dehydratase (translation) (2093 aa)	10	7.8
44	NCU01692T0	| NCU01692 | Neurospora crassa OR74A (finished) mitochondrial citrate synthase (translation) (470 aa)	10	19.8
45	NCU05850T0	| NCU05850 | Neurospora crassa OR74A (finished) rubredoxin-NAD(+) reductase (translation) (612 aa)	10	19.6
46	NCU01207T0	| NCU01207 | Neurospora crassa OR74A (finished) vacuolar membrane ATPase-1 (translation) (608 aa)	9	18.1
47	NCU07930T0	| NCU07930 | Neurospora crassa OR74A (finished) adenosylhomocysteinase (translation) (450 aa)	9	25.2
48	NCU04173T1	| NCU04173 | Neurospora crassa OR74A (finished) actin (translation) (376 aa)	9	30.7
49	NCU07404T0	| NCU07404 | Neurospora crassa OR74A (finished) alpha-mannosidase (translation) (1090 aa)	8	13.6
50	NCU00743T0	| NCU00743 | Neurospora crassa OR74A (finished) glycogen debranching enzyme (translation) (1562 aa)	8	10.3
51	NCU06211T1	| NCU06211 | Neurospora crassa OR74A (finished) malate dehydrogenase (translation) (332 aa)	10	35.4
52	NCU05429T1	| NCU05429 | Neurospora crassa OR74A (finished) 1,4-alpha-glucan branching enzyme (translation) (706 aa)	10	18.9
53	NCU02806T0	| NCU02806 | Neurospora crassa OR74A (finished) 14-3-3 family protein 7 (translation) (263 aa)	8	34.4
54	NCU01107T0	| NCU01107 | Neurospora crassa OR74A (finished) short-chain dehydrogenase (translation) (334 aa)	10	23.7
55	NCU06210T0	| NCU06210 | Neurospora crassa OR74A (finished) conserved hypothetical protein (translation) (151 aa)	9	48.0

56	NCU09285T0	| NCU09285 | Neurospora crassa OR74A (finished) zinc-containing alcohol dehydrogenase (translation) (347 aa)	9	34.4
57	NCU03125T0	| NCU03125 | Neurospora crassa OR74A (finished) NIMA-interacting protein TinC (translation) (796 aa)	9	11.2
58	NCU03102T0	| NCU03102 | Neurospora crassa OR74A (finished) 40S ribosomal protein S11 (translation) (162 aa)	11	49.7
59	NCU04482T0	| NCU04482 | Neurospora crassa OR74A (finished) conserved hypothetical protein (translation) (212 aa)	8	39.8
60	NCU03982T0	| NCU03982 | Neurospora crassa OR74A (finished) glucose regulated protein 78 (translation) (662 aa)	10	21.9
61	NCU05488T0	| NCU05488 | Neurospora crassa OR74A (finished) RNA-binding protein Vip1 (translation) (284 aa)	9	31.1
62	NCU01768T0	| NCU01768 | Neurospora crassa OR74A (finished) conserved hypothetical protein (translation) (1049 aa)	8	10.1
63	NCU02571T0	| NCU02571 | Neurospora crassa OR74A (finished) acetyl-CoA acetyltransferase (translation) (400 aa)	8	25.8
64	NCU10058T0	| NCU10058 | Neurospora crassa OR74A (finished) phosphoglucomutase 2 (translation) (555 aa)	10	20.0
65	NCU08515T0	| NCU08515 | Neurospora crassa OR74A (finished) vacuolar membrane ATPase-2 (translation) (514 aa)	8	20.7
66	NCU00726T0	| NCU00726 | Neurospora crassa OR74A (finished) cyclosporin-resistant-1 (translation) (224 aa)	11	37.7
67	NCU01824T0	| NCU01824 | Neurospora crassa OR74A (finished) UDP-galactopyranose mutase (translation) (518 aa)	8	17.2
68	NCU03703T0	| NCU03703 | Neurospora crassa OR74A (finished) 60S ribosomal protein L17 (translation) (187 aa)	7	43.6
69	NCU05288T0	| NCU05288 | Neurospora crassa OR74A (finished) rab GDP-dissociation inhibitor (translation) (466 aa)	9	18.1
70	NCU02919T0	| NCU02919 | Neurospora crassa OR74A (finished) cupin domain-containing protein (translation) (197 aa)	8	44.4

71	NCU00673T0	| NCU00673 | Neurospora crassa OR74A (finished) serine protease p2 (translation) (533 aa)	7	19.9
72	NCU02921T0	| NCU02921 | Neurospora crassa OR74A (finished) cupin domain-containing protein (translation) (197 aa)	8	41.3
73	NCU10008T0	| NCU10008 | Neurospora crassa OR74A (finished) fumarate hydratase (translation) (534 aa)	7	15.0
74	NCU08002T0	| NCU08002 | Neurospora crassa OR74A (finished) carnitine acetyl transferase (translation) (644 aa)	8	15.6
75	NCU09223T0	| NCU09223 | Neurospora crassa OR74A (finished) protein disulfide-isomerase (translation) (506 aa)	7	19.8
76	NCU00413T0	| NCU00413 | Neurospora crassa OR74A (finished) 60S ribosomal protein L2 (translation) (255 aa)	7	40.9
77	NCU07420T0	| NCU07420 | Neurospora crassa OR74A (finished) eIF4A (translation) (398 aa)	7	27.7
78	NCU07550T0	| NCU07550 | Neurospora crassa OR74A (finished) triosephosphate isomerase (translation) (249 aa)	7	29.0
79	NCU08828T0	| NCU08828 | Neurospora crassa OR74A (finished) peroxisomal hydratase-dehydrogenase-epimerase (translation) (895 aa)	7	12.6
80	NCU03038T0	| NCU03038 | Neurospora crassa OR74A (finished) 40S ribosomal protein S13 (translation) (152 aa)	7	39.1
81	NCU09475T0	| NCU09475 | Neurospora crassa OR74A (finished) 40s ribosomal protein s5 (translation) (214 aa)	8	35.2
82	NCU03753T0	| NCU03753 | Neurospora crassa OR74A (finished) clock-controlled gene-1 (translation) (72 aa)	8	78.9
83	NCU09111T0	| NCU09111 | Neurospora crassa OR74A (finished) glucose-6-phosphate 1-dehydrogenase (translation) (507 aa)	7	19.8
84	NCU06075T1	| NCU06075 | Neurospora crassa OR74A (finished) pyruvate kinase (translation) (528 aa)	7	11.8
85	NCU02263T0	| NCU02263 | Neurospora crassa OR74A (finished) Sec14 cytosolic factor (translation) (335 aa)	8	33.2

86	NCU07153T0	| NCU07153 | Neurospora crassa OR74A (finished) glutamate carboxypeptidase (translation) (534 aa)	7	14.8
87	NCU04930T0	| NCU04930 | Neurospora crassa OR74A (finished) conserved hypothetical protein (translation) (563 aa)	7	13.9
88	NCU00629T0	| NCU00629 | Neurospora crassa OR74A (finished) 6-phosphofructokinase (translation) (846 aa)	5	18.6
89	NCU00951T0	| NCU00951 | Neurospora crassa OR74A (finished) inorganic pyrophosphatase (translation) (445 aa)	6	17.6
90	NCU07830T0	| NCU07830 | Neurospora crassa OR74A (finished) cytoplasmic ribosomal protein-2 (translation) (151 aa)	6	36.7
91	NCU02701T0	| NCU02701 | Neurospora crassa OR74A (finished) dipeptidyl peptidase (translation) (707 aa)	5	12.9
92	NCU02549T0	| NCU02549 | Neurospora crassa OR74A (finished) processing enhancing protein (translation) (477 aa)	6	23.1
93	NCU02639T0	| NCU02639 | Neurospora crassa OR74A (finished) argininosuccinate synthase (translation) (418 aa)	5	23.5
94	NCU03806T0	| NCU03806 | Neurospora crassa OR74A (finished) ribosomal protein L27a.e (translation) (150 aa)	7	36.9
95	NCU00865T0	| NCU00865 | Neurospora crassa OR74A (finished) oxalate decarboxylase oxdC (translation) (456 aa)	6	24.0
96	NCU08500T0	| NCU08500 | Neurospora crassa OR74A (finished) 40S ribosomal protein S8 (translation) (203 aa)	6	48.0
97	NCU08336T0	| NCU08336 | Neurospora crassa OR74A (finished) succinate dehydrogenase flavoprotein subunit (translation) (649 aa)	6	15.6
98	NCU06783T0	| NCU06783 | Neurospora crassa OR74A (finished) ATP citrate lyase (translation) (488 aa)	6	15.6
99	NCU08693T0	| NCU08693 | Neurospora crassa OR74A (finished) heat shock protein 70-5 (translation) (669 aa)	7	20.1
100	NCU01765T0	| NCU01765 | Neurospora crassa OR74A (finished) NADH:ubiquinone oxidoreductase 78 (translation) (745 aa)	6	11.7

101	NCU04533T0	| NCU04533 | Neurospora crassa OR74A (finished) abundant perithecial protein (translation) (208 aa)	7	32.9
102	NCU09693T0	| NCU09693 | Neurospora crassa OR74A (finished) conserved hypothetical protein (translation) (323 aa)	7	20.5
103	NCU04140T0	| NCU04140 | Neurospora crassa OR74A (finished) FK506 resistant-2 (translation) (176 aa)	7	31.4
104	NCU03370T0	| NCU03370 | Neurospora crassa OR74A (finished) conserved hypothetical protein (translation) (184 aa)	7	36.1
105	NCU00935T0	| NCU00935 | Neurospora crassa OR74A (finished) conserved hypothetical protein (translation) (582 aa)	6	11.7
106	NCU11350T0	| NCU11350 | Neurospora crassa OR74A (finished) glucosamine-fructose-6-phosphate aminotransferase (translation) (701 aa)	5	16.1
107	NCU04100T0	| NCU04100 | Neurospora crassa OR74A (finished) vacuolar sorting protein 1 (translation) (707 aa)	5	14.0
108	NCU01827T0	| NCU01827 | Neurospora crassa OR74A (finished) 60S ribosomal protein L27 (translation) (136 aa)	6	45.2
109	NCU07449T0	| NCU07449 | Neurospora crassa OR74A (finished) conserved hypothetical protein (translation) (119 aa)	6	33.1
110	NCU06482T0	| NCU06482 | Neurospora crassa OR74A (finished) pyruvate dehydrogenase E1 component alpha subunit (translation) (418 aa)	5	19.7
111	NCU04924T0	| NCU04924 | Neurospora crassa OR74A (finished) hypothetical protein similar to phosphatidyl synthase (translation) (527 aa)	5	13.5
112	NCU04510T0	| NCU04510 | Neurospora crassa OR74A (finished) aldose reductase (translation) (327 aa)	6	18.1
113	NCU10007T1	| NCU10007 | Neurospora crassa OR74A (finished) malate synthase (translation) (543 aa)	4	11.6
114	NCU08389T0	| NCU08389 | Neurospora crassa OR74A (finished) 60S ribosomal protein L20 (translation) (175 aa)	5	47.1

115	NCU05810T0	| NCU05810 | Neurospora crassa OR74A (finished) cross pathway control-2 (translation) (317 aa)	5	20.9
116	NCU01484T0	| NCU01484 | Neurospora crassa OR74A (finished) rho-type GTPase (translation) (196 aa)	5	32.8
117	NCU01221T0	| NCU01221 | Neurospora crassa OR74A (finished) 60S ribosomal protein L16 (translation) (203 aa)	5	32.2
118	NCU08998T1	| NCU08998 | Neurospora crassa OR74A (finished) 4-aminobutyrate aminotransferase (translation) (470 aa)	5	17.3
119	NCU07240T0	| NCU07240 | Neurospora crassa OR74A (finished) aflatoxin B1 aldehyde reductase member 2 (translation) (351 aa)	5	22.0
120	NCU11655T0	| NCU11655 | Neurospora crassa OR74A (finished) outer mitochondrial membrane protein porin (translation) (284 aa)	6	24.0
121	NCU07446T0	| NCU07446 | Neurospora crassa OR74A (finished) vacuolar membrane ATPase-4 (translation) (231 aa)	5	29.1
122	NCU00634T0	| NCU00634 | Neurospora crassa OR74A (finished) ribosomal protein L14 (translation) (143 aa)	5	43.0
123	NCU10066T0	| NCU10066 | Neurospora crassa OR74A (finished) coatomer alpha subunit (translation) (1224 aa)	4	10.4
124	NCU03857T0	| NCU03857 | Neurospora crassa OR74A (finished) conserved hypothetical protein (translation) (463 aa)	4	17.8
125	NCU06251T0	| NCU06251 | Neurospora crassa OR74A (finished) KH domain RNA-binding protein (translation) (372 aa)	5	26.2
126	NCU00573T0	| NCU00573 | Neurospora crassa OR74A (finished) conserved hypothetical protein (translation) (749 aa)	5	12.2
127	NCU02629T0	| NCU02629 | Neurospora crassa OR74A (finished) bifunctional purine biosynthesis protein (translation) (595 aa)	5	10.9
128	NCU02744T0	| NCU02744 | Neurospora crassa OR74A (finished) 60S ribosomal protein L9 (translation) (194 aa)	5	33.2
129	NCU02510T0	| NCU02510 | Neurospora crassa OR74A (finished) clathrin heavy chain (translation) (1679 aa)	5	6.3

130	NCU02133T0	| NCU02133 | Neurospora crassa OR74A (finished) superoxide dismutase (translation) (155 aa)	5	48.1
131	NCU06265T0	| NCU06265 | Neurospora crassa OR74A (finished) conserved hypothetical protein (translation) (888 aa)	5	9.6
132	NCU00475T0	| NCU00475 | Neurospora crassa OR74A (finished) 40S ribosomal protein S18 (translation) (157 aa)	4	46.8
133	NCU04856T1	| NCU04856 | Neurospora crassa OR74A (finished) glutamine synthetase (translation) (395 aa)	5	17.0
134	NCU05275T0	| NCU05275 | Neurospora crassa OR74A (finished) ubiquitin fusion protein (translation) (129 aa)	5	36.7
135	NCU06031T0	| NCU06031 | Neurospora crassa OR74A (finished) mitochondrial peroxiredoxin PRX1 (translation) (226 aa)	4	30.2
136	NCU07697T0	| NCU07697 | Neurospora crassa OR74A (finished) isocitrate dehydrogenase subunit 2 (translation) (380 aa)	5	16.1
137	NCU02404T1	| NCU02404 | Neurospora crassa OR74A (finished) RNP domain-containing protein (translation) (484 aa)	5	19.9
138	NCU11288T0	| NCU11288 | Neurospora crassa OR74A (finished) xaa-Pro dipeptidase (translation) (514 aa)	5	13.3
139	NCU00714T0	| NCU00714 | Neurospora crassa OR74A (finished) heat shock protein STI1 (translation) (579 aa)	4	10.4
140	NCU11171T0	| NCU11171 | Neurospora crassa OR74A (finished) ssDNA binding protein (translation) (153 aa)	5	30.9
141	NCU08936T1	| NCU08936 | Neurospora crassa OR74A (finished) clock-controlled gene-15 (translation) (412 aa)	6	18.7
142	NCU04202T0	| NCU04202 | Neurospora crassa OR74A (finished) nucleoside diphosphate kinase-1 (translation) (153 aa)	6	40.8
143	NCU08418T0	| NCU08418 | Neurospora crassa OR74A (finished) tripeptidyl-peptidase (translation) (588 aa)	5	11.6
144	NCU04192T0	| NCU04192 | Neurospora crassa OR74A (finished) vacuolar aspartyl aminopeptidase Lap4 (translation) (536 aa)	5	13.5

145	NCU03358T0	| NCU03358 | Neurospora crassa OR74A (finished) ketoreductase (translation) (347 aa)	5	19.4
146	NCU04244T0	| NCU04244 | Neurospora crassa OR74A (finished) syntaxin 2 (translation) (336 aa)	5	16.1
147	NCU03748T0	| NCU03748 | Neurospora crassa OR74A (finished) saccharopine dehydrogenase (translation) (449 aa)	5	13.4
148	NCU03415T0	| NCU03415 | Neurospora crassa OR74A (finished) aldehyde dehydrogenase (translation) (495 aa)	4	18.2
149	NCU01949T0	| NCU01949 | Neurospora crassa OR74A (finished) 40S ribosomal protein S9 (translation) (191 aa)	6	32.1
150	NCU01776T0	| NCU01776 | Neurospora crassa OR74A (finished) 60S ribosomal protein L15 (translation) (204 aa)	5	25.1
151	NCU00040T0	| NCU00040 | Neurospora crassa OR74A (finished) eukaryotic translation initiation factor 3 110 kDa subunit (translation) (1060 aa)	4	12.6
152	NCU00915T0	| NCU00915 | Neurospora crassa OR74A (finished) aspartyl-tRNA synthetase (translation) (595 aa)	6	14.7
153	NCU07567T0	| NCU07567 | Neurospora crassa OR74A (finished) T-complex protein 1 subunit theta (translation) (548 aa)	4	18.1
154	NCU07829T0	| NCU07829 | Neurospora crassa OR74A (finished) 60S ribosomal protein L7 (translation) (249 aa)	4	33.5
155	NCU03779T0	| NCU03779 | Neurospora crassa OR74A (finished) dihydroxyacetone kinase-1 (translation) (650 aa)	4	11.3
156	NCU00775T0	| NCU00775 | Neurospora crassa OR74A (finished) isocitrate dehydrogenase subunit 1 (translation) (386 aa)	3	19.7
157	NCU00894T0	| NCU00894 | Neurospora crassa OR74A (finished) conserved hypothetical protein (translation) (673 aa)	4	14.3
158	NCU09109T0	| NCU09109 | Neurospora crassa OR74A (finished) 60S ribosomal protein L33 (translation) (110 aa)	4	41.3
159	NCU03393T0	| NCU03393 | Neurospora crassa OR74A (finished) ribosome-associated protein (translation) (291 aa)	5	20.0

160	NCU04185T0	| NCU04185 | Neurospora crassa OR74A (finished) protein kinase gsk3 (translation) (395 aa)	4	23.4
161	NCU06047T0	| NCU06047 | Neurospora crassa OR74A (finished) 40S ribosomal protein S2 (translation) (266 aa)	5	26.0
162	NCU08964T0	| NCU08964 | Neurospora crassa OR74A (finished) 60S ribosomal protein L10 (translation) (222 aa)	4	33.5
163	NCU00443T0	| NCU00443 | Neurospora crassa OR74A (finished) ran-specific GTPase-activating protein 1 (translation) (251 aa)	5	22.0
164	NCU09579T0	| NCU09579 | Neurospora crassa OR74A (finished) retinol dehydrogenase 12 (translation) (354 aa)	4	16.2
165	NCU09559T0	| NCU09559 | Neurospora crassa OR74A (finished) clock-controlled gene-9 (translation) (866 aa)	4	11.2
166	NCU03009T0	| NCU03009 | Neurospora crassa OR74A (finished) zuotin (translation) (446 aa)	4	15.5
167	NCU08332T0	| NCU08332 | Neurospora crassa OR74A (finished) hexagonal-1 (translation) (177 aa)	4	40.3
168	NCU08502T0	| NCU08502 | Neurospora crassa OR74A (finished) 40S ribosomal protein S6 (translation) (240 aa)	3	39.8
169	NCU07857T0	| NCU07857 | Neurospora crassa OR74A (finished) 60S ribosomal protein L34 (translation) (118 aa)	4	43.6
170	NCU07014T0	| NCU07014 | Neurospora crassa OR74A (finished) cytoplasmic ribosomal protein-3 (translation) (147 aa)	4	39.7
171	NCU04054T0	| NCU04054 | Neurospora crassa OR74A (finished) tubulin beta chain (translation) (448 aa)	4	17.5
172	NCU03795T0	| NCU03795 | Neurospora crassa OR74A (finished) cell division control protein 12 (translation) (386 aa)	4	19.2
173	NCU01948T0	| NCU01948 | Neurospora crassa OR74A (finished) ribosomal protein Srp1 (translation) (161 aa)	4	30.0
174	NCU01424T0	| NCU01424 | Neurospora crassa OR74A (finished) DUF636 domain-containing protein (translation) (138 aa)	6	48.9

175	NCU00549T0	| NCU00549 | Neurospora crassa OR74A (finished) glutathione transferase omega-1 (translation) (310 aa)	4	16.2
176	NCU03188T0	| NCU03188 | Neurospora crassa OR74A (finished) sugar 1,4-lactone oxidase (translation) (557 aa)	4	16.7
177	NCU01204T0	| NCU01204 | Neurospora crassa OR74A (finished) tropomyosin (translation) (162 aa)	4	37.3
178	NCU01175T0	| NCU01175 | Neurospora crassa OR74A (finished) farnesyl-pyrophosphate synthetase (translation) (348 aa)	4	12.7
179	NCU07831T0	| NCU07831 | Neurospora crassa OR74A (finished) eukaryotic translation initiation factor 3 (translation) (873 aa)	4	11.2
180	NCU06785T0	| NCU06785 | Neurospora crassa OR74A (finished) ATP-citrate synthase subunit 1 (translation) (671 aa)	4	8.8
181	NCU10067T0	| NCU10067 | Neurospora crassa OR74A (finished) 26S proteasome non-ATPase regulatory subunit 8 (translation) (290 aa)	5	14.2
182	NCU04600T0	| NCU04600 | Neurospora crassa OR74A (finished) protein phosphatase 2C isoform gamma (translation) (440 aa)	4	15.7
183	NCU09269T1	| NCU09269 | Neurospora crassa OR74A (finished) ran-like (translation) (216 aa)	4	20.0
184	NCU03290T0	| NCU03290 | Neurospora crassa OR74A (finished) dipeptidyl peptidase (translation) (752 aa)	4	6.8
185	NCU02097T0	| NCU02097 | Neurospora crassa OR74A (finished) short chain dehydrogenase (translation) (341 aa)	4	22.9
186	NCU03731T0	| NCU03731 | Neurospora crassa OR74A (finished) HAD superfamily hydrolase (translation) (251 aa)	4	19.2
187	NCU02509T0	| NCU02509 | Neurospora crassa OR74A (finished) 60S ribosomal protein L11 (translation) (175 aa)	4	21.3
188	NCU03813T0	| NCU03813 | Neurospora crassa OR74A (finished) formate dehydrogenase (translation) (376 aa)	4	15.5
189	NCU00575T0	| NCU00575 | Neurospora crassa OR74A (finished) glucokinase (translation) (531 aa)	4	10.0

190	NCU03804T0	| NCU03804 | Neurospora crassa OR74A (finished) serine/threonine-protein phosphatase 2B catalytic subunit (translation) (559 aa)	4	12.4
191	NCU08620T0	| NCU08620 | Neurospora crassa OR74A (finished) 40S ribosomal protein S16 (translation) (143 aa)	4	40.9
192	NCU00720T0	| NCU00720 | Neurospora crassa OR74A (finished) L-lactate dehydrogenase (translation) (325 aa)	4	12.7
193	NCU03463T0	| NCU03463 | Neurospora crassa OR74A (finished) vacuolar pH-sensitive ATPase-1 (translation) (857 aa)	4	6.9
194	NCU07826T0	| NCU07826 | Neurospora crassa OR74A (finished) 40S ribosomal protein S19 (translation) (150 aa)	4	29.5
195	NCU06035T0	| NCU06035 | Neurospora crassa OR74A (finished) elongation factor 1-beta (translation) (232 aa)	5	20.8
196	NCU01227T0	| NCU01227 | Neurospora crassa OR74A (finished) succinyl-CoA ligase alpha-chain (translation) (334 aa)	4	15.0
197	NCU09468T0	| NCU09468 | Neurospora crassa OR74A (finished) tubulin alpha-2 (translation) (450 aa)	4	12.0
198	NCU02435T0	| NCU02435 | Neurospora crassa OR74A (finished) histone H2B (translation) (138 aa)	5	27.0
199	NCU03302T0	| NCU03302 | Neurospora crassa OR74A (finished) 60S ribosomal protein L36 (translation) (105 aa)	4	43.3
200	NCU05299T0	| NCU05299 | Neurospora crassa OR74A (finished) NADH:ubiquinone oxidoreductase 29.9 (translation) (274 aa)	4	15.0
201	NCU03139T0	| NCU03139 | Neurospora crassa OR74A (finished) histidine-3 (translation) (871 aa)	4	8.5
202	NCU03118T0	| NCU03118 | Neurospora crassa OR74A (finished) conserved hypothetical protein (translation) (373 aa)	4	13.7
203	NCU00258T0	| NCU00258 | Neurospora crassa OR74A (finished) cytoplasmic ribosomal protein-15 (translation) (203 aa)	4	20.3

204	NCU05804T0	| NCU05804 | Neurospora crassa OR74A (finished) 60S ribosomal protein L19 (translation) (193 aa)	3	27.6
205	NCU04230T0	| NCU04230 | Neurospora crassa OR74A (finished) isocitrate lyase (translation) (549 aa)	4	12.8
206	NCU07659T0	| NCU07659 | Neurospora crassa OR74A (finished) pyruvate dehydrogenase complex (translation) (459 aa)	3	13.8
207	NCU00636T0	| NCU00636 | Neurospora crassa OR74A (finished) ATP synthase subunit D (translation) (174 aa)	3	28.9
208	NCU04331T0	| NCU04331 | Neurospora crassa OR74A (finished) cytoplasmic ribosomal protein-4 (translation) (302 aa)	4	17.3
209	NCU06743T0	| NCU06743 | Neurospora crassa OR74A (finished) predicted protein (translation) (164 aa)	4	35.6
210	NCU02273T0	| NCU02273 | Neurospora crassa OR74A (finished) PEP4 homolog (translation) (397 aa)	5	11.6
211	NCU11376T0	| NCU11376 | Neurospora crassa OR74A (finished) mitogen-activated protein kinase MKC1 (translation) (414 aa)	4	14.8
212	NCU00488T0	| NCU00488 | Neurospora crassa OR74A (finished) protein phosphatase PP2A regulatory subunit A (translation) (625 aa)	3	13.3
213	NCU02124T1	| NCU02124 | Neurospora crassa OR74A (finished) dienelactone hydrolase (translation) (256 aa)	4	23.5
214	NCU01438T0	| NCU01438 | Neurospora crassa OR74A (finished) nucleosome assembly protein (translation) (408 aa)	4	11.3
215	NCU08888T0	| NCU08888 | Neurospora crassa OR74A (finished) phenylalanyl-tRNA synthetase subunit beta (translation) (609 aa)	3	8.1
216	NCU04797T0	| NCU04797 | Neurospora crassa OR74A (finished) fructose-1,6-bisphosphatase (translation) (351 aa)	3	17.7
217	NCU02380T0	| NCU02380 | Neurospora crassa OR74A (finished) threonyl-tRNA synthetase (translation) (789 aa)	3	11.0

218	NCU03050T0	| NCU03050 | Neurospora crassa OR74A (finished) ARP2/3 complex 34 kDa subunit (translation) (320 aa)	2	21.0
219	NCU02464T0	| NCU02464 | Neurospora crassa OR74A (finished) neuronal-specific septin-3 (translation) (391 aa)	4	15.6
220	NCU07723T0	| NCU07723 | Neurospora crassa OR74A (finished) norsolorinic acid reductase (translation) (381 aa)	4	11.1
221	NCU02438T0	| NCU02438 | Neurospora crassa OR74A (finished) dihydrolipoamide succinyltransferase (translation) (422 aa)	4	8.3
222	NCU10061T0	| NCU10061 | Neurospora crassa OR74A (finished) proteasome subunit alpha type 6 (translation) (255 aa)	3	23.2
223	NCU08344T0	| NCU08344 | Neurospora crassa OR74A (finished) 60s ribosomal protein (translation) (123 aa)	3	41.0
224	NCU01966T1	| NCU01966 | Neurospora crassa OR74A (finished) 60S ribosomal protein L37 (translation) (93 aa)	3	27.2
225	NCU04370T0	| NCU04370 | Neurospora crassa OR74A (finished) ubiquitin-activating enzyme E1 1 (translation) (1036 aa)	3	6.0
226	NCU02325T0	| NCU02325 | Neurospora crassa OR74A (finished) GMP synthase (translation) (544 aa)	3	10.9
227	NCU01369T0	| NCU01369 | Neurospora crassa OR74A (finished) ATP-dependent RNA helicase ded-1 (translation) (689 aa)	3	12.4
228	NCU08471T0	| NCU08471 | Neurospora crassa OR74A (finished) succinyl-CoA ligase beta-chain (translation) (448 aa)	4	13.0
229	NCU00477T0	| NCU00477 | Neurospora crassa OR74A (finished) carboxypeptidase Y (translation) (555 aa)	3	10.8
230	NCU03108T0	| NCU03108 | Neurospora crassa OR74A (finished) glutamate carboxypeptidase (translation) (800 aa)	3	8.4
231	NCU02252T0	| NCU02252 | Neurospora crassa OR74A (finished) phosphoglycerate mutase (translation) (520 aa)	3	14.8
232	NCU05095T0	| NCU05095 | Neurospora crassa OR74A (finished) phenylalanyl-tRNA synthetase subunit alpha (translation) (518 aa)	4	10.3

233	NCU05828T0	| NCU05828 | Neurospora crassa OR74A (finished) conserved hypothetical protein (translation) (957 aa)	3	6.4
234	NCU01317T0	| NCU01317 | Neurospora crassa OR74A (finished) 60S ribosomal protein L12 (translation) (166 aa)	3	31.5
235	NCU05805T0	| NCU05805 | Neurospora crassa OR74A (finished) serine hydroxymethyltransferase (translation) (547 aa)	3	10.1
236	NCU07267T0	| NCU07267 | Neurospora crassa OR74A (finished) blue light-induced-3 (translation) (210 aa)	3	23.0
237	NCU07308T0	| NCU07308 | Neurospora crassa OR74A (finished) fatty acid synthase alpha subunit reductase (translation) (1865 aa)	3	6.0
238	NCU10498T0	| NCU10498 | Neurospora crassa OR74A (finished) 60S ribosomal protein L35 (translation) (126 aa)	2	30.4
239	NCU06661T0	| NCU06661 | Neurospora crassa OR74A (finished) 60S ribosomal protein L22 (translation) (127 aa)	3	31.0
240	NCU03897T0	| NCU03897 | Neurospora crassa OR74A (finished) RNA binding effector protein Scp160 (translation) (1284 aa)	3	9.4
241	NCU09821T0	| NCU09821 | Neurospora crassa OR74A (finished) oxidoreductase (translation) (301 aa)	3	11.7
242	NCU05764T0	| NCU05764 | Neurospora crassa OR74A (finished) conserved hypothetical protein (translation) (333 aa)	3	15.7
243	NCU09572T0	| NCU09572 | Neurospora crassa OR74A (finished) ARP2/3 complex 21 kDa subunit (translation) (193 aa)	3	22.9
244	NCU09123T0	| NCU09123 | Neurospora crassa OR74A (finished) Ca/CaM-dependent kinase-1 (translation) (414 aa)	3	11.1
245	NCU07408T1	| NCU07408 | Neurospora crassa OR74A (finished) 60S ribosomal protein P0 (translation) (314 aa)	3	14.1
246	NCU01550T0	| NCU01550 | Neurospora crassa OR74A (finished) adenylate kinase cytosolic (translation) (279 aa)	3	14.0
247	NCU03608T0	| NCU03608 | Neurospora crassa OR74A (finished) ketol-acid reductoisomerase (translation) (403 aa)	3	14.4

248	NCU06226T0	| NCU06226 | Neurospora crassa OR74A (finished) 60S ribosomal protein L25 (translation) (157 aa)	3	21.8
249	NCU04474T0	| NCU04474 | Neurospora crassa OR74A (finished) sulfite oxidase (translation) (519 aa)	3	12.6
250	NCU09267T0	| NCU09267 | Neurospora crassa OR74A (finished) copper radical oxidase (translation) (1106 aa)	3	4.4
251	NCU02807T1	| NCU02807 | Neurospora crassa OR74A (finished) hypothetical protein (translation) (96 aa)	2	32.6
252	NCU09715T0	| NCU09715 | Neurospora crassa OR74A (finished) alpha,alpha-trehalose-phosphate synthase (translation) (524 aa)	3	7.1
253	NCU07562T0	| NCU07562 | Neurospora crassa OR74A (finished) 60S ribosomal protein L43 (translation) (93 aa)	3	37.0
254	NCU01195T0	| NCU01195 | Neurospora crassa OR74A (finished) amination-deficient (translation) (455 aa)	3	10.6
255	NCU00263T0	| NCU00263 | Neurospora crassa OR74A (finished) serin endopeptidase (translation) (877 aa)	3	5.3
256	NCU01443T0	| NCU01443 | Neurospora crassa OR74A (finished) seryl-tRNA synthetase (translation) (466 aa)	3	12.7
257	NCU05345T0	| NCU05345 | Neurospora crassa OR74A (finished) zearalenone lactonase (translation) (296 aa)	3	10.9
258	NCU03738T0	| NCU03738 | Neurospora crassa OR74A (finished) 40S ribosomal protein S29 (translation) (57 aa)	3	64.3
259	NCU00627T0	| NCU00627 | Neurospora crassa OR74A (finished) conserved hypothetical protein (translation) (570 aa)	3	15.1
260	NCU09463T0	| NCU09463 | Neurospora crassa OR74A (finished) leucine-6 (translation) (1124 aa)	3	5.3
261	NCU03992T0	| NCU03992 | Neurospora crassa OR74A (finished) fimbrin (translation) (650 aa)	3	8.0
262	NCU00225T0	| NCU00225 | Neurospora crassa OR74A (finished) conserved hypothetical protein (translation) (319 aa)	3	14.5

263	NCU05137T0	| NCU05137 | Neurospora crassa OR74A (finished) non-anchored cell wall protein-1 (translation) (692 aa)	3	6.1
264	NCU02407T0	| NCU02407 | Neurospora crassa OR74A (finished) dihydrolipoyl dehydrogenase (translation) (505 aa)	3	9.5
265	NCU00644T0	| NCU00644 | Neurospora crassa OR74A (finished) ATP synthase subunit G (translation) (188 aa)	3	27.3
266	NCU09707T0	| NCU09707 | Neurospora crassa OR74A (finished) conserved hypothetical protein (translation) (238 aa)	3	16.0
267	NCU03300T0	| NCU03300 | Neurospora crassa OR74A (finished) DNA damage checkpoint protein rad24 (translation) (248 aa)	4	22.3
268	NCU02707T0	| NCU02707 | Neurospora crassa OR74A (finished) 60S ribosomal protein L6 (translation) (202 aa)	3	24.4
269	NCU11369T1	| NCU11369 | Neurospora crassa OR74A (finished) BAR domain-containing protein (translation) (319 aa)	3	12.9
270	NCU00979T0	| NCU00979 | Neurospora crassa OR74A (finished) 60S acidic ribosomal protein P2 (translation) (111 aa)	3	36.4
271	NCU11339T0	| NCU11339 | Neurospora crassa OR74A (finished) cytochrome c oxidase subunit VIb (translation) (85 aa)	3	31.0
272	NCU11239T0	| NCU11239 | Neurospora crassa OR74A (finished) glutamine synthetase (translation) (485 aa)	3	8.1
273	NCU09331T0	| NCU09331 | Neurospora crassa OR74A (finished) HMF1 (translation) (163 aa)	3	14.8
274	NCU06880T0	| NCU06880 | Neurospora crassa OR74A (finished) AhpC/TSA family protein (translation) (197 aa)	3	16.8
275	NCU06416T0	| NCU06416 | Neurospora crassa OR74A (finished) thymine dioxygenase (translation) (334 aa)	3	9.6
276	NCU06397T1	| NCU06397 | Neurospora crassa OR74A (finished) profilin (translation) (134 aa)	3	24.1
277	NCU05518T0	| NCU05518 | Neurospora crassa OR74A (finished) peroxisomal copper amine oxidase (translation) (704 aa)	3	4.8

		| NCU01360 | Neurospora crassa OR74A (finished)		
278	NCU01360T0	NADH:ubiquinone oxidoreductase 11.5kD subunit (translation) (106 aa)	3	29.5
		| NCU06457 | Neurospora crassa OR74A (finished)		
279	NCU06457T0	asparaginyl-tRNA synthetase (translation) (581 aa)	3	17.1
		| NCU09043 | Neurospora crassa OR74A (finished) caleosin		
280	NCU09043T0	domain-containing protein (translation) (300 aa)	3	20.1
		| NCU08923 | Neurospora crassa OR74A (finished) zinc		
281	NCU08923T0	knuckle domain-containing protein (translation) (184 aa)	2	32.2
		| NCU06009 | Neurospora crassa OR74A (finished)		
282	NCU06009T0	oxidoreductase (translation) (360 aa)	2	12.5
		| NCU09476 | Neurospora crassa OR74A (finished) 40S		
283	NCU09476T0	ribosomal protein S25 (translation) (98 aa)	3	36.1
		| NCU07719 | Neurospora crassa OR74A (finished)		
284	NCU07719T0	isopentenyl-diphosphate delta-isomerase (translation) (256 aa)	2	21.2
		| NCU02650 | Neurospora crassa OR74A (finished) 26S		
285	NCU02650T0	proteasome non-ATPase regulatory subunit 12 (translation) (495 aa)	3	7.9
		| NCU01861 | Neurospora crassa OR74A (finished) short		
286	NCU01861T0	chain dehydrogenase/reductase family (translation) (360 aa)	3	9.2
		| NCU09610 | Neurospora crassa OR74A (finished) sey-1		
287	NCU09610T0	(translation) (863 aa)	3	7.9
		| NCU04020 | Neurospora crassa OR74A (finished) lysyl-		
288	NCU04020T0	tRNA synthetase (translation) (619 aa)	2	10.2
		| NCU16027 | Neurospora crassa OR74A mito cytochrome c		
289	NCU16027T0	oxidase subunit 2 (translation) (251 aa)	3	13.6
		| NCU04676 | Neurospora crassa OR74A (finished)		
290	NCU04676T0	glutathione S-transferase (translation) (267 aa)	3	18.1
		| NCU03126 | Neurospora crassa OR74A (finished)		
291	NCU03126T0	conserved hypothetical protein (translation) (315 aa)	3	11.2

292	NCU00294T0	| NCU00294 | Neurospora crassa OR74A (finished) 60S ribosomal protein L10a (translation) (218 aa)	3	28.6
293	NCU06702T0	| NCU06702 | Neurospora crassa OR74A (finished) yop-1 (translation) (169 aa)	3	22.6
294	NCU00695T0	| NCU00695 | Neurospora crassa OR74A (finished) conserved hypothetical protein (translation) (537 aa)	3	6.2
295	NCU11386T0	| NCU11386 | Neurospora crassa OR74A (finished) DUF52 domain-containing protein (translation) (356 aa)	3	18.0
296	NCU08791T0	| NCU08791 | Neurospora crassa OR74A (finished) catalase-1 (translation) (766 aa)	4	10.6
297	NCU04069T0	| NCU04069 | Neurospora crassa OR74A (finished) 3'-phosphoadenosine 5'-phosphatase isoform B (translation) (429 aa)	3	6.1
298	NCU04796T0	| NCU04796 | Neurospora crassa OR74A (finished) 3-ketoacyl-CoA thiolase (translation) (420 aa)	2	20.8
299	NCU00378T0	| NCU00378 | Neurospora crassa OR74A (finished) aldehyde dehydrogenase (translation) (547 aa)	3	10.1
300	NCU07458T0	| NCU07458 | Neurospora crassa OR74A (finished) N-acetylglucosamine-phosphate mutase (translation) (548 aa)	2	11.2
301	NCU09076T0	| NCU09076 | Neurospora crassa OR74A (finished) ATP-dependent RNA helicase (translation) (435 aa)	3	13.4
302	NCU09002T0	| NCU09002 | Neurospora crassa OR74A (finished) NADH:ubiquinone oxidoreductase 10.6kD subunit (translation) (94 aa)	3	20.4
303	NCU02393T1	| NCU02393 | Neurospora crassa OR74A (finished) mitogen-activated protein kinase-2 (translation) (353 aa)	3	17.3
304	NCU08477T0	| NCU08477 | Neurospora crassa OR74A (finished) small GTP-binding protein (translation) (204 aa)	3	13.8
305	NCU11456T0	| NCU11456 | Neurospora crassa OR74A (finished) IMP-specific 5'-nucleotidase 1 (translation) (432 aa)	2	19.5

306	NCU08550T0	| NCU08550 | Neurospora crassa OR74A (finished) conserved hypothetical protein (translation) (288 aa)	3	12.9
307	NCU05390T0	| NCU05390 | Neurospora crassa OR74A (finished) mitochondrial phosphate carrier protein (translation) (320 aa)	2	21.6
308	NCU00422T1	| NCU00422 | Neurospora crassa OR74A (finished) curved DNA-binding protein (translation) (411 aa)	3	7.3
309	NCU01634T0	| NCU01634 | Neurospora crassa OR74A (finished) histone H4-1 (translation) (104 aa)	2	35.0
310	NCU00502T0	| NCU00502 | Neurospora crassa OR74A (finished) ATP synthase subunit 4 (translation) (242 aa)	2	13.7
311	NCU03690T0	| NCU03690 | Neurospora crassa OR74A (finished) importin beta-2 subunit (translation) (945 aa)	1	5.2
312	NCU01021T0	| NCU01021 | Neurospora crassa OR74A (finished) eukaryotic translation initiation factor 3 subunit EifCf (translation) (370 aa)	1	15.7
313	NCU01368T1	| NCU01368 | Neurospora crassa OR74A (finished) proteasome component C11 (translation) (204 aa)	3	14.8
314	NCU07542T0	| NCU07542 | Neurospora crassa OR74A (finished) rad23-like (translation) (384 aa)	2	11.2
315	NCU00742T0	| NCU00742 | Neurospora crassa OR74A (finished) glycerol-3-phosphate dehydrogenase (translation) (525 aa)	3	10.3
316	NCU06687T0	| NCU06687 | Neurospora crassa OR74A (finished) glycogen synthase-1 (translation) (707 aa)	2	7.1
317	NCU00414T0	| NCU00414 | Neurospora crassa OR74A (finished) adenosine kinase (translation) (455 aa)	2	10.6
318	NCU03944T0	| NCU03944 | Neurospora crassa OR74A (finished) WD repeat containing protein 2 (translation) (619 aa)	2	9.1
319	NCU02905T0	| NCU02905 | Neurospora crassa OR74A (finished) 60S ribosomal protein L23 (translation) (140 aa)	2	28.8
320	NCU08894T0	| NCU08894 | Neurospora crassa OR74A (finished) glutamyl-tRNA synthetase (translation) (637 aa)	2	7.7

321	NCU04109T0	| NCU04109 | Neurospora crassa OR74A (finished) theta class glutathione S-transferase (translation) (291 aa)	2	20.0
322	NCU06892T0	| NCU06892 | Neurospora crassa OR74A (finished) 40S ribosomal protein S20 (translation) (118 aa)	2	35.9
323	NCU07941T0	| NCU07941 | Neurospora crassa OR74A (finished) aspartate aminotransferase (translation) (483 aa)	2	8.7
324	NCU02260T0	| NCU02260 | Neurospora crassa OR74A (finished) 26S protease regulatory subunit 6B (translation) (422 aa)	3	16.9
325	NCU00127T0	| NCU00127 | Neurospora crassa OR74A (finished) conserved hypothetical protein (translation) (593 aa)	2	11.3
326	NCU08195T0	| NCU08195 | Neurospora crassa OR74A (finished) arginyl-tRNA synthetase (translation) (735 aa)	2	6.5
327	NCU01587T1	| NCU01587 | Neurospora crassa OR74A (finished) cofilin (translation) (155 aa)	2	38.3
328	NCU01219T0	| NCU01219 | Neurospora crassa OR74A (finished) glutaredoxin (translation) (125 aa)	2	36.3
329	NCU06153T0	| NCU06153 | Neurospora crassa OR74A (finished) monooxygenase (translation) (585 aa)	2	7.0
330	NCU03911T0	| NCU03911 | Neurospora crassa OR74A (finished) F-actin-capping protein subunit alpha (translation) (274 aa)	2	12.1
331	NCU01918T0	| NCU01918 | Neurospora crassa OR74A (finished) ARP2/3 complex 20 kDa subunit (translation) (210 aa)	3	13.4
332	NCU00326T0	| NCU00326 | Neurospora crassa OR74A (finished) calcium homeostasis protein Regucalcin (translation) (306 aa)	2	14.4
333	NCU01240T0	| NCU01240 | Neurospora crassa OR74A (finished) conserved hypothetical protein (translation) (543 aa)	2	7.4
334	NCU10852T0	| NCU10852 | Neurospora crassa OR74A (finished) exochitinase (translation) (629 aa)	2	8.0
335	NCU07129T0	| NCU07129 | Neurospora crassa OR74A (finished) amino-acid permease inda1 (translation) (569 aa)	2	5.8

336	NCU04245T0	| NCU04245 | Neurospora crassa OR74A (finished) translocase of outer mitochondrial membrane 70 (translation) (623 aa)	2	8.7
337	NCU02547T0	| NCU02547 | Neurospora crassa OR74A (finished) conserved hypothetical protein (translation) (277 aa)	2	13.0
338	NCU02044T0	| NCU02044 | Neurospora crassa OR74A (finished) GTP-binding protein (translation) (396 aa)	2	7.8
339	NCU00959T0	| NCU00959 | Neurospora crassa OR74A (finished) succinate dehydrogenase iron-sulfur protein (translation) (283 aa)	1	23.8
340	NCU09535T0	| NCU09535 | Neurospora crassa OR74A (finished) conserved hypothetical protein (translation) (494 aa)	1	8.3
341	NCU08991T1	| NCU08991 | Neurospora crassa OR74A (finished) hypothetical protein (translation) (172 aa)	2	17.5
342	NCU00884T0	| NCU00884 | Neurospora crassa OR74A (finished) NAD dependent epimerase/dehydratase (translation) (417 aa)	2	12.7
343	NCU02810T0	| NCU02810 | Neurospora crassa OR74A (finished) eukaryotic translation initiation factor 2 gamma subunit (translation) (512 aa)	2	15.7
344	NCU01965T0	| NCU01965 | Neurospora crassa OR74A (finished) valyl-tRNA synthetase (translation) (1051 aa)	2	3.6
345	NCU02948T0	| NCU02948 | Neurospora crassa OR74A (finished) non-anchored cell wall protein-4 (translation) (206 aa)	2	17.6
346	NCU02109T0	| NCU02109 | Neurospora crassa OR74A (finished) UDP-N-acetylglucosamine pyrophosphorylase (translation) (488 aa)	2	7.6
347	NCU07894T0	| NCU07894 | Neurospora crassa OR74A (finished) oligopeptide transporter 2 (translation) (887 aa)	2	3.7
348	NCU09210T0	| NCU09210 | Neurospora crassa OR74A (finished) dyp-type peroxidase (translation) (514 aa)	2	9.0
349	NCU07874T0	| NCU07874 | Neurospora crassa OR74A (finished) nuclear and cytoplasmic polyadenylated RNA-binding protein pub1 (translation) (481 aa)	2	12.3

350	NCU07926T0	| NCU07926 | Neurospora crassa OR74A (finished) glutaminyl-tRNA synthetase (translation) (652 aa)	2	7.5
351	NCU02287T0	| NCU02287 | Neurospora crassa OR74A (finished) acyl-CoA dehydrogenase (translation) (547 aa)	2	11.7
352	NCU06606T0	| NCU06606 | Neurospora crassa OR74A (finished) iron-sulfur subunit-1 (translation) (232 aa)	2	17.3
353	NCU09175T0	| NCU09175 | Neurospora crassa OR74A (finished) GPI-anchored cell wall beta-1,3-endoglucanase EglC (translation) (411 aa)	2	11.0
354	NCU05041T0	| NCU05041 | Neurospora crassa OR74A (finished) trehalose-phosphatase (translation) (1016 aa)	2	3.8
355	NCU07608T1	| NCU07608 | Neurospora crassa OR74A (finished) ribose 5-phosphate isomerase A (translation) (365 aa)	2	12.9
356	NCU08287T0	| NCU08287 | Neurospora crassa OR74A (finished) pyrABCN (translation) (1833 aa)	2	4.2
357	NCU00050T0	| NCU00050 | Neurospora crassa OR74A (finished) pyruvate dehydrogenase X component (translation) (427 aa)	2	13.9
358	NCU03559T0	| NCU03559 | Neurospora crassa OR74A (finished) ubiquinol-cytochrome c reductase complex core protein 2 precursor (translation) (455 aa)	2	12.8
359	NCU02887T0	| NCU02887 | Neurospora crassa OR74A (finished) voltage-gated potassium channel beta-2 subunit (translation) (400 aa)	2	6.3
360	NCU01962T0	| NCU01962 | Neurospora crassa OR74A (finished) conserved hypothetical protein (translation) (137 aa)	2	20.6
361	NCU07721T0	| NCU07721 | Neurospora crassa OR74A (finished) 26S proteasome regulatory subunit rpn1 (translation) (903 aa)	2	4.1
362	NCU07182T0	| NCU07182 | Neurospora crassa OR74A (finished) 40S ribosomal protein S24 (translation) (137 aa)	2	20.6
363	NCU03339T0	| NCU03339 | Neurospora crassa OR74A (finished) glutathione reductase (translation) (504 aa)	2	9.5

364	NCU09897T0	| NCU09897 | Neurospora crassa OR74A (finished) vacuolar membrane ATPase-5 (translation) (392 aa)	1	9.2
365	NCU03755T0	| NCU03755 | Neurospora crassa OR74A (finished) flavin dependent monooxygenase (translation) (478 aa)	2	8.2
366	NCU04380T0	| NCU04380 | Neurospora crassa OR74A (finished) acyl-CoA synthetase (translation) (707 aa)	2	4.4
367	NCU03893T0	| NCU03893 | Neurospora crassa OR74A (finished) short-chain dehydrogenase/reductase SDR (translation) (365 aa)	2	11.3
368	NCU07929T0	| NCU07929 | Neurospora crassa OR74A (finished) eukaryotic translation initiation factor 3 subunit 3 (translation) (360 aa)	2	10.0
369	NCU09024T0	| NCU09024 | Neurospora crassa OR74A (finished) conserved hypothetical protein (translation) (624 aa)	2	8.7
370	NCU06431T0	| NCU06431 | Neurospora crassa OR74A (finished) 40S ribosomal protein S22 (translation) (131 aa)	2	29.2
371	NCU04442T0	| NCU04442 | Neurospora crassa OR74A (finished) GAL10 (translation) (376 aa)	2	6.4
372	NCU08330T0	| NCU08330 | Neurospora crassa OR74A (finished) conserved hypothetical protein (translation) (291 aa)	2	12.8
373	NCU11181T0	| NCU11181 | Neurospora crassa OR74A (finished) Ras superfamily GTPase (translation) (190 aa)	2	19.6
374	NCU07853T0	| NCU07853 | Neurospora crassa OR74A (finished) uricase (translation) (296 aa)	2	13.2
375	NCU09290T0	| NCU09290 | Neurospora crassa OR74A (finished) proteasome component PRE3 (translation) (230 aa)	2	13.1
376	NCU02829T0	| NCU02829 | Neurospora crassa OR74A (finished) phosphomannomutase (translation) (274 aa)	2	14.7
377	NCU04799T0	| NCU04799 | Neurospora crassa OR74A (finished) polyadenylate-binding protein (translation) (765 aa)	2	5.0
378	NCU02695T0	| NCU02695 | Neurospora crassa OR74A (finished) conserved hypothetical protein (translation) (325 aa)	2	10.5

379	NCU01449T1	| NCU01449 | Neurospora crassa OR74A (finished) GTP cyclohydrolase II (translation) (508 aa)	2	7.3
380	NCU01756T0	| NCU01756 | Neurospora crassa OR74A (finished) actin (translation) (440 aa)	2	7.7
381	NCU08535T0	| NCU08535 | Neurospora crassa OR74A (finished) acetyl-CoA carboxylase (translation) (2276 aa)	1	4.9
382	NCU03515T0	| NCU03515 | Neurospora crassa OR74A (finished) cell division control protein 10 (translation) (338 aa)	2	17.8
383	NCU09119T0	| NCU09119 | Neurospora crassa OR74A (finished) ATP synthase subunit gamma (translation) (300 aa)	2	14.1
384	NCU04044T0	| NCU04044 | Neurospora crassa OR74A (finished) NADH2 dehydrogenase flavoprotein 1 (translation) (494 aa)	2	7.7
385	NCU01446T0	| NCU01446 | Neurospora crassa OR74A (finished) uracil phosphoribosyltransferase (translation) (245 aa)	2	14.3
386	NCU00692T0	| NCU00692 | Neurospora crassa OR74A (finished) chaperone dnaK (translation) (572 aa)	2	7.7
387	NCU11745T0	| NCU11745 | Neurospora crassa OR74A (finished) conserved hypothetical protein (translation) (72 aa)	2	39.4
388	NCU10521T0	| NCU10521 | Neurospora crassa OR74A (finished) conserved hypothetical protein (translation) (231 aa)	2	14.8
389	NCU09041T0	| NCU09041 | Neurospora crassa OR74A (finished) L-xylulose reductase (translation) (272 aa)	2	10.7
390	NCU08333T0	| NCU08333 | Neurospora crassa OR74A (finished) bleomycin hydrolase (translation) (517 aa)	2	6.2
391	NCU07467T0	| NCU07467 | Neurospora crassa OR74A (finished) conserved hypothetical protein (translation) (199 aa)	2	12.1
392	NCU04857T0	| NCU04857 | Neurospora crassa OR74A (finished) 2-hydroxyacid dehydrogenase (translation) (412 aa)	2	7.3
393	NCU03558T0	| NCU03558 | Neurospora crassa OR74A (finished) conserved hypothetical protein (translation) (79 aa)	2	29.5

		| NCU01142 | Neurospora crassa OR74A (finished)		
394	NCU01142T0	NADH:ubiquinone oxidoreductase 13.4kD subunit (translation) (138 aa)	2	25.6
		| NCU02634 | Neurospora crassa OR74A (finished)		
395	NCU02634T0	conserved hypothetical protein (translation) (394 aa)	2	11.5
		| NCU03870 | Neurospora crassa OR74A (finished)		
396	NCU03870T1	conserved hypothetical protein (translation) (834 aa)	2	4.7
		| NCU09237 | Neurospora crassa OR74A (finished) KH		
397	NCU09237T0	domain RNA binding protein (translation) (482 aa)	2	6.7
		| NCU08669 | Neurospora crassa OR74A (finished) betaine		
398	NCU08669T0	aldehyde dehydrogenase 2 (translation) (468 aa)	2	5.4
		| NCU08627 | Neurospora crassa OR74A (finished)		
399	NCU08627T1	cytoplasmic ribosomal protein-7 (translation) (88 aa)	3	26.4
		| NCU07167 | Neurospora crassa OR74A (finished)		
400	NCU07167T0	isoflavone reductase (translation) (344 aa)	2	7.9
		| NCU06695 | Neurospora crassa OR74A (finished)		
401	NCU06695T1	cytochrome c oxidase polypeptide VI (translation) (149 aa)	2	12.2
		| NCU05454 | Neurospora crassa OR74A (finished) glycerol-		
402	NCU05454T0	3-phosphate dehydrogenase (translation) (695 aa)	2	4.3
		| NCU05295 | Neurospora crassa OR74A (finished)		
403	NCU05295T0	proteasome component PUP2 (translation) (246 aa)	2	11.8
		| NCU03859 | Neurospora crassa OR74A (finished) MYG1		
404	NCU03859T0	protein (translation) (367 aa)	2	6.0
		| NCU03749 | Neurospora crassa OR74A (finished)		
405	NCU03749T1	hydroxyacylglutathione hydrolase (translation) (283 aa)	2	11.7
		| NCU03150 | Neurospora crassa OR74A (finished) 60S		
406	NCU03150T0	ribosomal protein L24 (translation) (157 aa)	2	16.0
		| NCU01552 | Neurospora crassa OR74A (finished)		
407	NCU01552T1	ribosomal protein S28 (translation) (146 aa)	2	18.6
		| NCU11213 | Neurospora crassa OR74A (finished)		
408	NCU11213T0	mannose-1-phosphate guanyltransferase (translation) (365	2	5.2

		aa)		
409	NCU09995T1	| NCU09995 | Neurospora crassa OR74A (finished) hypothetical protein (translation) (104 aa)	2	16.5
410	NCU09265T0	| NCU09265 | Neurospora crassa OR74A (finished) calreticulin (translation) (566 aa)	2	1.8
411	NCU08949T2	| NCU08949 | Neurospora crassa OR74A (finished) conserved hypothetical protein (translation) (170 aa)	2	16.6
412	NCU08947T0	| NCU08947 | Neurospora crassa OR74A (finished) ubiquinol-cytochrome-c reductase chain VIII (translation) (108 aa)	2	26.2
413	NCU08162T0	| NCU08162 | Neurospora crassa OR74A (finished) argininosuccinate lyase (translation) (467 aa)	2	5.2
414	NCU07439T0	| NCU07439 | Neurospora crassa OR74A (finished) conserved hypothetical protein (translation) (78 aa)	2	37.7
415	NCU07332T0	| NCU07332 | Neurospora crassa OR74A (finished) conserved hypothetical protein (translation) (539 aa)	2	4.6
416	NCU07159T0	| NCU07159 | Neurospora crassa OR74A (finished) proteinase T (translation) (397 aa)	4	6.3
417	NCU06968T0	| NCU06968 | Neurospora crassa OR74A (finished) conserved hypothetical protein (translation) (287 aa)	2	8.0
418	NCU06561T0	| NCU06561 | Neurospora crassa OR74A (finished) rho-gdp dissociation inhibitor (translation) (202 aa)	2	11.0
419	NCU06543T0	| NCU06543 | Neurospora crassa OR74A (finished) acyl-CoA dehydrogenase (translation) (434 aa)	2	3.9
420	NCU06464T0	| NCU06464 | Neurospora crassa OR74A (finished) hypothetical protein (translation) (171 aa)	2	10.6
421	NCU05457T0	| NCU05457 | Neurospora crassa OR74A (finished) cytochrome a-4 (translation) (172 aa)	2	12.9
422	NCU05008T0	| NCU05008 | Neurospora crassa OR74A (finished) predicted protein (translation) (135 aa)	2	12.7

423	NCU04479T0	| NCU04479 | Neurospora crassa OR74A (finished) LAP2 (translation) (403 aa)	2	5.2
424	NCU04371T0	| NCU04371 | Neurospora crassa OR74A (finished) peptidyl-prolyl cis-trans isomerase fkr-3 (translation) (114 aa)	2	18.6
425	NCU03306T0	| NCU03306 | Neurospora crassa OR74A (finished) conserved hypothetical protein (translation) (121 aa)	2	20.0
426	NCU03151T0	| NCU03151 | Neurospora crassa OR74A (finished) peroxisomal membrane protein (translation) (167 aa)	2	10.8
427	NCU02786T0	| NCU02786 | Neurospora crassa OR74A (finished) conserved hypothetical protein (translation) (348 aa)	2	4.9
428	NCU02437T0	| NCU02437 | Neurospora crassa OR74A (finished) histone H2A (translation) (135 aa)	2	11.9
429	NCU01754T0	| NCU01754 | Neurospora crassa OR74A (finished) alcohol dehydrogenase I (translation) (354 aa)	2	6.5
430	NCU01169T0	| NCU01169 | Neurospora crassa OR74A (finished) NADH:ubiquinone oxidoreductase 24 (translation) (264 aa)	2	6.8
431	NCU00706T0	| NCU00706 | Neurospora crassa OR74A (finished) 60S ribosomal protein L44 (translation) (107 aa)	2	10.4
432	NCU08977T0	| NCU08977 | Neurospora crassa OR74A (finished) long chain fatty alcohol oxidase (translation) (764 aa)	2	5.1
433	NCU00793T0	| NCU00793 | Neurospora crassa OR74A (finished) trehalose phosphate synthase (translation) (930 aa)	1	4.5
434	NCU02319T0	| NCU02319 | Neurospora crassa OR74A (finished) aminopeptidase (translation) (1060 aa)	2	7.2
435	NCU00618T0	| NCU00618 | Neurospora crassa OR74A (finished) 40S ribosomal protein S27 (translation) (83 aa)	1	37.8
436	NCU08356T0	| NCU08356 | Neurospora crassa OR74A (finished) acetamidase (translation) (574 aa)	2	7.7
437	NCU07459T0	| NCU07459 | Neurospora crassa OR74A (finished) protein arginine N-methyltransferase 1 (translation) (347 aa)	2	9.2

		| NCU02280 | Neurospora crassa OR74A (finished) NADH:ubiquinone oxidoreductase 21.3kD subunit b		
438	NCU02280T0	(translation) (201 aa)	2	16.0
		| NCU00831 | Neurospora crassa OR74A (finished)		
439	NCU00831T0	extracellular serine carboxypeptidase (translation) (572 aa)	2	8.6
		| NCU02480 | Neurospora crassa OR74A (finished) short-		
440	NCU02480T0	chain dehydrogenase/reductase (translation) (283 aa)	2	8.5
		| NCU06617 | Neurospora crassa OR74A (finished) myosin		
441	NCU06617T0	regulatory light chain cdc4 (translation) (140 aa)	2	30.9
		| NCU11027 | Neurospora crassa OR74A (finished) zinc		
442	NCU11027T0	metalloprotease (translation) (1064 aa)	1	7.1
		| NCU07365 | Neurospora crassa OR74A (finished) 20S		
443	NCU07365T0	proteasome subunit (translation) (269 aa)	2	7.8
		| NCU01596 | Neurospora crassa OR74A (finished) 26S proteasome non-ATPase regulatory subunit 11 (translation)		
444	NCU01596T0	(425 aa)	2	9.7
		| NCU07997 | Neurospora crassa OR74A (finished)		
445	NCU07997T0	conserved hypothetical protein (translation) (342 aa)	2	12.0
		| NCU01820 | Neurospora crassa OR74A (finished) exportin-		
446	NCU01820T0	1 (translation) (1079 aa)	2	6.3
		| NCU06413 | Neurospora crassa OR74A (finished)		
447	NCU06413T0	conserved hypothetical protein (translation) (762 aa)	1	3.7
		| NCU06836 | Neurospora crassa OR74A (finished) acetyl-		
448	NCU06836T0	coenzyme A synthetase (translation) (668 aa)	1	11.7
		| NCU05498 | Neurospora crassa OR74A (finished)		
449	NCU05498T0	conserved hypothetical protein (translation) (181 aa)	1	23.3
		| NCU03980 | Neurospora crassa OR74A (finished) T-		
450	NCU03980T0	complex protein 1 subunit epsilon (translation) (551 aa)	2	5.5
		| NCU00122 | Neurospora crassa OR74A (finished) aspartyl		
451	NCU00122T0	aminopeptidase (translation) (538 aa)	2	8.0

452	NCU07471T0	| NCU07471 | Neurospora crassa OR74A (finished) F-actin-capping protein subunit beta (translation) (290 aa)	2	17.3
453	NCU06448T0	| NCU06448 | Neurospora crassa OR74A (finished) enoyl-CoA hydratase (translation) (300 aa)	2	15.7
454	NCU07067T0	| NCU07067 | Neurospora crassa OR74A (finished) mannosyl-oligosaccharide alpha-1,2-mannosidase (translation) (711 aa)	2	4.9
455	NCU06720T0	| NCU06720 | Neurospora crassa OR74A (finished) carboxypeptidase cpdS (translation) (578 aa)	2	3.1
456	NCU04334T0	| NCU04334 | Neurospora crassa OR74A (finished) chaperonin (translation) (105 aa)	2	21.2
457	NCU03877T0	| NCU03877 | Neurospora crassa OR74A (finished) C-1-tetrahydrofolate synthase (translation) (942 aa)	1	8.3
458	NCU09808T0	| NCU09808 | Neurospora crassa OR74A (finished) dynamin-1 (translation) (802 aa)	3	8.2
459	NCU03340T0	| NCU03340 | Neurospora crassa OR74A (finished) cytochrome-c oxidase chain VIIc (translation) (83 aa)	2	23.2
460	NCU02013T0	| NCU02013 | Neurospora crassa OR74A (finished) conserved hypothetical protein (translation) (164 aa)	1	27.0
461	NCU01744T0	| NCU01744 | Neurospora crassa OR74A (finished) glutamate synthase (translation) (2117 aa)	1	4.7
462	NCU09861T0	| NCU09861 | Neurospora crassa OR74A (finished) Ser/Thr protein phosphatase (translation) (696 aa)	1	5.3
463	NCU07451T0	| NCU07451 | Neurospora crassa OR74A (finished) methionyl-tRNA synthetase (translation) (664 aa)	1	9.0
464	NCU07083T0	| NCU07083 | Neurospora crassa OR74A (finished) conserved hypothetical protein (translation) (561 aa)	1	4.6
465	NCU06722T0	| NCU06722 | Neurospora crassa OR74A (finished) tryptophanyl-tRNA synthetase (translation) (492 aa)	1	4.7
466	NCU01200T1	| NCU01200 | Neurospora crassa OR74A (finished) peptidyl-prolyl cis-trans isomerase B (translation) (286 aa)	1	9.5

467	NCU01635T0	| NCU01635 | Neurospora crassa OR74A (finished) histone H3 (translation) (137 aa)	1	22.8
468	NCU00350T0	| NCU00350 | Neurospora crassa OR74A (finished) epoxide hydrolase (translation) (373 aa)	2	7.5
469	NCU08847T0	| NCU08847 | Neurospora crassa OR74A (finished) conserved hypothetical protein (translation) (568 aa)	1	5.1
470	NCU09356T0	| NCU09356 | Neurospora crassa OR74A (finished) conserved hypothetical protein (translation) (555 aa)	1	3.8
471	NCU09646T0	| NCU09646 | Neurospora crassa OR74A (finished) 3-ketoacyl-CoA thiolase (translation) (416 aa)	1	13.3
472	NCU04221T0	| NCU04221 | Neurospora crassa OR74A (finished) trehalase-2 (translation) (745 aa)	1	6.9
473	NCU04129T0	| NCU04129 | Neurospora crassa OR74A (finished) gamma-tocopherol methyltransferase (translation) (337 aa)	1	11.9
474	NCU02493T0	| NCU02493 | Neurospora crassa OR74A (finished) proteasome component C1 (translation) (298 aa)	1	7.4
475	NCU05069T0	| NCU05069 | Neurospora crassa OR74A (finished) FAD dependent oxidoreductase (translation) (541 aa)	1	8.1
476	NCU06578T0	| NCU06578 | Neurospora crassa OR74A (finished) KapG (translation) (1032 aa)	1	5.7
477	NCU11271T0	| NCU11271 | Neurospora crassa OR74A (finished) 26S protease regulatory subunit 4 (translation) (460 aa)	1	8.3
478	NCU04387T0	| NCU04387 | Neurospora crassa OR74A (finished) vacuolar membrane ATPase-7 (translation) (125 aa)	1	16.1
479	NCU09469T0	| NCU09469 | Neurospora crassa OR74A (finished) EF hand domain-containing protein (translation) (1286 aa)	1	2.0
480	NCU03310T0	| NCU03310 | Neurospora crassa OR74A (finished) prohibitin-2 (translation) (311 aa)	1	6.8
481	NCU02746T0	| NCU02746 | Neurospora crassa OR74A (finished) vacuolar membrane ATPase-13 (translation) (482 aa)	1	4.2

482	NCU08092T0	| NCU08092 | Neurospora crassa OR74A (finished) nipsnap family protein (translation) (332 aa)	1	8.2
483	NCU08505T0	| NCU08505 | Neurospora crassa OR74A (finished) DUF866 domain-containing protein (translation) (161 aa)	1	17.5
484	NCU00464T0	| NCU00464 | Neurospora crassa OR74A (finished) 60S ribosomal protein L32 (translation) (132 aa)	1	20.6
485	NCU00202T0	| NCU00202 | Neurospora crassa OR74A (finished) coronin-6 (translation) (607 aa)	1	6.6
486	NCU04826T0	| NCU04826 | Neurospora crassa OR74A (finished) conserved hypothetical protein (translation) (1423 aa)	1	1.3
487	NCU02208T0	| NCU02208 | Neurospora crassa OR74A (finished) eukaryotic translation initiation factor 3 (translation) (748 aa)	1	2.5
488	NCU03156T0	| NCU03156 | Neurospora crassa OR74A (finished) NUO (translation) (95 aa)	1	18.1
489	NCU10360T0	| NCU10360 | Neurospora crassa OR74A (finished) conserved hypothetical protein (translation) (543 aa)	1	11.6
490	NCU08920T0	| NCU08920 | Neurospora crassa OR74A (finished) ATP-binding cassette sub-family F member 2 (translation) (614 aa)	1	7.2
491	NCU04449T0	| NCU04449 | Neurospora crassa OR74A (finished) prolyl-tRNA synthetase (translation) (559 aa)	1	5.7
492	NCU00405T0	| NCU00405 | Neurospora crassa OR74A (finished) glycyl-tRNA synthetase 1 (translation) (733 aa)	1	10.0
493	NCU07415T0	| NCU07415 | Neurospora crassa OR74A (finished) proline iminopeptidase (translation) (483 aa)	1	9.5
494	NCU06346T0	| NCU06346 | Neurospora crassa OR74A (finished) conserved hypothetical protein (translation) (102 aa)	1	24.8
495	NCU00104T0	| NCU00104 | Neurospora crassa OR74A (finished) heat shock protein 98 (translation) (928 aa)	1	8.3
496	NCU11129T0	| NCU11129 | Neurospora crassa OR74A (finished) carboxypeptidase s (translation) (597 aa)	1	4.5

497	NCU01816T0	| NCU01816 | Neurospora crassa OR74A (finished) allantoicase-l (translation) (355 aa)	1	7.1
498	NCU07024T0	| NCU07024 | Neurospora crassa OR74A (finished) osmotic sensitive-2 (translation) (359 aa)	2	12.3
499	NCU10283T0	| NCU10283 | Neurospora crassa OR74A (finished) tryptophan synthetase (translation) (709 aa)	1	6.1
500	NCU03127T0	| NCU03127 | Neurospora crassa OR74A (finished) urease Ure (translation) (843 aa)	1	4.2
501	NCU00880T0	| NCU00880 | Neurospora crassa OR74A (finished) phospholipase A-2-activating protein (translation) (810 aa)	1	3.7
502	NCU08771T0	| NCU08771 | Neurospora crassa OR74A (finished) acetolactate synthase (translation) (609 aa)	1	8.4
503	NCU03988T0	| NCU03988 | Neurospora crassa OR74A (finished) 60S ribosomal protein L18 (translation) (184 aa)	1	16.4
504	NCU02397T0	| NCU02397 | Neurospora crassa OR74A (finished) pyruvate decarboxylase (translation) (519 aa)	1	8.3
505	NCU03635T0	| NCU03635 | Neurospora crassa OR74A (finished) 60S ribosomal protein L38 (translation) (81 aa)	1	18.8
506	NCU08963T0	| NCU08963 | Neurospora crassa OR74A (finished) 60S ribosomal protein L30 (translation) (110 aa)	1	23.9
507	NCU04074T0	| NCU04074 | Neurospora crassa OR74A (finished) NADH:ubiquinone oxidoreductase 30.4 (translation) (284 aa)	1	17.7
508	NCU03112T0	| NCU03112 | Neurospora crassa OR74A (finished) NADH-cytochrome b5 reductase 2 (translation) (344 aa)	1	7.6
509	NCU06432T0	| NCU06432 | Neurospora crassa OR74A (finished) 40S ribosomal protein S12 (translation) (148 aa)	1	12.9
510	NCU03949T0	| NCU03949 | Neurospora crassa OR74A (finished) FMN-dependent 2-nitropropane dioxygenase (translation) (379 aa)	1	4.5
511	NCU08003T0	| NCU08003 | Neurospora crassa OR74A (finished) RSC complex subunit (translation) (691 aa)	1	4.3

512	NCU07465T0	| NCU07465 | Neurospora crassa OR74A (finished) mitochondrial phosphate carrier protein 2 (translation) (383 aa)	1	5.8
513	NCU08882T0	| NCU08882 | Neurospora crassa OR74A (finished) NAD binding Rossmann fold oxidoreductase (translation) (371 aa)	1	7.8
514	NCU08823T0	| NCU08823 | Neurospora crassa OR74A (finished) band (translation) (214 aa)	1	7.0
515	NCU02534T0	| NCU02534 | Neurospora crassa OR74A (finished) NADH:ubiquinone oxidoreductase 49kD subunit (translation) (479 aa)	1	3.8
516	NCU03575T0	| NCU03575 | Neurospora crassa OR74A (finished) isoleucyl-tRNA synthetase (translation) (1080 aa)	1	6.7
517	NCU01689T0	| NCU01689 | Neurospora crassa OR74A (finished) mitochondrial DNA replication protein YHM2 (translation) (317 aa)	1	11.1
518	NCU01606T0	| NCU01606 | Neurospora crassa OR74A (finished) ATP synthase subunit 5 (translation) (221 aa)	1	21.8
519	NCU09816T0	| NCU09816 | Neurospora crassa OR74A (finished) cytochrome-1 (translation) (322 aa)	1	14.0
520	NCU09366T0	| NCU09366 | Neurospora crassa OR74A (finished) proteasome component C5 (translation) (266 aa)	1	7.2
521	NCU05079T0	| NCU05079 | Neurospora crassa OR74A (finished) MFS peptide transporter (translation) (630 aa)	1	3.8
523	NCU07280T0	| NCU07280 | Neurospora crassa OR74A (finished) serine/threonine-protein kinase gad8 (translation) (645 aa)	1	5.1
524	NCU05387T0	| NCU05387 | Neurospora crassa OR74A (finished) hydrolase (translation) (477 aa)	1	7.1
525	NCU04164T0	| NCU04164 | Neurospora crassa OR74A (finished) conserved hypothetical protein (translation) (341 aa)	1	12.7
526	NCU06712T0	| NCU06712 | Neurospora crassa OR74A (finished) proteasome component PRE5 (translation) (266 aa)	1	7.5

527	NCU03200T0	| NCU03200 | Neurospora crassa OR74A (finished) serine/threonine-protein kinase sck1 (translation) (912 aa)	1	5.6
528	NCU02274T0	| NCU02274 | Neurospora crassa OR74A (finished) serine hydroxymethyltransferase (translation) (481 aa)	2	9.6
529	NCU08924T0	| NCU08924 | Neurospora crassa OR74A (finished) acyl-CoA dehydrogenase (translation) (523 aa)	1	9.0
530	NCU02542T1	| NCU02542 | Neurospora crassa OR74A (finished) hexokinase (translation) (502 aa)	1	10.0
531	NCU01140T0	| NCU01140 | Neurospora crassa OR74A (finished) NAD(P) transhydrogenase (translation) (1124 aa)	1	3.1
532	NCU05495T0	| NCU05495 | Neurospora crassa OR74A (finished) CVNH domain-containing protein (translation) (112 aa)	1	22.5
533	NCU07735T0	| NCU07735 | Neurospora crassa OR74A (finished) Grp1p (translation) (355 aa)	1	17.5
534	NCU02134T0	| NCU02134 | Neurospora crassa OR74A (finished) transcription factor (translation) (881 aa)	1	7.5
535	NCU03953T0	| NCU03953 | Neurospora crassa OR74A (finished) NADH:ubiquinone oxidoreductase 19.3 (translation) (227 aa)	1	15.5
536	NCU05889T0	| NCU05889 | Neurospora crassa OR74A (finished) eukaryotic translation initiation factor 3 subunit 6 (translation) (444 aa)	1	6.3
537	NCU05633T0	| NCU05633 | Neurospora crassa OR74A (finished) stomatin family protein (translation) (432 aa)	1	9.3
538	NCU11395T0	| NCU11395 | Neurospora crassa OR74A (finished) S-(hydroxymethyl)glutathione dehydrogenase (translation) (456 aa)	1	4.8
539	NCU03387T0	| NCU03387 | Neurospora crassa OR74A (finished) vesicular-fusion protein SEC18 (translation) (854 aa)	1	3.6
540	NCU10477T0	| NCU10477 | Neurospora crassa OR74A (finished) ubiquitin-conjugating enzyme E2 (translation) (171 aa)	1	18.8

541	NCU01318T0	| NCU01318 | Neurospora crassa OR74A (finished) protein transporter sec-23 (translation) (776 aa)	1	4.9
542	NCU04133T0	| NCU04133 | Neurospora crassa OR74A (finished) peptidase family M28 (translation) (1073 aa)	1	2.7
543	NCU09132T0	| NCU09132 | Neurospora crassa OR74A (finished) alpha tubulin (translation) (455 aa)	1	4.2
544	NCU07580T0	| NCU07580 | Neurospora crassa OR74A (finished) cyclin-dependent protein kinase (translation) (338 aa)	1	7.4
545	NCU01439T0	| NCU01439 | Neurospora crassa OR74A (finished) D-3-phosphoglycerate dehydrogenase 1 (translation) (467 aa)	1	8.6
546	NCU00680T0	| NCU00680 | Neurospora crassa OR74A (finished) 2-methylcitrate dehydratase (translation) (566 aa)	1	6.5
547	NCU04496T0	| NCU04496 | Neurospora crassa OR74A (finished) conserved hypothetical protein (translation) (222 aa)	1	14.9
548	NCU01981T0	| NCU01981 | Neurospora crassa OR74A (finished) translation factor sui1 (translation) (118 aa)	1	18.0
549	NCU03061T0	| NCU03061 | Neurospora crassa OR74A (finished) translation initiation factor RLI1 (translation) (608 aa)	1	4.9
550	NCU01632T0	| NCU01632 | Neurospora crassa OR74A (finished) pentafunctional AROM polypeptide (translation) (1564 aa)	1	3.1
551	NCU05689T0	| NCU05689 | Neurospora crassa OR74A (finished) cytochrome c oxidase polypeptide IV (translation) (187 aa)	1	14.0
552	NCU01523T0	| NCU01523 | Neurospora crassa OR74A (finished) GTP-binding protein ypt3 (translation) (215 aa)	1	17.8
553	NCU04448T0	| NCU04448 | Neurospora crassa OR74A (finished) T-complex protein 1 subunit alpha (translation) (567 aa)	1	6.9
554	NCU04076T0	| NCU04076 | Neurospora crassa OR74A (finished) copper resistance-associated P-type ATPase (translation) (1293 aa)	1	4.7
555	NCU11202T0	| NCU11202 | Neurospora crassa OR74A (finished) cytoskeleton assembly control protein Sla2 (translation) (1054 aa)	1	4.7

556	NCU01992T0	| NCU01992 | Neurospora crassa OR74A (finished) coatomer subunit gamma (translation) (917 aa)	1	5.0
557	NCU09866T0	| NCU09866 | Neurospora crassa OR74A (finished) thyroid hormone receptor interactor 12 (translation) (1973 aa)	1	1.7
558	NCU10732T0	| NCU10732 | Neurospora crassa OR74A (finished) mitochondrial dicarboxylate transporter (translation) (332 aa)	1	8.5
559	NCU09194T0	| NCU09194 | Neurospora crassa OR74A (finished) nuclease S1 (translation) (325 aa)	1	7.1
560	NCU06187T0	| NCU06187 | Neurospora crassa OR74A (finished) adenylosuccinate lyase (translation) (483 aa)	1	7.1
561	NCU10292T0	| NCU10292 | Neurospora crassa OR74A (finished) porphobilinogen deaminase (translation) (338 aa)	1	8.0
562	NCU06603T0	| NCU06603 | Neurospora crassa OR74A (finished) ThiJ/PfpI family protein (translation) (243 aa)	1	6.2
563	NCU06348T0	| NCU06348 | Neurospora crassa OR74A (finished) myo-inositol-1-monophosphotase (translation) (306 aa)	1	6.9
564	NCU06698T0	| NCU06698 | Neurospora crassa OR74A (finished) glycogenin (translation) (687 aa)	1	7.3
565	NCU08469T0	| NCU08469 | Neurospora crassa OR74A (finished) conserved hypothetical protein (translation) (449 aa)	1	8.7
566	NCU04115T0	| NCU04115 | Neurospora crassa OR74A (finished) clathrin light chain (translation) (245 aa)	1	11.1
567	NCU01667T0	| NCU01667 | Neurospora crassa OR74A (finished) arginine-12 (translation) (386 aa)	1	5.5
568	NCU00905T0	| NCU00905 | Neurospora crassa OR74A (finished) N-acylethanolamine amidohydrolase (translation) (611 aa)	1	2.5
569	NCU09169T0	| NCU09169 | Neurospora crassa OR74A (finished) NmrA family transcriptional regulator (translation) (325 aa)	1	6.8
570	NCU03876T0	| NCU03876 | Neurospora crassa OR74A (finished) eukaryotic translation initiation factor 3 subunit 2 (translation) (347 aa)	1	9.5

571	NCU05526T1	| NCU05526 | Neurospora crassa OR74A (finished) lysine-5 (translation) (314 aa)	1	6.4
572	NCU06300T0	| NCU06300 | Neurospora crassa OR74A (finished) guanylate kinase (translation) (216 aa)	1	11.2
573	NCU09485T0	| NCU09485 | Neurospora crassa OR74A (finished) chaperone dnaK (translation) (1006 aa)	1	3.8
574	NCU07618T0	| NCU07618 | Neurospora crassa OR74A (finished) conserved hypothetical protein (translation) (1801 aa)	1	1.3
575	NCU06240T0	| NCU06240 | Neurospora crassa OR74A (finished) protein kinase A catalytic subunit-1 (translation) (537 aa)	1	6.0
576	NCU04415T0	| NCU04415 | Neurospora crassa OR74A (finished) conserved hypothetical protein (translation) (562 aa)	1	3.2
577	NCU05942T0	| NCU05942 | Neurospora crassa OR74A (finished) proteasome component Y13 (translation) (252 aa)	1	13.2
578	NCU09794T0	| NCU09794 | Neurospora crassa OR74A (finished) NAD-binding Rossmann fold oxidoreductase (translation) (358 aa)	1	4.2
579	NCU06615T0	| NCU06615 | Neurospora crassa OR74A (finished) conserved hypothetical protein (translation) (204 aa)	1	9.4
580	NCU06440T0	| NCU06440 | Neurospora crassa OR74A (finished) proteasome component PRE6 (translation) (270 aa)	1	5.9
581	NCU05599T0	| NCU05599 | Neurospora crassa OR74A (finished) 40S ribosomal protein S28 (translation) (69 aa)	1	22.1
582	NCU04907T0	| NCU04907 | Neurospora crassa OR74A (finished) conserved hypothetical protein (translation) (377 aa)	1	7.4
583	NCU10273T0	| NCU10273 | Neurospora crassa OR74A (finished) Hsc70 cochaperone (translation) (366 aa)	1	11.5
584	NCU08434T0	| NCU08434 | Neurospora crassa OR74A (finished) 5-methyltetrahydropteroyltriglutamate-homocysteine methyltransferase (translation) (402 aa)	1	5.5
585	NCU03399T0	| NCU03399 | Neurospora crassa OR74A (finished) conserved hypothetical protein (translation) (472 aa)	1	6.4

586	NCU01272T0	| NCU01272 | Neurospora crassa OR74A (finished) mitochondrial presequence protease (translation) (1013 aa)	1	3.1
587	NCU09309T0	| NCU09309 | Neurospora crassa OR74A (finished) proteasome component PRE2 (translation) (292 aa)	1	6.5
588	NCU08549T0	| NCU08549 | Neurospora crassa OR74A (finished) UDP-galactose 4-epimerase (translation) (286 aa)	1	5.3
589	NCU04242T0	| NCU04242 | Neurospora crassa OR74A (finished) ATP-dependent helicase NAM7 (translation) (1091 aa)	1	1.5
590	NCU03636T1	| NCU03636 | Neurospora crassa OR74A (finished) conserved hypothetical protein (translation) (89 aa)	1	22.7
591	NCU02541T0	| NCU02541 | Neurospora crassa OR74A (finished) oligosaccharyltransferase alpha subunit (translation) (502 aa)	1	1.8
592	NCU06556T0	| NCU06556 | Neurospora crassa OR74A (finished) thioredoxin II (translation) (148 aa)	1	16.3
593	NCU07574T0	| NCU07574 | Neurospora crassa OR74A (finished) conserved hypothetical protein (translation) (528 aa)	1	6.5
594	NCU11265T0	| NCU11265 | Neurospora crassa OR74A (finished) predicted protein (translation) (200 aa)	1	13.1
595	NCU04404T0	| NCU04404 | Neurospora crassa OR74A (finished) coatomer beta subunit (translation) (958 aa)	1	3.2
596	NCU03076T0	| NCU03076 | Neurospora crassa OR74A (finished) delta-1-pyrroline-5-carboxylate dehydrogenase (translation) (602 aa)	1	4.0
597	NCU02813T0	| NCU02813 | Neurospora crassa OR74A (finished) eukaryotic translation initiation factor 3 subunit M (translation) (435 aa)	1	7.4
598	NCU00410T0	| NCU00410 | Neurospora crassa OR74A (finished) eukaryotic release factor 1 (translation) (435 aa)	1	6.2
599	NCU00261T0	| NCU00261 | Neurospora crassa OR74A (finished) CTP synthase (translation) (586 aa)	1	4.4
600	NCU11755T0	| NCU11755 | Neurospora crassa OR74A (finished) conserved hypothetical protein (translation) (92 aa)	1	15.4

601	NCU06764T0	| NCU06764 | Neurospora crassa OR74A (finished) 20S proteasome subunit Y7 (translation) (287 aa)	1	4.9
602	NCU05881T0	| NCU05881 | Neurospora crassa OR74A (finished) DUF500 and UBA/TS-N domain-containing protein (translation) (702 aa)	1	3.1
603	NCU05274T0	| NCU05274 | Neurospora crassa OR74A (finished) eukaryotic initiation factor 5A (translation) (164 aa)	1	9.2
604	NCU03010T0	| NCU03010 | Neurospora crassa OR74A (finished) L-aminoadipate-semialdehyde dehydrogenase large subunit (translation) (1175 aa)	1	1.3
605	NCU00102T0	| NCU00102 | Neurospora crassa OR74A (finished) conserved hypothetical protein (translation) (373 aa)	1	4.0
606	NCU02455T0	| NCU02455 | Neurospora crassa OR74A (finished) FKBP-type peptidyl-prolyl cis-trans isomerase (translation) (218 aa)	2	9.7
607	NCU09721T0	| NCU09721 | Neurospora crassa OR74A (finished) AP-1 complex subunit beta-1 (translation) (750 aa)	1	4.4
608	NCU09895T0	| NCU09895 | Neurospora crassa OR74A (finished) thioesterase (translation) (296 aa)	1	10.9
609	NCU09553T0	| NCU09553 | Neurospora crassa OR74A (finished) 3-hydroxybutyryl CoA dehydrogenase (translation) (317 aa)	1	7.0
610	NCU09089T1	| NCU09089 | Neurospora crassa OR74A (finished) hypothetical protein (translation) (63 aa)	1	41.9
611	NCU07363T0	| NCU07363 | Neurospora crassa OR74A (finished) conserved hypothetical protein (translation) (350 aa)	1	7.7
612	NCU05156T0	| NCU05156 | Neurospora crassa OR74A (finished) conserved hypothetical protein (translation) (488 aa)	1	4.9
613	NCU04768T0	| NCU04768 | Neurospora crassa OR74A (finished) electron transfer flavoprotein-ubiquinone oxidoreductase (translation) (646 aa)	1	4.5
614	NCU04762T0	| NCU04762 | Neurospora crassa OR74A (finished) conserved hypothetical protein (translation) (493 aa)	1	5.9

615	NCU02016T0	| NCU02016 | Neurospora crassa OR74A (finished) conserved hypothetical protein (translation) (129 aa)	1	22.7
616	NCU01821T0	| NCU01821 | Neurospora crassa OR74A (finished) alanine-glyoxylate aminotransferase (translation) (447 aa)	1	6.3
617	NCU00461T0	| NCU00461 | Neurospora crassa OR74A (finished) NAD-specific glutamate dehydrogenase (translation) (1052 aa)	1	2.3
618	NCU09755T0	| NCU09755 | Neurospora crassa OR74A (finished) conserved hypothetical protein (translation) (412 aa)	1	3.9
619	NCU09732T0	| NCU09732 | Neurospora crassa OR74A (finished) acetyl-CoA acetyltransferase (translation) (431 aa)	1	3.5
620	NCU09266T0	| NCU09266 | Neurospora crassa OR74A (finished) methylmalonate-semialdehyde dehydrogenase (translation) (584 aa)	1	2.7
621	NCU08909T0	| NCU08909 | Neurospora crassa OR74A (finished) beta-1,3-glucanosyltransferase (translation) (543 aa)	1	3.3
622	NCU08578T0	| NCU08578 | Neurospora crassa OR74A (finished) oxysterol binding protein (translation) (419 aa)	1	4.5
623	NCU07787T0	| NCU07787 | Neurospora crassa OR74A (finished) Epl1 protein (translation) (139 aa)	1	10.9
624	NCU06875T0	| NCU06875 | Neurospora crassa OR74A (finished) conserved hypothetical protein (translation) (203 aa)	1	10.4
625	NCU06588T0	| NCU06588 | Neurospora crassa OR74A (finished) conserved hypothetical protein (translation) (182 aa)	1	9.4
626	NCU06530T0	| NCU06530 | Neurospora crassa OR74A (finished) palmitoyl-protein thioesterase (translation) (331 aa)	1	6.4
627	NCU06307T0	| NCU06307 | Neurospora crassa OR74A (finished) multisynthetase complex auxiliary component p43 (translation) (420 aa)	1	5.0
628	NCU06071T0	| NCU06071 | Neurospora crassa OR74A (finished) 2-dehydropantoate 2-reductase (translation) (363 aa)	1	4.7

629	NCU05841T0	| NCU05841 | Neurospora crassa OR74A (finished) UMTA (translation) (388 aa)	1	5.7
630	NCU05512T0	| NCU05512 | Neurospora crassa OR74A (finished) copper resistance protein Crd2 (translation) (113 aa)	1	19.6
631	NCU05290T0	| NCU05290 | Neurospora crassa OR74A (finished) orotate phosphoribosyltransferase (translation) (234 aa)	1	11.2
632	NCU04721T0	| NCU04721 | Neurospora crassa OR74A (finished) neutral ceramidase (translation) (772 aa)	1	2.7
633	NCU03329T0	| NCU03329 | Neurospora crassa OR74A (finished) conserved hypothetical protein (translation) (295 aa)	1	7.5
634	NCU03148T0	| NCU03148 | Neurospora crassa OR74A (finished) nascent polypeptide-associated complex beta subunit (translation) (153 aa)	1	11.8
635	NCU02781T0	| NCU02781 | Neurospora crassa OR74A (finished) conserved hypothetical protein (translation) (369 aa)	1	4.9
636	NCU02657T0	| NCU02657 | Neurospora crassa OR74A (finished) ethionine resistant-1 (translation) (396 aa)	1	5.3
637	NCU02160T0	| NCU02160 | Neurospora crassa OR74A (finished) small GTPase RAC (translation) (201 aa)	1	9.0
638	NCU02011T0	| NCU02011 | Neurospora crassa OR74A (finished) importin subunit beta-1 (translation) (877 aa)	1	1.8
639	NCU01645T0	| NCU01645 | Neurospora crassa OR74A (finished) conserved hypothetical protein (translation) (314 aa)	1	6.1
640	NCU01258T1	| NCU01258 | Neurospora crassa OR74A (finished) cyanase (translation) (182 aa)	1	12.7
641	NCU01197T0	| NCU01197 | Neurospora crassa OR74A (finished) cell wall biogenesis protein phosphatase Ssd1 (translation) (1366 aa)	1	1.5
642	NCU01092T0	| NCU01092 | Neurospora crassa OR74A (finished) 3-oxoacyl-(acyl-carrier-protein) reductase (translation) (315 aa)	1	6.4

643	NCU00243T0	| NCU00243 | Neurospora crassa OR74A (finished) microtubule-associated protein RP/EB family member 1 (translation) (249 aa)	1	9.7
644	NCU00116T2	| NCU00116 | Neurospora crassa OR74A (finished) am alpha binding protein-1 (translation) (272 aa)	1	5.2
645	NCU16006T0	| NCU16006 | Neurospora crassa OR74A mito NADH dehydrogenase subunit 2 (translation) (584 aa)	1	2.2
646	NCU11647T0	| NCU11647 | Neurospora crassa OR74A (finished) conserved hypothetical protein (translation) (277 aa)	1	3.3
647	NCU10046T0	| NCU10046 | Neurospora crassa OR74A (finished) ubiquitin conjugating enzyme Ubc8 (translation) (173 aa)	1	5.2
648	NCU09904T0	| NCU09904 | Neurospora crassa OR74A (finished) glucan 1,3-beta-glucosidase (translation) (468 aa)	1	2.1
649	NCU09600T0	| NCU09600 | Neurospora crassa OR74A (finished) dienelactone hydrolase (translation) (296 aa)	1	3.1
650	NCU09560T0	| NCU09560 | Neurospora crassa OR74A (finished) superoxide dismutase (translation) (229 aa)	1	6.1
651	NCU09429T0	| NCU09429 | Neurospora crassa OR74A (finished) flavin-containing monooxygenase (translation) (667 aa)	1	1.8
652	NCU08930T0	| NCU08930 | Neurospora crassa OR74A (finished) NADH:ubiquinone oxidoreductase 21.3kD subunit a (translation) (202 aa)	1	5.5
653	NCU08605T0	| NCU08605 | Neurospora crassa OR74A (finished) proteasome subunit beta type 7 (translation) (276 aa)	1	2.9
654	NCU08300T1	| NCU08300 | Neurospora crassa OR74A (finished) conserved hypothetical protein (translation) (92 aa)	1	7.7
655	NCU08133T0	| NCU08133 | Neurospora crassa OR74A (finished) carbonic anhydrase 2 (translation) (284 aa)	1	6.4
656	NCU08095T0	| NCU08095 | Neurospora crassa OR74A (finished) conserved hypothetical protein (translation) (246 aa)	1	4.5

657	NCU07456T0	| NCU07456 | Neurospora crassa OR74A (finished) riboflavin synthase subunit alpha (translation) (256 aa)	1	4.3
658	NCU07273T0	| NCU07273 | Neurospora crassa OR74A (finished) conserved hypothetical protein (translation) (160 aa)	1	8.8
659	NCU06740T0	| NCU06740 | Neurospora crassa OR74A (finished) conserved hypothetical protein (translation) (97 aa)	1	11.5
660	NCU06666T0	| NCU06666 | Neurospora crassa OR74A (finished) inositol-3-phosphate synthase (translation) (538 aa)	1	2.0
661	NCU05780T0	| NCU05780 | Neurospora crassa OR74A (finished) glutathione transferase (translation) (237 aa)	1	4.7
662	NCU05598T0	| NCU05598 | Neurospora crassa OR74A (finished) ascus development-1 (translation) (541 aa)	1	2.6
663	NCU04940T0	| NCU04940 | Neurospora crassa OR74A (finished) reticulon-4-interacting protein 1 (translation) (348 aa)	1	2.9
664	NCU04759T0	| NCU04759 | Neurospora crassa OR74A (finished) nuclear transport factor 2 (translation) (125 aa)	1	6.5
665	NCU04743T0	| NCU04743 | Neurospora crassa OR74A (finished) tubulin-tyrosine ligase (translation) (855 aa)	1	1.6
666	NCU04552T0	| NCU04552 | Neurospora crassa OR74A (finished) cytoplasmic ribosomal protein-5 (translation) (120 aa)	1	7.6
667	NCU04452T0	| NCU04452 | Neurospora crassa OR74A (finished) 12-oxophytodienoate reductase 1 (translation) (380 aa)	1	2.9
668	NCU04337T0	| NCU04337 | Neurospora crassa OR74A (finished) survival factor 1 (translation) (382 aa)	1	2.6
669	NCU03882T0	| NCU03882 | Neurospora crassa OR74A (finished) conserved hypothetical protein (translation) (162 aa)	1	6.8
670	NCU03803T0	| NCU03803 | Neurospora crassa OR74A (finished) sorbitol utilization protein SOU2 (translation) (293 aa)	1	3.4
671	NCU02555T0	| NCU02555 | Neurospora crassa OR74A (finished) actin (translation) (470 aa)	1	3.0

672	NCU02472T0	| NCU02472 | Neurospora crassa OR74A (finished) NADH:ubiquinone oxidoreductase 20.8kD subunit (translation) (184 aa)	1	8.2
673	NCU02399T0	| NCU02399 | Neurospora crassa OR74A (finished) conserved hypothetical protein (translation) (625 aa)	1	2.2
674	NCU02156T0	| NCU02156 | Neurospora crassa OR74A (finished) dsDNA-binding protein PDCD5 (translation) (142 aa)	1	12.1
675	NCU02041T0	| NCU02041 | Neurospora crassa OR74A (finished) anchored cell wall protein-11 (translation) (196 aa)	1	4.1
676	NCU01919T0	| NCU01919 | Neurospora crassa OR74A (finished) ubiquitin C-terminal hydrolase (translation) (549 aa)	1	1.6
677	NCU01914T0	| NCU01914 | Neurospora crassa OR74A (finished) sorting nexin-3 (translation) (143 aa)	1	5.6
678	NCU01859T0	| NCU01859 | Neurospora crassa OR74A (finished) NADH:ubiquinone oxidoreductase 20.9kD subunit (translation) (190 aa)	1	3.7
679	NCU01838T0	| NCU01838 | Neurospora crassa OR74A (finished) nitrilase (translation) (358 aa)	1	4.2
680	NCU01766T0	| NCU01766 | Neurospora crassa OR74A (finished) conserved hypothetical protein (translation) (253 aa)	1	4.4
681	NCU01759T0	| NCU01759 | Neurospora crassa OR74A (finished) aldo-keto reductase family 1 member C13 (translation) (323 aa)	1	3.4
682	NCU00903T0	| NCU00903 | Neurospora crassa OR74A (finished) conserved hypothetical protein (translation) (351 aa)	1	2.9
683	NCU00768T0	| NCU00768 | Neurospora crassa OR74A (finished) mRNA binding post-transcriptional regulator (translation) (392 aa)	1	2.3
684	NCU00635T0	| NCU00635 | Neurospora crassa OR74A (finished) nascent polypeptide-associated complex subunit alpha (translation) (201 aa)	1	7.0
685	NCU00578T0	| NCU00578 | Neurospora crassa OR74A (finished) peptidyl-prolyl cis-trans isomerase-like 1 (translation) (164 aa)	1	4.9

686	NCU00236T0	| NCU00236 | Neurospora crassa OR74A (finished) flavoprotein oxygenase (translation) (367 aa)	1	3.8
687	NCU00173T0	| NCU00173 | Neurospora crassa OR74A (finished) esterase D (translation) (296 aa)	1	4.1
688	NCU00160T0	| NCU00160 | Neurospora crassa OR74A (finished) NADH:ubiquinone oxidoreductase 6.6kD subunit (translation) (76 aa)	1	12.0
691	NCU09209T0	| NCU09209 | Neurospora crassa OR74A (finished) galactose oxidase (translation) (717 aa)	1	3.6
692	NCU04368T0	| NCU04368 | Neurospora crassa OR74A (finished) glutathione S-transferase Gst3 (translation) (420 aa)	1	7.9
693	NCU07380T0	| NCU07380 | Neurospora crassa OR74A (finished) eukaryotic translation initiation factor 3 (translation) (592 aa)	1	6.6
694	NCU02373T0	| NCU02373 | Neurospora crassa OR74A (finished) NADH-ubiquinone oxidoreductase 40 kDa subunit (translation) (376 aa)	1	8.3
696	NCU08297T1	| NCU08297 | Neurospora crassa OR74A (finished) cell division control protein 3 (translation) (419 aa)	2	8.9
697	NCU06216T0	| NCU06216 | Neurospora crassa OR74A (finished) nuclear condensin complex subunit 3 (translation) (1263 aa)	1	2.9
698	NCU02515T0	| NCU02515 | Neurospora crassa OR74A (finished) dipeptidyl aminopeptidase (translation) (896 aa)	1	2.5
699	NCU02175T0	| NCU02175 | Neurospora crassa OR74A (finished) phosphatidyl inositol-specific phospholipase C (translation) (675 aa)	1	4.0
700	NCU01648T0	| NCU01648 | Neurospora crassa OR74A (finished) dolichyl-phosphate-mannose-protein mannosyltransferase 2 (translation) (751 aa)	1	2.0
701	NCU01517T0	| NCU01517 | Neurospora crassa OR74A (finished) glucoamylase precursor (translation) (664 aa)	1	3.0

702	NCU09783T0	| NCU09783 | Neurospora crassa OR74A (finished) D-isomer specific 2-hydroxyacid dehydrogenase (translation) (338 aa)	1	2.1
703	NCU09013T0	| NCU09013 | Neurospora crassa OR74A (finished) UPF0047 domain-containing protein (translation) (149 aa)	1	4.1
704	NCU06844T0	| NCU06844 | Neurospora crassa OR74A (finished) conserved hypothetical protein (translation) (170 aa)	1	8.3
705	NCU06318T0	| NCU06318 | Neurospora crassa OR74A (finished) ATP-dependent RNA helicase DHX8 (translation) (1180 aa)	1	0.8
706	NCU01654T0	| NCU01654 | Neurospora crassa OR74A (finished) long-chain-fatty-acid-CoA ligase 1 (translation) (706 aa)	1	4.0
708	NCU09141T0	| NCU09141 | Neurospora crassa OR74A (finished) pyridoxal reductase (translation) (329 aa)	1	7.3
709	NCU03166T0	| NCU03166 | Neurospora crassa OR74A (finished) phosphoribosylaminoimidazole-succinocarboxamide synthase (translation) (308 aa)	1	7.2
710	NCU07296T0	| NCU07296 | Neurospora crassa OR74A (finished) colonial temperature sensitive-1 (translation) (599 aa)	1	6.5
712	NCU05683T0	| NCU05683 | Neurospora crassa OR74A (finished) dihydroxy-acid dehydratase (translation) (641 aa)	1	5.5
713	NCU03797T0	| NCU03797 | Neurospora crassa OR74A (finished) ubiquitin C-terminal hydrolase (translation) (1163 aa)	1	2.5
714	NCU00649T0	| NCU00649 | Neurospora crassa OR74A (finished) Npt1p (translation) (478 aa)	1	3.6
715	NCU05363T0	| NCU05363 | Neurospora crassa OR74A (finished) 26S protease regulatory subunit 8 (translation) (390 aa)	2	6.4
716	NCU09709T0	| NCU09709 | Neurospora crassa OR74A (finished) T-complex protein 1 subunit zeta (translation) (545 aa)	1	3.9
717	NCU07029T0	| NCU07029 | Neurospora crassa OR74A (finished) conserved hypothetical protein (translation) (1266 aa)	1	1.2

719	NCU08561T0	| NCU08561 | Neurospora crassa OR74A (finished) succinate/fumarate mitochondrial transporter (translation) (325 aa)	1	3.7
720	NCU07171T0	| NCU07171 | Neurospora crassa OR74A (finished) actin-6 (translation) (396 aa)	1	2.3
721	NCU05220T0	| NCU05220 | Neurospora crassa OR74A (finished) ATP synthase subunit F (translation) (102 aa)	1	6.9
722	NCU01939T0	| NCU01939 | Neurospora crassa OR74A (finished) nonsense-mediated mRNA decay protein (translation) (1048 aa)	1	0.8
723	NCU00971T0	| NCU00971 | Neurospora crassa OR74A (finished) ribosomal protein S12 (translation) (153 aa)	1	4.6
724	NCU00867T0	| NCU00867 | Neurospora crassa OR74A (finished) conserved hypothetical protein (translation) (304 aa)	1	4.0
725	NCU11348T0	| NCU11348 | Neurospora crassa OR74A (finished) NADH-ubiquinone oxidoreductase B18 subunit (translation) (88 aa)	1	26.4
727	NCU01938T0	| NCU01938 | Neurospora crassa OR74A (finished) conserved hypothetical protein (translation) (400 aa)	1	5.3
728	NCU10497T0	| NCU10497 | Neurospora crassa OR74A (finished) oligosaccharyl transferase STT3 subunit (translation) (750 aa)	1	5.5
729	NCU03297T1	| NCU03297 | Neurospora crassa OR74A (finished) cytochrome c peroxidase (translation) (359 aa)	1	4.7
730	NCU01190T0	| NCU01190 | Neurospora crassa OR74A (finished) DUF410 domain-containing protein (translation) (344 aa)	1	7.3
731	NCU16012T0	| NCU16012 | Neurospora crassa OR74A mito cytochrome b (translation) (390 aa)	1	5.9
732	NCU06417T0	| NCU06417 | Neurospora crassa OR74A (finished) uracil-5-carboxylate decarboxylase (translation) (395 aa)	1	7.1
733	NCU02110T0	| NCU02110 | Neurospora crassa OR74A (finished) NADPH oxidase-1 (translation) (554 aa)	1	2.5

734	NCU07120T0	| NCU07120 | Neurospora crassa OR74A (finished) DUF1264 domain-containing protein (translation) (253 aa)	1	4.0
735	NCU02888T0	| NCU02888 | Neurospora crassa OR74A (finished) conserved hypothetical protein (translation) (250 aa)	1	3.6
737	NCU05858T0	| NCU05858 | Neurospora crassa OR74A (finished) fatty acid oxygenase (translation) (1135 aa)	1	1.9
740	NCU06062T0	| NCU06062 | Neurospora crassa OR74A (finished) aerobactin siderophore biosynthesis protein iucB (translation) (447 aa)	1	5.8
742	NCU07295T0	| NCU07295 | Neurospora crassa OR74A (finished) mitochondrial import inner membrane translocase subunit tim-54 (translation) (469 aa)	1	4.7
743	NCU04790T0	| NCU04790 | Neurospora crassa OR74A (finished) eukaryotic peptide chain release factor GTP-binding subunit (translation) (730 aa)	1	4.7

VITA

Stephanie Marie Cologna
MS 3255 TAMU
College Station, TX 77843
e-mail: scologna@mail.chem.tamu.edu

EDUCATION

December 2010 **Ph.D. Chemistry**
Texas A&M University, College Station, TX
Advisor: Dr. David H. Russell
Dissertation Title: Isoelectric Trapping and Mass Spectrometry: Tools for Proteomics

August 2005 **B.S. Chemistry**
University of Arizona, Tucson, AZ
Advisor: Dr. Katrina M. Miranda

EXPERIENCE

2005-current Research Assistant –Department of Chemistry, Texas A&M University

- Method development and application of coupling isoelectric trapping offline with mass spectrometry for proteomic applications using MALDI, ESI and LC-MS/MS techniques.
- Perform research collaborations for protein identification, peptide identification and characterization using mass spectrometry including the use of database searching.

SELECTED PUBLICATIONS

B.W. Newton*, **S.M. Cologna*,** C. Moya, D.H. Russell, W. K. Russell and A. Jayaraman "*Proteomic Analysis of 3T3-L1 Adipocyte Mitochondria During Differentiation, Maturation and Hypertrophic Enlargement*," *submitted,* **2010**. (*authors contributed equally)

S.M. Cologna, W.K. Russell, P.J. Lim, G. Vigh, and D.H. Russell "*Combining Isoelectric Point Fractionation, Liquid Chromatography and Mass Spectrometry to Increase Peptide Detection and Protein Identification*," Journal of the American Society for Mass Spectrometry*, in press,* **2010**.